Canadian Journal of
Earth Sciences

Article

The mid-Cretaceous Peninsular Ranges orogeny: a new slant on Cordilleran tectonics? III: the orogenic foredeep

Robert S. Hildebrand[a], **Janok P. Bhattacharya**[b], **and Joseph B. Whalen**[c]

[a]1401 N. Camino de Juan, Tucson, AZ 85745, USA; [b]School of Geography and Earth Sciences, McMaster University, 1280 Main St. West, Hamilton, ON L8S 4L8, Canada; [c]Geological Survey of Canada, 601 Booth Street, Ottawa, ON K1A 0E8, Canada

Corresponding author: **Robert S. Hildebrand** (email: bob@roberthildebrand.com)

Abstract

The Cretaceous Western Interior Basin reflects the interplay between the North American craton and allochthonous terranes to the west. We divide the basinal stratigraphy into three successions, Aptian–Albian, Cenomanian–Turonian, and Santonian–Maastrichtian, each related to periods of deformation in the adjacent fold-thrust belt. Here we focus on the Cenomanian–Turonian succession, where progressive west to east uplift and fluvial incision of older Aptian–Albian sedimentary rocks (Cedar Mtn–San Pitch–Thermopolis–Skull Creek–Mannville) are interpreted as a migrating forebulge. Uplift was underway at 103 Ma in the west (Paddy–Blackleaf–Muddy sandstones) and propagated eastward throughout the trough by 99.5 Ma (Viking–Bow Island–Newcastle sandstones). The incised fluvial valleys were subsequently filled by swampy and shallow marine facies, then overlain by dark, marine *Neogastroplites*-bearing shale and associated bentonites of the 100–97.5 Ma Shell Creek–Mowry–Slater River–Goodrich–Shaftesbury–Westgate shales. The shales are characterized by a distinctive condensed horizon with abundant fish scales, teeth, and bones. They are interpreted as outer-trench slope deposits, with the overlying anoxic horizon representing a starved isochronous unit formed atop the slope deposits. The starved horizon is overlain by prodeltaic muddy clinoforms of easterly migrating clastic wedges (Trevor–Dunvegan–Frontier–Cintura–Mexcala) that can be traced 800 km atop the fish-scale hash and contain hinterland-derived 99–90 Ma detrital zircons. Although the Western Interior Basin has long been considered a retro-arc trough, the overall succession instead suggests that the Cretaceous–Turonian part represents a collisional foredeep created during the ~100 Ma collision between the arc-bearing Peninsular Ranges composite terrane and North America. The accretion brought tyrannosaurids, pachycephalosaurs, snakes, and marsupials to North America.

Key words: foredeep basin, dinosaur invasion, Cordillera, Peninsular Ranges orogeny, stratigraphy, Western Interior Basin

Introduction

Much of the western half of Cretaceous North America comprised a northerly trending couplet of distinct, yet intimately interrelated, tectonic entities: the Cordillera and the Western Interior Basin (Fig. 1). The mostly high-standing Cordillera consists of varied geological terranes, complexly mingled, mixed, rifted, and amalgamated, and mainly Phanerozoic; whereas to the east, the Cretaceous Western Interior Basin was generally a subdued, low-lying, asymmetric drainage trough, built on cratonic North America, and received sediment from Cordilleran uplands to the west, as well as more muted cratonic topography to the east (Roberts and Kirschbaum 1995; Carpenter 2014; Finzel 2014; Miall and Catuneanu 2019). From time to time, the trough was continuous from the Tethyan realm of the Gulf of Mexico to the Boreal realm of the Arctic Ocean (see Kauffman and Caldwell 1993), and so is commonly referred to as the Western Interior seaway.

Rocks of the Western Interior Basin unconformably overlie platformal siliciclastic and carbonate rocks of the west-facing Cambrian to Mesozoic platformal margin of North America. In contrast, rocks of the Cordilleran terranes are largely considered to be composite, allochthonous, and exotic to North America, although in some cases their provenance remains equivocal (Helwig 1974; Coney et al. 1980; Coney 1981; Monger et al. 1982; Hildebrand 2013). The boundary between the two geologic regions is represented by a linear belt of easterly vergent folds and thrusts of widely different ages, but collectively known as the Cordilleran fold-thrust belt, with an eastern limit that closely coincides with the cratonic hingeline (Stokes 1976; Aitken 1989).

During the mid-1960s while working in the fold-thrust belt of the Idaho–Wyoming border region, Armstrong and Oriel (1965) recognized that Mesozoic folds and thrust faults were progressively younger eastward, and as the deformation migrated, coarse detritus was deposited in front of the thrusts. In a related paper, Bally et al. (1966) used seismic data to demonstrate that the Canadian portion of the fold-thrust belt, along with high-grade gneiss and granitic plutons farther west, sat structurally upon the western edge of cratonic North America and that the progressively eastward-migrating thrust stack, not only loaded and depressed the subjacent

Fig. 1. Location of the Western Interior Basin in the proposed paleogeography of North America during the Cretaceous. Source map © 2013 Colorado Plateau Geosystems Inc.

lithosphere, but that it shed clastic detritus into an asymmetrical basin migrating eastward in front of the thrust wedge. Their synthesis implied, as they noted, that the structurally higher and more westerly thrust sheets formed prior to those to the east.

By 1969, in their zeal to explore and understand the landward implications of plate tectonics, early advocates used a Cenozoic Andean framework to interpret the strongly deformed Mesozoic rocks of the high-pressure, low-temperature Franciscan thrust complex, located in western California, with similar age sedimentary rocks of the Great Valley Group, plutons of the Sierran-Klamath batholith, and the Cordilleran fold-thrust belt as a two-sided orogen: bound on both sides by major, but opposed, structural elements that collectively reflected eastward subduction of the Pacific seafloor beneath North America from the Jurassic to the Eocene (Dickinson 1970; DeCelles 2004; Yonkee and Weil 2015; Pavlis et al. 2020).

This long-standing and generally accepted hypothesis has created problems for those working in the Western Interior Basin, as phases of thrusting, thought to range in age from the Jurassic to Eocene, were active intermittently, and so are difficult to link genetically to specific events farther west (e.g., Cant and Stockmal 1989; Price 1994; Liu et al. 2005; Plint et al. 2012; Pana and van der Pluijm 2015; Quinn et al. 2016).

Some workers (Ducea and Barton 2007; DeCelles et al. 2009; Ducea et al. 2015) tried to resolve the problems by developing a complex model where magmatic high-flux events in the arc were linked to retro-arc thrusting, which, in turn, led to increased sedimentation and subsidence within the Western Interior Basin. In this model, ~400 km of upper crustal sedimentary rocks were progressively detached from crystalline basement and transported eastward on thrusts, causing an equal length of middle to lower crust and subjacent lithospheric mantle to be underthrust beneath the hinterland and Sierran arc, where they hypothesized that the crust melted to provide more than 50% of Sierran arc magmatism.

However, there are several problems with this model. First, they provide no sound mechanism for how 400 km of buoyant cratonic lithosphere was thrust beneath the Sierra Nevada nor where the heat to melt it might have come from. Second, the underthrust lithosphere would still have had a dry lower crust and refractory, intact mantle root, typical of old cratons, which would have amplified the difficulty of generating melts. Third, given that the Sierran high-flux plutons have bulk compositions no more than 10%–12% different than bulk lower and middle crust (Ducea 2002), a mechanism must be found to melt nearly all of that crust, implying a paucity of dense restite to delaminate and sink into the mantle. Fourth, the lack of delamination, coupled with the underthrusting of such large volumes of material, creates severe room problems. Finally, the plutonic rocks of the high-flux events can have, where there is no old, enriched subcratonic lithospheric mantle, positive εNd_T and Sr_i <0.704 that rule out significant input of continental crust (Wetmore and Ducea 2009; Cecil et al. 2021), or, as in the case of the Sierran Crest magmatic suite of Coleman and Glazner (1998), have $\delta^{18}O_{zircon}$ values more typical of the mantle than continental crust (Lackey et al. 2008; Hildebrand et al. 2018).

Other models envisaged flexural loading and isostatic compensation caused by the accreted terranes, the thrust stack, and their eroded sediments as the main driver for subsidence in the basin (Price 1973; Beaumont 1981; Jordan 1981). Over the next couple of decades, models were invoked to better constrain the development of the basinal subsidence not only in terms of thrust load and lithospheric flexure (Stockmal et al. 1986; Stockmal and Beaumont 1987) but also by accounting for the shape of the orogen, the rifted margin, the shape of the basal detachment, and the way their interaction developed through time (e.g., Jamieson and Beaumont 1988; Beaumont et al. 1993). However, at times the basin subsided to extend eastward to the Dakotas and beyond, which is simply too far to be explained by isostatic loads in the Cordillera. As a result, some researchers invoked dynamic pressure variations in the asthenosphere above shallowly dipping oceanic lithosphere beneath the craton (Mitrovica et al. 1989; Gurnis 1992; Burgess and Moresi 1999; Liu et al. 2014; Li and Aschoff 2022). In every case, the models assumed the basin was in a retro-arc position above a persistently eastward-dipping slab of oceanic lithosphere beneath cratonic North America—but as dynamic topography is governed by transient variations in the mantle density and flow, it is difficult to interpret surface heights (topography) from mantle convection processes (Molnar et al. 2015), especially where the isostatic components are so poorly known that they cannot be removed to better isolate the dynamic contribution (Yang and Gurnis 2016). Additionally, slab break-off and migration of a broken slab beneath a continent as it moved laterally can also produce a downward pull on the surface, much in the way the Indian foredeep basin (Siwaliks) was apparently deepened when the torn and bent oceanic slab passed beneath

it (Husson et al. 2014). Overall, better geological constraints are necessary to understand the sources of the variations in surface topography.

In this paper, we examine the mid-Cretaceous stratigraphy of the Western Interior Basin, from the latest Albian into the Cenomanian–Turonian. We start with a brief overview of our tectono-sedimentary divisions for the basin to better integrate our results within the larger continuum of plate interactions that bear on its overall development. Then we describe mid-Cretaceous stratigraphic units throughout the basin to demonstrate their along-strike similarities in both lithology and timing. We end with a model that ties the stratigraphy within the Cenomanian–Turonian sector of the Western Interior Basin directly to interactions between the Peninsular Ranges composite terrane and the North American craton during the mid-Cretaceous Peninsular Ranges orogeny of Hildebrand and Whalen (2021*a*, 2021*b*).

Tectono-sedimentary subdivisions of the basinal stratigraphy

The bulk of the Western Interior Basin developed during the Cretaceous (Kauffman and Caldwell 1993); although some workers, most notably Royse (1993), along with DeCelles and colleagues (DeCelles and Currie 1996; DeCelles 2004; DeCelles and Coogan 2006; Fuentes et al. 2011), suggested that the basin initially formed during the Late Jurassic; but in either case, the Jurassic rocks were uplifted and eroded prior to the deposition of Cretaceous sediments as old as Aptian–Albian (see Heller et al. 1986). Within the southern Canadian sector of the basin, Pana et al. (2018*a*, 2019) presented the results of U-Pb dating of ash beds, along with biostratigraphy and sedimentology, from units as old as Lower Jurassic, which support the concept of one or more Jurassic foredeep basins. Within the US portion of the basin, remnant sedimentary rocks of the Upper Jurassic Morrison Formation are known to be 155–148 Ma (Kowallis et al. 1998, 2007) and could be equivalent to the youngest stratigraphic units of the Canadian Jurassic.

Regardless of the interpretation of the Jurassic stratigraphy, the Western Interior Basin is dominantly a Cretaceous basin (Fig. 2). Here we divide its Cretaceous rocks into three major intervals: Aptian–Albian (125–100.5 Ma), Cenomanian–Turonian (100.5–90 Ma), and Coniacian–Maastrichtian (90–66 Ma), each apparently related to recognized periods of shortening, uplift, and exhumation in the adjacent fold-thrust belt to the west. We use the terms Sevier (~124 Ma), Peninsular Ranges (~100 Ma), and Laramide to refer to the three orogenies, respectively, with the Laramide subdivided into an early thin-skin orthogonal phase (90–72 Ma) and a younger thick-skin transpressive phase (72–50 Ma) as per Hildebrand and Whalen (2017).

Unconformably overlying, and cutting downward into paleosols of the Jurassic Morrison Formation are incised paleovalleys filled with a regional pebble conglomerate (Yingling and Heller 1992; Currie 1998; Heller et al. 1986; Heller and Paola 1989), a regional gravelly conglomerate, that was traced eastward as far as the Black Hills of South Dakota, which

Fig. 2. Schematic west to east US cross section illustrating our tripartite divisions of the Cretaceous stratigraphy within the Western Interior Basin. Each succession is correlative with the named periods of shortening, uplift, and exhumation recognized in the adjacent fold-thrust belt. Modified from Weimer (1986).

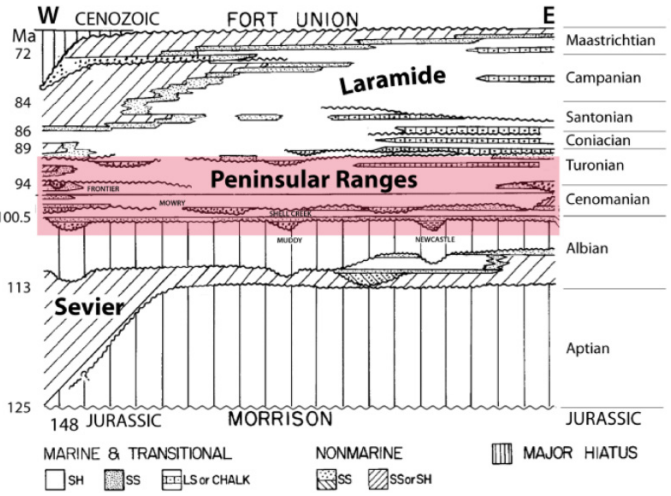

suggests that the regional surface sloped gently eastward (Heller et al. 2003). In Utah, the conglomerates are overlain by synorogenic sedimentary rocks of the Ruby Ranch Member of the Cedar Mountain Formation and the San Pitch Formation, which on the basis of detrital zircon populations, are interpreted to have been derived largely from thrust sheets located to the west, such as the Canyon Range thrust (Lawton et al. 2010), and interpreted, on the basis of $\delta^{18}O$ in dinosaur ingested water, to have been deposited in the arid lee of mountains to the west (Suarez et al. 2014). The onset of Early Cretaceous thrusting in the Great Basin segment is constrained to be ~124–120 Ma based on (i) detrital zircon peaks in sedimentary units beneath the Ruby Ranch Member (Greenhalgh 2006; Greenhalgh and Britt 2007; Britt et al. 2007; Mori 2009), (ii) a 119.4 ± 2.6 Ma U-Pb age of palustrine carbonate, and (iii) a good match between $\delta^{13}C_{org}$ excursions in early terrestrial foredeep sedimentary rocks and well-dated Albian features of the global carbon isotope chemostratigraphy (Ludvigson et al. 2010). More recent dating of detrital zircons in mudstone palaeosols from the lowermost member of the Cedar Mountain Formation, known as the Yellow Cat Member, produced a maximum depositional age (MDA) of 136.3 ± 1.3 Ma (Joeckel et al. 2020). However, most researchers consider the overlying, more continuous, and westward thickening Ruby Ranch Member to represent the earliest basinal fill related to Sevier thrusting in Utah (Kirkland et al. 2016).

Regional thrusting, originally assigned to the Sevier orogeny by Armstrong (1968), stopped during the mid-Albian at about 105 Ma, as documented by alluvial fan and fluvial sedimentary rocks of the Canyon Range wedge-top basin that unconformably overstep the Canyon Range thrust (Lawton et al. 2007). In the Wyoming sector of the belt the Ephraim Conglomerate, which was deposited unconformably upon Jurassic strata, is inferred on the basis of detrital zircon spectra

and conglomerate clast types to be debris shed from the oldest Paris thrust sheet. The Ephraim Conglomerate contains Aptian charophytes (Gentry et al. 2018; Heller et al. 1986). Additionally, apatite fission track ages of 117 ± 6 Ma and 111 ± 8 Ma collected along the Paris thrust attest to significant cooling at that time (Burtner and Nigrini 1994). In southern Canada, thrusts were shown to predate 108 Ma as they are cut by post-kinematic plutons of the Bayonne suite (Logan 2002; Larson et al. 2006). The sedimentary package in Canada starts with a basal Aptian pebbly conglomerate (Cadomin Formation), which sits unconformably upon Jurassic strata (Leckie and Cheel 1997; Leier and Gehrels 2011). The regional conglomerate unit is overlain by a thick package of siliciclastic strata contained within the Blairmore, Mannville, Luscar, and Bullhead groups (Hayes et al. 1994), which locally contain volcanic and plutonic clasts, and more elevated εNd (epsilon Nd) than rocks of the Cadomin Formation (Ross et al. 2005), consistent with uplift and erosion of young volcano-plutonic material to the west.

Throughout the basin, an unconformity within the uppermost Albian strata forms the base of a new cycle of sedimentation and co-genetic thrust activity to the west, during which movement on the thrust faults folded the earlier thrusts to form structural culminations, that are more or less coeval with part of the Cenomanian–Turonian succession of sedimentary rocks within the basin (Pujols et al. 2020; Yonkee and Weil 2015). These rocks are the main focus of this contribution.

More thrusts, active some 15 Myr later during the Santonian–Early Campanian, document another pulse of shortening (Yonkee and Weil 2015) and are unconformably overlain by large eastward-prograding, fluvial megafans deposited during the Campanian–Maastrichtian (DeCelles and Cavazza 1999). This thrusting marks what we term the early Laramide phase of deformation and related sedimentation (Hildebrand 2014; Hildebrand and Whalen 2017) when the shortening direction was approximately NE-SW. This early Laramide event involved some northward migration of the foredeep (Catuneanu et al. 2000), followed by contraction and local inversion of the Western Interior Basin during the Maastrichtian–Paleocene when the more localized thick-skin Laramide basins and uplifts (Dickinson et al. 1988) formed as shortening progressed to N-S (Gries 1983) and produced large-scale meridional migration of much of the Cordillera (Enkin 2006; Gladwin and Johnston 2006; Hildebrand 2014, 2015).

The mid-Cretaceous of the Western Interior Basin

During the early part of the late Albian, central to western North America (Fig. 3) was covered by an epeiric seaway that extended from the Gulf of Mexico to the Arctic Ocean, known as the Joli Fou-Skull Creek Sea (Porter et al. 1998; Cobban and Reeside 1952). By the latest Albian, a marine regression resulted in the southern margin of the basin migrating northward to Montana, Wyoming, north-central Colorado, and the western Dakotas (Roberts and Kirschbaum 1995). During this regression, incised valleys were cut into the older units progressively from west to east and subsequently filled with sinuous bodies of sandstone, such as occur in the dominantly non-marine Newcastle and Muddy sandstones. Later, as the Boreal Sea transgressed from west to east into northwestern Colorado and northeastern Utah, rocks of the Muddy/Newcastle were overlain by shales, siltstones, and bentonites of the Shell Creek and upper Thermopolis formations, which in turn were covered by shales of the siliceous Mowry Formation, a dominantly anoxic, condensed unit containing abundant disarticulated fish bones, teeth, and scales, as well as numerous bentonite beds (Walaszczyk and Cobban 2016). These units have equivalents to the north in Canada, and in both countries the condensed units holding abundant fish hash were abruptly overlain by eastward-prograding clastic wedges containing abundant 99–90 Ma detrital zircons derived from the orogenic hinterland to the west.

Fig. 3. Hypothesized paleogeography from Blakey (2014) for the Western Interior Basin or seaway from Late Albian to Middle Cenomanian. Source maps © 2014 Colorado Plateau Geosystems Inc.

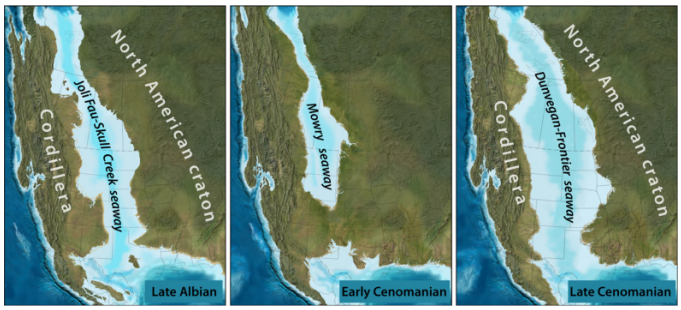

Thermopolis Formation

This succession of rocks, which largely predates rocks we are interested in, is widely known from Wyoming where it underlies the Muddy Sandstone and is commonly subdivided into several informal members (Fig. 4): Rusty beds, "lower" Thermopolis shale, middle silt, and "upper" Thermopolis shale. Although rocks of the formation occur in the Black Hills of South Dakota (Fig. 5), they are only about 5 m thick and so undivided (Eicher 1958). In the upper Thermopolis Shale, a bentonite bed collected below the base of the Muddy Sandstone yielded a $^{40}Ar/^{39}Ar$ sanidine age of 101.36 ± 0.11 Ma (Singer et al. 2021), which constrains the Muddy Sandstone and the Shell Creek Shale to be younger, whereas the underlying Thermopolis Shale is about 5 million years older (Fig. 4). In the Big Horn and Powder River basins (Fig. 5), "upper" Thermopolis Shale is a black, nearly silt-free shale 20–35 m thick containing scarce ironstone beds, a couple of bentonites near the top, and in only the Big Horn Basin, radiolarians in its upper layers (Eicher 1958). Some workers include the Muddy Sandstone and overlying Shell Creek Shale in the Thermopolis Shale, but as they are demonstrably younger and represent in part non-marine successions, we treat them

Fig. 4. Middle Cretaceous stratigraphic chart with $^{40}Ar/^{39}Ar$ sanadine ages after Singer et al. (2021) and additions in Canada from sources cited in text. Note the eastward younging of the Muddy and Newcastle sandstones.

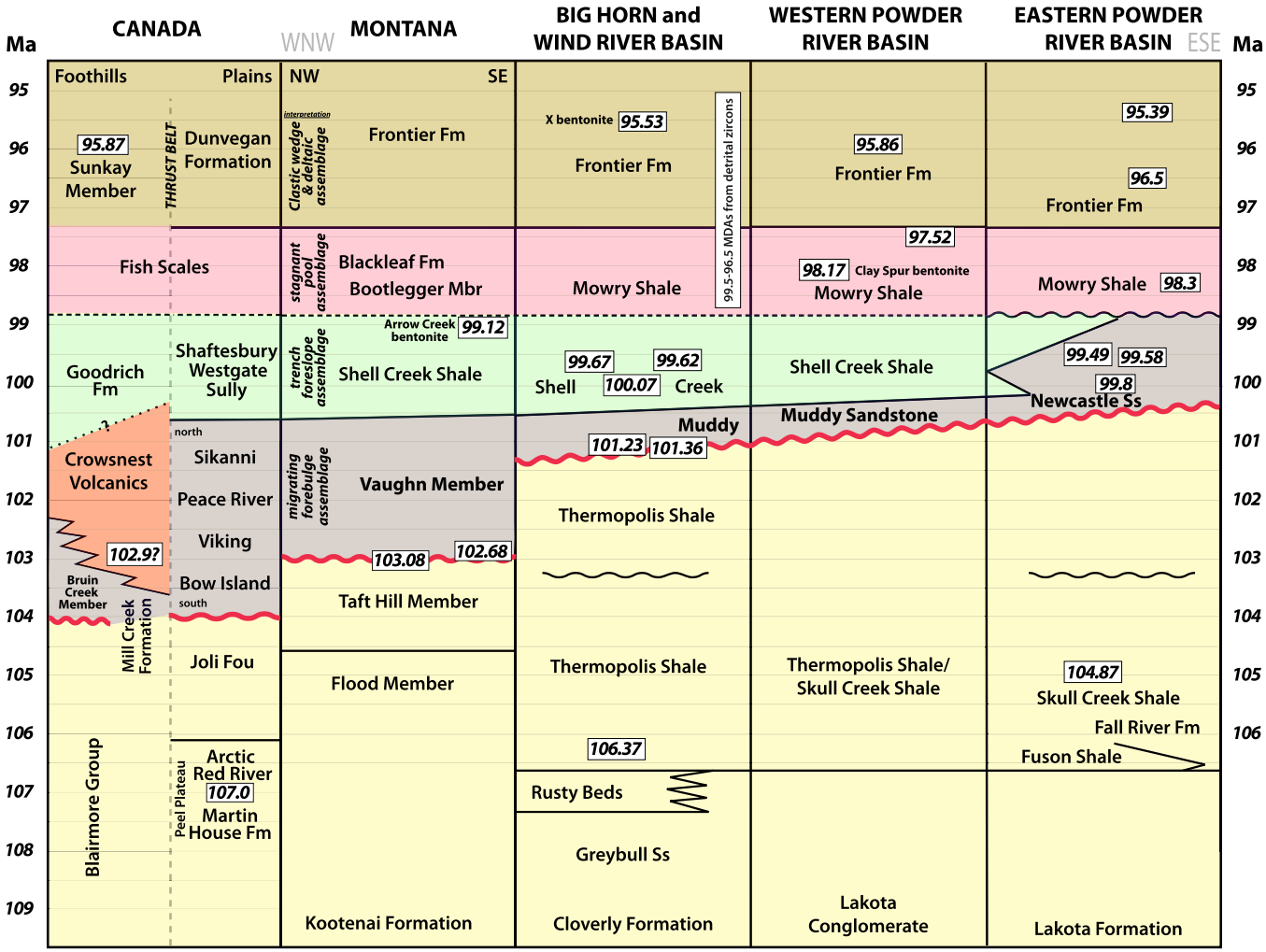

as separate units (see also Kirschbaum and Mercier 2013; Bremer 2016).

Muddy Sandstone

The Muddy Sandstone (Fig. 4) is known from much of Wyoming, but in the southwest is commonly termed the Dakota Sandstone. Eicher (1962) originally argued for separation of the Muddy Sandstone from adjacent units and for it to be given formational status. As this formation is a major petroleum reservoir, there is plenty of available data. Waring (1976) used it to show that in the northeast Powder River Basin of Wyoming (Fig. 5) and southeastern Montana the unit represented infilled channels of a dendritic river system. Whiteford (1962), Dresser (1974), and Curry (1962) studied rocks of the Muddy Formation in the Wind River Basin (Fig. 5) and found quartzose and chert-bearing sandstone, siltstones, silty shales, carbonaceous sandstones, conglomerates, rare bentonite, black and gray shale, and lignitic shale lying atop the Thermopolis Shale. In places, the Muddy Sandstone is up to 50 m thick, but more typically ranges from 3 to 13 m thick, and is overlain disconformably by the Shell Creek Shale (Curry 1962), which consists of shallow marine sedimentary rocks (Gustason 1988). Depending on location, the basal 1–10 m of the Muddy Sandstone consists of sandy or silty mudstone, muddy sandstone, lignite, and scarce bentonites, one of which was dated using $^{40}Ar/^{39}Ar$ by Singer et al. (2021) as 101.23 ± 0.09 Ma (Fig. 4). Plant remains such as leaves, amber, fusain, ferns, conifers, and dicots are abundant (Curry 1962). The basal succession shoals upwards to a non-marine sandy shoreline and (or) swampy section.

The middle sector of the formation comprises local, irregularly distributed bar, channel, and deltaic facies of a distributary river system, with some trough crossbedded sandstone filling channels as wide as several kilometers cut 30 m deep into the finer grained units below (Whiteford 1962). Dresser (1974) also reported facies diagnostic of a northeast-trending siliciclastic shoreline. Gustason (1988) documented that the middle parts of the formation contain foraminifera characteristic of the *Miliammina manitobensis* zone as do the overlying Shell Creek and Mowry shales, whereas the lower parts of the formation were more similar to the Skull Creek facies

Fig. 5. Sketch map of part of western North America after Reed et al. (2005) showing distribution of Cretaceous sedimentary rocks of the Western Interior Basin and geologic elements discussed in text. Not all geological units are shown.

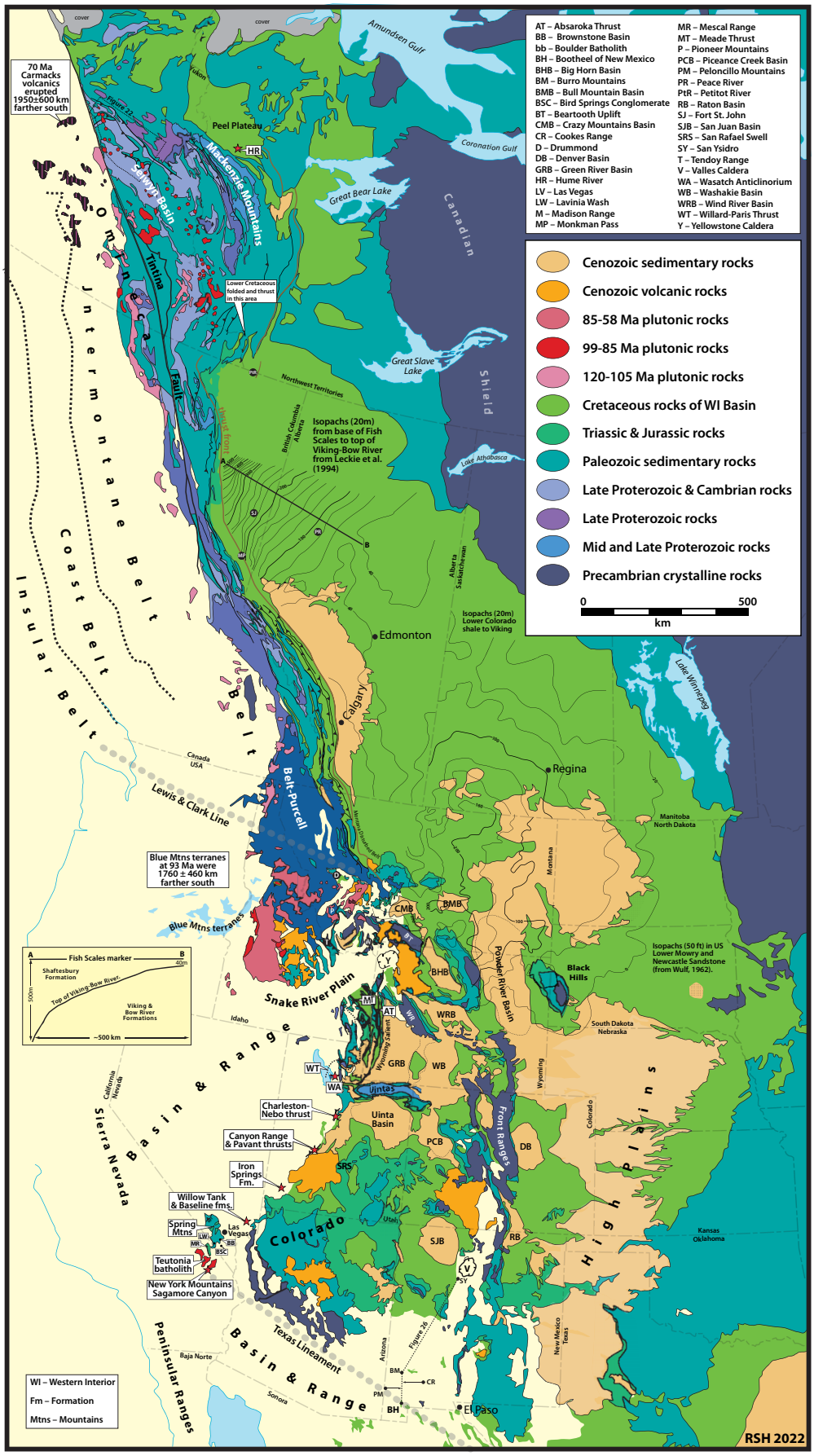

Fig. 6. Paleontological zonation of various formations described and discussed in text (from Walaszczyk and Cobban 2016).

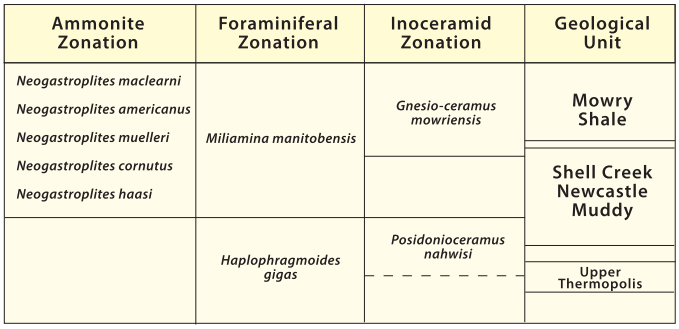

and contain the late Albian *Haplophragmoides gigas* biofacies (Fig. 6).

In the upper part of the unit, lagoonal, shallow marine sediments buried the sandy channels and covered the shoreline with shallow-water muds, detrital lignites, paleosols, fine sands with abundant ripple marks and mud cracks, with thin, burrowed tidal flat sands, and silts (Dresser 1974). According to Curry (1962), the uppermost shallow marine facies contains brachiopods.

Dolson et al. (1991) used published subsurface maps, more than 1000 core descriptions, a 900-well cross-section grid, and a computerized regional formation-top file of over 30 000 wells to reconstruct the Muddy Sandstone. Their earliest sedimentation, sheet sands that migrated westward, are several million years older than the Muddy and relate to the Kiowa-Skull Creek Sea (Singer et al. 2021). However, these studies recognized younger valley fill, alluvial plain channel fill, and transgressive marine units. They point out that valley incision and the development of at least 10 different drainage basins took place during a relative fall in sea level and that the incised valleys were filled by both fluvial and transgressive marine facies.

Newcastle Sandstone

The Newcastle Sandstone (Fig. 4), partly overlaps in age with, but is mostly slightly younger than, the Muddy Sandstone (Singer et al. 2021). Rocks of the formation are mainly of fluvial to neritic origin and were largely deposited in incised paleovalleys cut into Skull Creek Shale and oriented westerly, northwesterly, and northerly. Throughout its outcrop area of the western Dakotas, Wyoming, and southeastern Montana, the formation contains anastomosing sand bodies of a dendritic drainage system and generally ranges from 30 to 50 m thick (Stapp 1967; Finzel 2017). Examination of more than 9000 wireline logs and 23 drill cores over its outcrop area by LeFever and McCloskey (1995) documented a basal alluvial sandstone, incised during a subsequent lowstand, then overlain and infilled by a package consisting of a westward-deepening, marginal to offshore transgressive succession of sandstones, mudstones, and minor coal, similar to units of the upper Muddy Sandstone to the west. During the eastward-migrating transgression, the older fluvial and shoreline systems were reworked and deposited as shallow to marginal marine deposits. Recent age determinations show rocks of the formation (Fig. 4) to be Lower Cenomanian with $^{40}Ar/^{39}Ar$ sanidine ages of 99.49 ± 0.07 (lower), 99.58 ± 0.12 Ma (middle), and 99.8 ± 0.4 Ma (upper) for bentonites intercalated with sandstone, mudstones, and coal (Singer et al. 2021). Finzel (2017) reported six detrital zircons with ages ranging from 103 to 98 Ma, which probably represent zircons from ash beds eroded and redeposited within the fluvial unit as the Newcastle Sandstone is confined to the far eastern sector of the trough.

Shell Creek Shale

The Shell Creek Shale (Fig. 4) is the basal marine shale unit deposited during the rise and transgression of the Shell Creek-Mowry Sea (Kirschbaum and Roberts 2005). It was first given formational status separate from both the overlying Mowry and underlying Thermopolis Shale by Eicher (1962). Rocks of the Shell Creek Shale are dominated by fissile, dark-gray shale and thin bentonite beds that overlie either the Thermopolis Shale or the Muddy Sandstone in the Green River and Bighorn basins (Fig. 5), pinch out to the west, and can be traced intermittently to the Black Hills of South Dakota (Redden and DeWitt 2008). Locally, a thin, poorly sorted, granular to pebbly conglomerate and pebbly sandstone, containing crocodile and fish teeth, interpreted as a transgressive lag, occurs on top of the Muddy Sandstone (Bremer 2016). Curry (1962) pointed out that rocks of the Muddy Sandstone contained Boreal, but no Tethyan faunas, implying that the trough was not connected to the Gulf of Mexico at that time. Singer et al. (2021) dated three bentonite beds using $^{40}Ar/^{39}Ar$ on sanidine (100.07 ± 0.07 Ma, 99.67 ± 0.13 Ma, and 99.62 ± 0.07 Ma) in the Shell Creek Shale from outcrops in the Big Horn Basin of Wyoming and Montana (Figs. 4 and 5). They noted that the 99.62 Ma bentonite in the lower Shell Creek Shale is indistinguishable in age from the middle Newcastle Sandstone to the east (Fig. 4), and so their correlation constrains the location of the eastern shoreface during the Early Cenomanian.

Mowry Shale

The Mowry Shale (Fig. 4) is widespread in Wyoming, southern Montana, northern Utah and Colorado, and in the Black Hills of western South Dakota. It extends the width of the trough from the thrust belt, where it is called Aspen Shale, to the east side of the Black Hills. It was originally described at the northern end of the Bighorn Mountains of Wyoming by Darton (1904), who identified abundant fish scales, bones, and teeth. It was distinguished from shales above and below by its ridge-forming nature, attributed to the presence of abundant siliceous ash beds or porcellanites (Rubey 1929). The Mowry Shale overlies a variety of units including black Thermopolis Shale, Shell Creek Shale, and Muddy Sandstone, Dakota Formation, and (or) Newcastle Sandstone, depending on location, and is overlain by the Belle Fourche or Chalk Creek members of the Frontier Formation (Reeside and Cobban 1960; Kirschbaum and Roberts 2005; Lichtner et al. 2020).

In most locations, the Mowry Shale is a dark siliceous shale with abundant bentonite or porcellanite beds: Reeside and Cobban (1960) describe a section just under 60 m thick containing 55 bentonite beds with several beds extending for hundreds of kilometers (Kauffman 1977). Due to its high silica content, rocks of the formation tend to form ridges of silvery colored shale. In addition to the volcanic debris, the unit is rich in disarticulated fish remains, especially scales and teeth. It thickens westward from 60 to 72 m thick in the Black Hills, where it contains abundant bentonite beds (Cobban and Larson 1997) to about 200 m in western Wyoming. Singer et al. (2021) obtained $^{40}Ar/^{39}Ar$ sanidine ages of 98.17 ± 0.11 Ma and 97.52 ± 0.09 Ma for bentonites in the Mowry Shale of the western Powder River basin (Fig. 4). Hannon (2020) dated one bentonite from the Mowry Shale in the Black Hills by U-Pb inductively coupled plasma mass spectrometry (ICP-MS) on zircon to be 98.3 ± 1.1 Ma (Fig. 4).

Reeside and Cobban (1960) recognized five gastroplitine ammonite zones in the Mowry Shale of Wyoming, from oldest to youngest: *Neogastroplites haasi, Neogastroplites cornutus, Neogastroplites muelleri, Neogastroplites americanus,* and *Neogastroplites maclearni* (Fig. 6). These species of ammonite were apparently endemic to the early Cenomanian of the Mowry Sea (Cobban and Kennedy 1989). In the Black Hills of South Dakota, Cobban and Larson (1997) documented *Neogastroplites americanus and Metengonoceras aspenanum* in the upper part of the formation.

Within the Wind River Basin of Wyoming, Finn (2021) included the Shell Creek Shale as the lower member of the Mowry Shale and constructed isopach maps for the total thickness, as well as both the upper siliceous member and the lower Shell Creek Member. All three maps showed thinning to the east-southeast, with the thickness of the Mowry Shale decreasing from about 190 m thick in the western part of the basin to about 75 m in the extreme eastern sector of the basin.

Another succession rich in porcellanite that appears correlative with the Mowry Shale occurs just west of the Boulder batholith in the Flint Creek basin near Drummond, Montana (Fig. 5) and southward through the eastern Pioneer Range (Fig. 5) into the Snowcrest Range, Centennial Mountains, and Lima Peaks area (Tysdal et al. 1989; Vuke 1984; see also Hildebrand and Whalen 2021*b*). In the Madison (Fig. 5) and Gallatin ranges, 1 km of sedimentary rocks and abundant intercalated porcellanite beds of the Blackleaf/Mowry formations lie just east of the Tendoy thrust (Dyman and Nichols 1988; Wallace et al. 1990; Dyman et al. 2000). Detrital zircons collected from the Vaughn member of the Blackleaf Formation to the north near Drummond (Fig. 5) yielded a peak of 100 Ma (Stroup et al. (2008). Also, Zartman et al. (1995) dated three porcellanites from the middle of the Vaughn member of the Blackleaf as 97–95 Ma by U-Pb on zircon; whereas Dyman et al. (2000) used Ar-Ar laser fusion geochronometry to date a sample from the uppermost Vaughn of the Lima Peaks area as 99.78 Ma.

Although the above units are superficially similar to strata of the Blackleaf Formation to the east and northeast in the Montana Disturbed Belt (Fig. 5), on the basis of the available radiometric ages, they are several million years younger. These units, as well as rocks of the Blackleaf Formation to the east in the Disturbed Belt, were transported on thrust faults of potentially very different ages and so are difficult to restore palinspastically.

To the northeast of the Montana Disturbed Belt, Cobban et al. (1976) correlated rocks of the 100 m thick Bootlegger Member of the Blackleaf Formation (Fig. 4) with the Mowry Shale and suggested that it was a near-shore facies. The Bootlegger Formation consists of very fine interlaminated marine sandstone, siltstone, shale, bentonite, and pebbly lags of chert, including an uppermost sandy unit holding chert pebbles to 5 cm and abundant fish bones, overlain by the Floweree Member of the Marias River Shale, which contains no bentonites and only sparse fish debris. The Arrow Creek bentonite (Fig. 4), which occurs in the Shell Creek Shale directly below the Bootlegger Formation, was recently dated to be 99.12 ± 0.14 Ma (Singer et al. 2021). Arnott (1988) studied the Bootlegger Formation near Great Falls, Montana, and found it to contain five stacked successions comprising coarsening upward cycles grading upwards from low to moderate bioturbated offshore shelf mudstone to shoreface sandstone capped by a transgressive lag deposit of chert pebble conglomerate sitting on an erosional surface.

Outcrops of Mowry Shale continue to the south into northeastern Utah, where they consist of siliceous marine shales containing abundant disarticulated fish bones, scales, and shark teeth that overlie a nonmarine section of the Dakota Formation and underlie the Frontier Formation (Sprinkel et al. 2012). A U-Pb age from a bentonite in the middle Dakota Formation beneath the Mowry Shale was dated as 101.4 ± 0.4 Ma (Sprinkel et al. 2012), which constrains the maximum age of the Mowry Shale in northeastern Utah. Sprinkel (personal communication, 2022) now considers the Dakota there as Muddy Sandstone, with the dated bentonite just beneath it in Thermopolis Shale, consistent with the work of Singer et al. (2021) farther north (Fig. 4).

Anderson and Kowallis (2005) also examined a section of Mowry Shale in extreme northeastern Utah, but near its southwestern extent, and concluded that, although fish fossil debris occurs throughout the unit, they are particularly concentrated on bedding planes as a result of material trapped in bottom scours by storm currents on a gently sloping shelf starved of coarse sediment.

In a study of the paleoenvironments of the Mowry Shale, Byers and Larson (1979) used bentonite datum planes to demonstrate an eastward progradation of the shoreline over an east-dipping paleoslope, which they estimated at 0°0.3′. In their study, they found that the Mowry/Frontier contact is isochronous, but that Mowry facies are oblique to the contact with lower Mowry mudstones characterized as anoxic and lethal, with facies becoming richer in oxygen upwards, in what is overall a time transgressive succession from west to east, They found, as did others, that the thickest sections occurred in the thrust belt to the west. We turn now to some of those equivalent units.

Aspen and Sage Junction formations

The Aspen Shale and Sage Junction Formation are stratigraphic equivalents to the Mowry Shale that are exposed

Fig. 7. Wide-angle view looking north at an easterly dipping section of Frontier Formation near Willow Creek, Powder River Basin of Wyoming showing Mowry Shale with white bentonite on the left overlain by sandstones and shales of the Frontier Formation capped by Turonian sandstone of the Wall Creek Member (Zupanic 2017) along the ridgeline. The labeled bentonite occurs between the Mowry and Frontier formations and, although not dated at this locale, is likely the same as that dated as 97.52 ± 0.09 Ma by Singer et al. (2021).

in relatively thick sections in the fold-thrust belt of the Wyoming salient to the west (location AT on Fig. 5). In southwesternmost Wyoming and eastern Idaho, the Aspen Shale, which ranges in thickness from 200 to 600 m, is considered correlative with the Mowry Shale, and comprises shales containing *Neogastroplites cornutus* and *N. americanus*, abundant fish scales and porcellanites; overlies the shallow marine to nonmarine Bear River Formation, as well as nonmarine sandstones and conglomerates of the Kelvin Formation; and sits beneath the coal-bearing sandstones and shales of the Frontier Formation (Reeside and Cobban 1960). About 25 miles to the west, they describe a nearly 2 km-thick succession of sandstones, shales, porcellanites, bentonites, coal beds, and limestone that suggested to them a more shoreward facies of the Aspen Shale. When describing the two formations, Reeside and Cobban (1960, p. 11) wrote that "the conspicuous rocks of both the Mowry and Aspen shales are so similar to each other and so different from other rocks in the Cretaceous sequence that it is difficult not to believe them the product of one series of events".

West of the Green River basin in Wyoming, the Aspen Shale is exposed in the footwall successions below the much younger Absaroka thrust (Fig. 5), where it was described by M'Gonigle and Dover (1992) to consist of 245–370 m of dark and light-silvery weathering marine shale, siltstone, siliceous sandstone, and ridge-forming porcellanites. They reported that the unit contains abundant fish scales. A tuff in the Aspen Shale produced a U-Pb tuffzirc age of 98.8 ± 0.4 Ma (Gentry et al. 2018). Rocks of the formation are overlain by 300–430 m of largely non-marine shale, bentonitic shale, tuff, sandstone carbonaceous shale, coal, and planar to cross-bedded sandstone of the Chalk Creek Member of the Frontier Formation (M'Gonigle and Dover 1992).

The hanging wall of the Absaroka thrust fault (Fig. 5) contains a different, but equivalent, succession of rocks known as the Wayan and Sage Junction formations (Oriel and Platt 1980; M'Gonigle and Dover 1992). The Wayan Formation, about 1200 m thick, comprises variegated red, purple, and gray mudstone, siltstone, and sandstone with minor porcellenite, bentonite, and coal (Oriel and Platt 1980). The Wayan Formation is, on the basis of fauna, early Cenomanian and contains the burrowing dinosaur *Oryctodromeus* as well as flora similar to the dated flora of the 98 Ma Dakota Sandstone near Westwater, Utah (Krumenacker 2010; Barclay et al. 2015). Rubey, who had earlier defined and named the units, considered the Sage Junction Formation, which comprises slightly more than 1 km of gray siltstone and mudstone with sandstone, quartzite, and thin, but common interbeds of porcellanite throughout, except in the upper 80 m or so, to be the most probable equivalent of the Aspen Formation (Rubey 1973), but he wondered if the upper non-porcellanite facies could be a correlative of the Frontier Formation, as it contained more grit and conglomerate.

Frontier clastic wedge

The Frontier Formation (Fig. 4) of Wyoming, Utah, Montana, and Colorado is well known from both outcrops and drill holes in the eastern part of the thrust belt and even farther east in the Green River, Bighorn, and Powder River basins (Fig. 5), where it consists of southeastward prograding marine and non-marine sandstone, siltstone, shale, conglomerate, coal, and bentonite (Cobban and Reeside 1952; Merewether et al. 1984; Merewether and Cobban 1986). Within the thrust belt, the sections of Frontier are nonmarine, up to 2.1 km thick, and were transported eastward on younger thrust faults (Royse et al. 1975; Dyman and Tysdal 1998).

In the western Powder River basin of central Wyoming, rocks of the Frontier Formation (Fig. 4) constitute a Cenomanian to Turonian clastic wedge that prograded east and southeastward over the Mowry Shale, holding the 98.17 ± 0.11 Ma Clay Spur bentonite ($^{40}Ar/^{39}Ar$ sanidine age; Singer et al. 2021), and was studied in detail by Bhattacharya and Willis (2001). In western Wyoming and eastern Utah, thick

Fig. 8. Relatively immobile elements from 101.5 to 95 Ma bentonites (Hannon 2020) plotted on Nb vs. Y and Ta vs. Yb discrimination diagrams of Whalen and Hildebrand (2019) illustrating their probable slab failure origin.

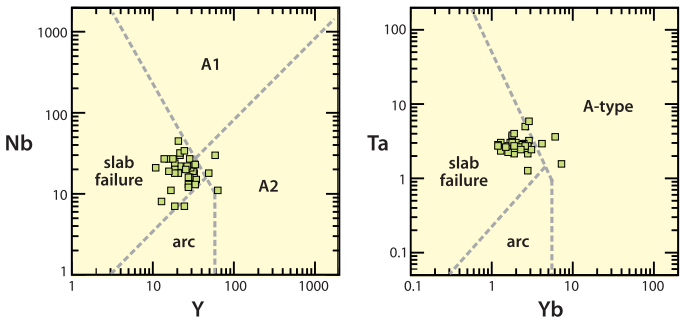

fluvial conglomeratic facies were interpreted to fill incised valleys, but in the eastern Powder River basin (Fig. 7) several hundred kilometers to the east, three unconformity-bound sandstone members are separated by marine shales (Hamlin 1996; Bhattacharya and Willis 2001). Within the basal Belle Fourche Member, Bhattacharya and Willis (2001) correlated six, meter-thick, bentonite beds through 50 outcrop sections and 550 well logs to produce a "grid of isochronous surfaces" spanning about 25 000 km^2 from which they were able to demonstrate several coarsening upward cycles grading from little to moderately bioturbated mudstone to sandstone capped by coarse-grained lag deposits sitting on disconformities. They used the overall lobate to elongate form of the sandstone bodies, radiating paleocurrent measurements, clinoforms, low to moderate shallow marine burrowing, and top-truncated beds to infer low-stand deltaic environments fed by river systems to the northwest for each of the main three bodies studied.

Hutsky et al. (2012) measured 26 outcropping sections of the Frontier Formation in the northeastern Bighorn Basin. They found tidal and wave-influenced fluvio-deltaic successions that prograded southeastward into a shallow marine environment with low accommodation space and sea-floor gradient. They also identified six bentonite beds, in addition to what they called the Clay Spur Bentonite, recently re-dated using $^{40}Ar/^{39}Ar$ sanidine to be 98.17 ± 0.11 Ma (Singer et al. 2021) at the base of the formation, in dark-gray laminated mudstone units, which they correlated through 26 measured sections. The X-Bentonite, located about 75 m above the base in their composite section, yielded an age of 95.53 ± 0.09 Ma (Ogg and Hinnov 2012).

Hannon (2020) collected several bentonites from the Frontier Formation in the Black Hills area and, in addition to dating them by U-Pb zircon methods, analyzed them for whole rock geochemistry as well as Sr and Nd isotopes (Hannon et al. 2019). Discrimination plots using relatively immobile high field strength trace elements point to a slab failure, not arc, origin (Fig. 8). Their isotopic results, $^{87/86}Si_i = 0.708$ and ENd_T ranging from −7 to −9.5. suggest interaction with subcratonic lithospheric mantle as hypothesized by Hildebrand et al. (2018) for post-collisional magmatism elsewhere. Five of his dated bentonites were collected from the Belle Fourche Member of the Frontier Formation, and dated by ICP-MS, with the Clay Spur at 97.19 ± 0.9 Ma and others at 96.87 ± 0.81 Ma, 96.8 ± 1.1 Ma, 96.5 ± 1.0 Ma, and 96.0 ± 1.3 Ma.

May et al. (2013*a*, 2013*b*) collected and studied detrital zircons from the Cenomanian–Coniacian sedimentary units in the northern Bighorn Basin and found detrital populations dominated by young peaks that approximate the age of the units, with the youngest peak ages in the Mowry Shale and Frontier Formation ranging in age mainly from 99.4 to 96.5 Ma (Fig. 9), which agree with the stratigraphic age, as there the Lower Mowry contains the ammonite *Neogastroplites cornutus*, which is considered by Reeside and Cobban (1960) to be an index fossil for the Mowry Shale. Whereas most, if not all, zircons within the Mowry Shale were derived from airfall eruptions into the basin, many of the zircons with ages <100 Ma in the Frontier clastic wedge were likely derived during uplift and exhumation of the hinterland belt as Hannon (2020) reported igneous clasts in the Frontier Formation. Painter et al. (2014) also examined detrital zircon suites from the Frontier and younger formations in Wyoming and found consistent peaks between 100 and 90 Ma in formations younger than the Dakota, whereas older formations were dominated by detrital zircon populations older than 100 Ma. Because rocks of the Frontier Formation contain abundant zircons derived from rocks <100 Ma (Fig. 9), we consider the Frontier clastic wedge to represent molasse shed during exhumation and uplift of the hinterland.

In northern Utah, major exhumation and cooling of the 125–115 Ma Willard-Paris thrust sheets (Fig. 5) also occurred at 105–95 Ma, which led to increased subsidence to the east and deposition of the 100–96 Ma Aspen and Frontier formations in the foreland basin and conglomeratic debris adjacent to the Paris thrust (Yonkee et al. 2019; Pujols et al. 2020). A thrust duplex of Paleoproterozoic crystalline rocks, known as the Farmington complex, seemingly sits on the Archean basement of the Wyoming—Grouse Creek block (Mueller et al. 2011; Yonkee et al. 2003). The band of Paleoproterozoic crystalline rocks likely continues northward into Idaho, where Paleoproterozoic crystalline basement occurs within the Cabin—Medicine Lake thrust system just east of the Idaho batholith (Skipp 1987) and the Tendoy thrust (Fig. 5) of southwestern Montana (Skipp and Hait 1977; DuBois 1982).

Farther north in the Montana sector of the thrust belt, Carrapa et al. (2019) studied exhumation and uplift using low-temperature thermochronology. Although they were focused on the geology of the younger Laramide orogeny, their zircon (U-Th)/He modeling results for several mountainous massifs in that sector showed that exhumation commenced at 100 Ma (Fig. 10) similar to areas farther south.

Mussentuchit Member and correlative units in Utah

To the south in central Utah (Fig. 11), the smectite-rich, 25–40 m thick Mussentuchit Member of the Cedar Mountain Formation appears to be bentonite-rich and temporally equivalent to the Mowry Shale, but is non-marine. There, a discontinuous, basal black-chert-pebble lag separates the Mussentu-

Fig. 9. Detrital zircon data (May et al. 2013*a*, 2013*b*) from several units within the Bighorn basin. The Graybull samples are from the older Aptian–Albian succession and have a strong similarity to samples from the Alleghanian foredeep as shown (Benyon et al. (2014). The sample from Newcastle Sandstone of the Black Hills is from Finzel (2017) and is similar to the Alleghanian and Graybull profiles, plus an ~100 Ma peak that presumably represents airfall reaching this far eastern location. Samples from the Muddy, Mowry, and Frontier are entirely dissimilar to the Greybull and Newcastle, except for the ~100 Ma airfall and hinterland detrital peaks, which suggest the difficulty of getting Appalachian Alleghanian detritus across the eastward-migrating bulge. Plotted with detritalPy (Sharman et al. 2018).

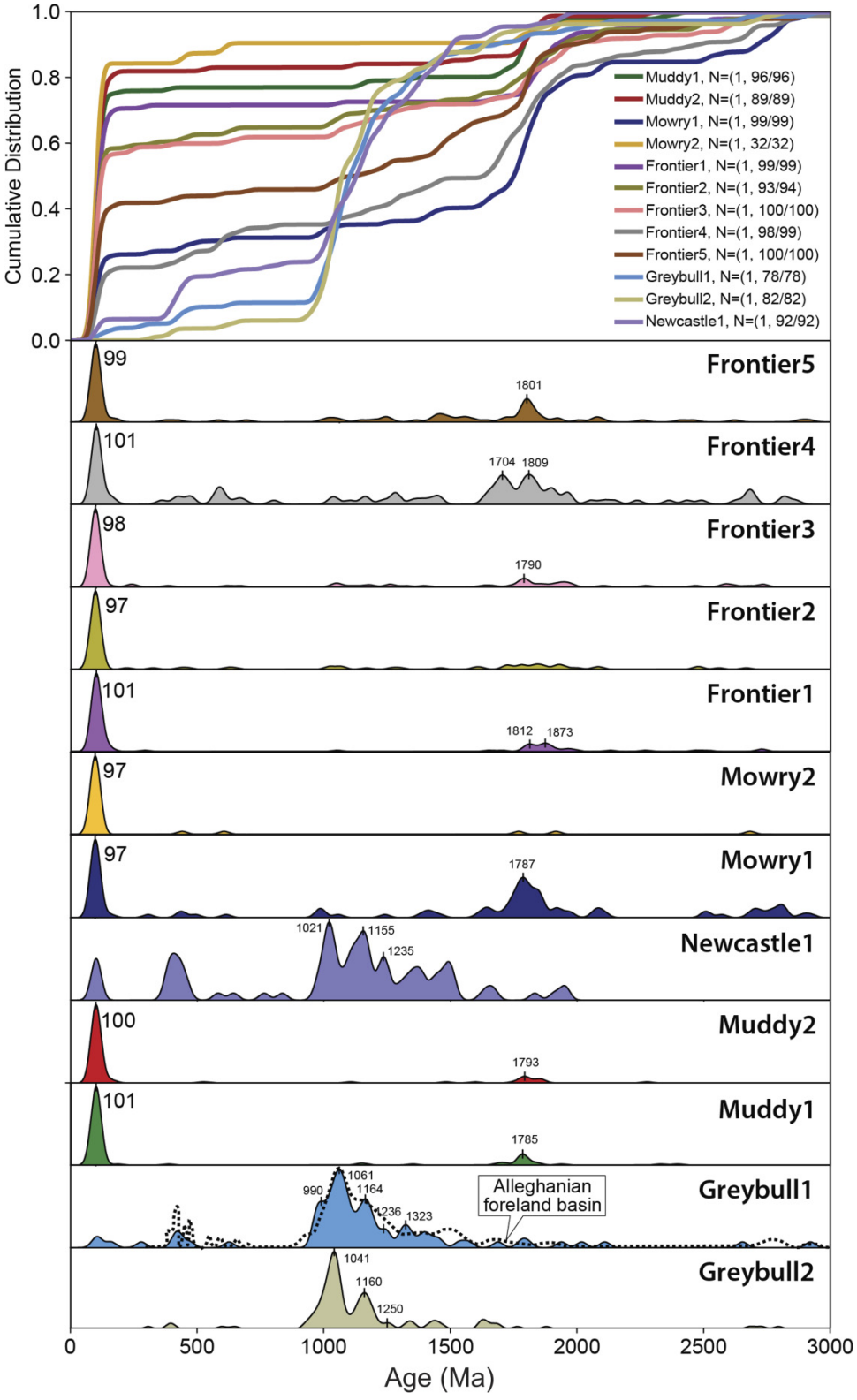

Fig. 10. Thermochronological models using zircon (U-Th)/He) from the Helena Salient area (Carrapa et al. 2019), indicating initial cooling and exhumation of several Precambrian-cored, mountain blocks starting at 100 Ma. (See Fig. 5 for locations of uplifted massifs.) Those authors suggest that the observed cooling/exhumation was tectonically driven as opposed to magmatic cooling. (See original work for modeling techniques and error propagation.)

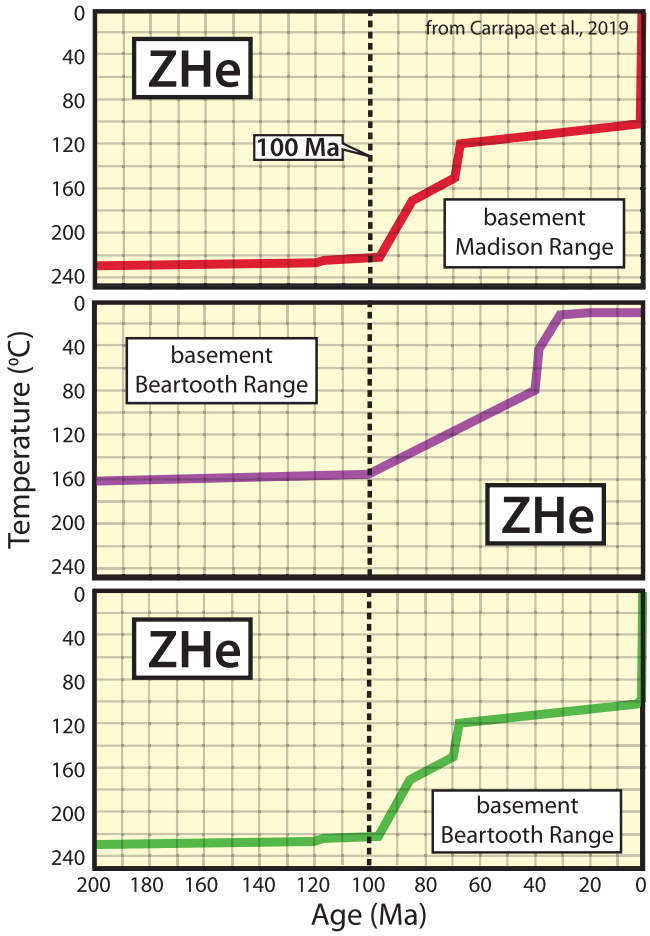

chit from the underlying Ruby Ranch Member of the Cedar Mountain Formation, interpreted to represent debris shed eastward from the ~120 Ma Sevier orogeny (Lawton et al. 2010; Hunt et al. 2011). Rocks of the Mussentuchit Member are overlain by shales of the Naturita/Dakota Formation, but to the east where the Naturita was eroded, rocks of the member are overlain by the Tununk Member of the Mancos Shale, also with a basal pebble lag (Kirkland and Madsen 2007). The Mussentuchit Member is best known along the western side of the San Rafael Swell (Figs. 5 and 11) where it overlies a distinctive cobbly conglomerate up to 5 m thick holding quartzite clasts (Doelling and Kuehne 2013). The member is dominated by gray, silty mudstone and muddy siltstone high in organic carbon from fossil plant material with local beds of lignite, all deposited on a broad coastal plain (Kirkland et al. 2016). Tucker et al. (2020) also reported variably preserved shell hash.

Several bentonites within the Mussentuchit Member on the San Rafael Swell were dated by $^{40}Ar/^{39}Ar$ to be 98.2–96.7 Ma, but generally have high analytical errors and do not match their stratigraphic order (Garrison et al. 2007). For this reason, we prefer to use the average of four bentonite ages, likely from the same bed, and with a weighted mean age of 98.39 ± 0.07 Ma (Cifelli et al. 1997) consistent with ages from the Mowry Shale (Fig. 4). Tucker et al. (2020) collected detrital zircons from volcaniclastic rocks in the member and argued that it was deposited no earlier than 96–94 Ma, an interpretation which conflicts with the $^{40}Ar/^{39}Ar$ sanidine ages from bentonite beds, and their own age from the lower Mussentuchit of 102.1 Ma, as determined by averaging seven different methods of determining the MDA.

Kirkland et al. (2016, p. 160) point out that dinosaur eggshells are common in the Mussentuchit Member and that vertebrate fauna from the member "is the oldest dinosaur fauna with representatives of each family characteristic of the remainder of the Late Cretaceous in North America" as documented by Cifelli et al. (1997). Researchers have recognized at least 22 species of mammals, albanerpetonids, salamanders, adocid turtles, the oldest North American snakes, marsupials, bird teeth, and a wealth of dinosaur teeth representing brachiosaurids and a diverse group of meat-eating dinosaurs, such as velociraptors and North America's oldest tyrannosaurids (Cifelli et al. 1997, 1999; Kirkland et al. 1997, 1999, 2016; Kirkland and Madsen 2007). Scientists also note that several dinosaurs collected from rocks of the Mussentuchit Member, such as the tyrannosaurids and pachycephalosaurs, as well as other vertebrates such as snakes, anocid turtles, and the world's most primitive marsupials, have Asian affinities and are hypothesized to have immigrated to North America over a polar land bridge (Cifelli et al. 1997; Gardner and Cifelli 1999; Kirkland et al. 2016; Avrahami et al. 2018). Their arrival may have led to extinction of native North American dinosaur clades, such as Sauropods, which went extinct at about the same time (Kirkland et al. 1997, 1999). Cifelli et al. (1997) suggested that perhaps the accretion of Wrangellia to southern Alaska might have brought the Asian family groups to North America at ~100 Ma.

Other formations of the same age within the basin also contain new fauna. The first discovery of both trace and body fossils of a burrowing and denning dinosaur, *Oryctodromeus*, occur in the Blackleaf Formation of Montana (Varricchio et al. 2007), which also hosts a similar dinosaur fauna as the Mussentuchit Member (Ullmann et al. 2012).

Mid-Cretaceous thrust-related stratigraphy of southwest Utah, Nevada, and California

To the west of the San Rafael swell, in the Sanpete and San Pitch mountains (Fig. 11), rocks of the Cedar Mountain Formation and overlying Indianola Group represent the foredeep stratigraphy in the thrust belt of the Pavant Valley, and Canyon Ranges, where coarse conglomeratic facies, known as the Canyon Range Conglomerate, overstep the Pavant thrust (Figs. 5 and 11) and lie unconformably upon the Canyon Range culmination (Spieker 1946; Sprinkel 1994; Schwans 1995; Sprinkel et al. 1999; Lawton et al. 2007).

Fig. 11. Stratigraphic units with ages in Ma for some lower to mid-Cretaceous stratigraphic successions in Utah and southern Nevada. Data from sources cited in text. MDA–maximum depositional age from detrital zircons; Fm—formation. Broad gray line is approximate location of cratonic hingeline. Thrust symbols provide approximate locations of important thrust faults mentioned in text with ages in Ma.

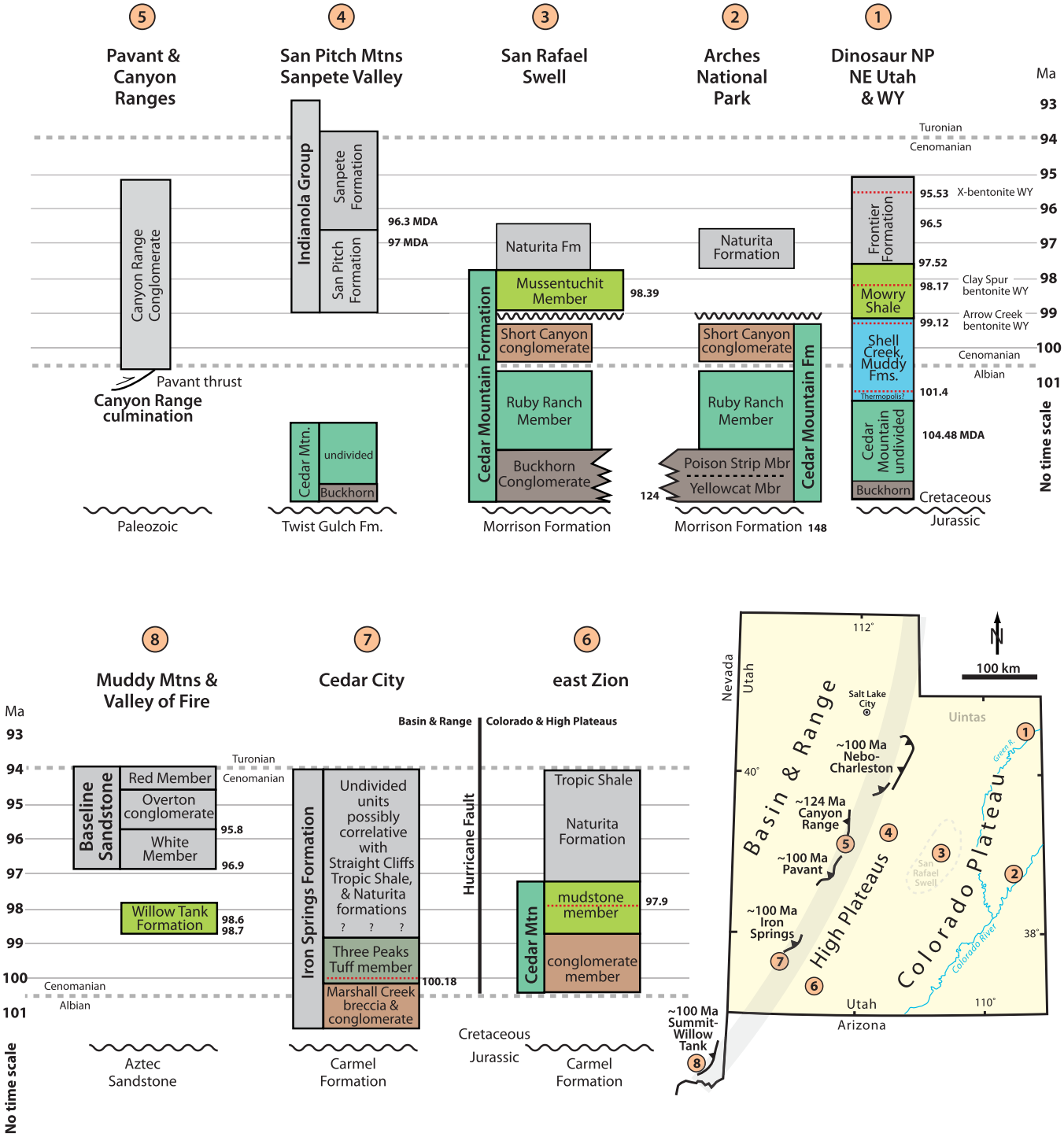

The Pavant thrust fault and Canyon Range culmination are one segment of the mid-Cretaceous thrust belt of the US Cordillera (Sevier of Armstrong 1968). It occurs in central Utah as well as western Wyoming where it is known as the Wyoming salient (Fig. 5). Thrust faults of the Pavant–Charleston–Nebo thrust system transported Neoproterozoic metasedimentary rocks, Paleoproterozoic crystalline basement of the Santaquin complex (Nelson et al. 2002), and a Phanerozoic sedimentary succession, eastward, and led to the development of a large nearly recumbent anticline. The Pavant sector of the thrust system deformed and elevated the Canyon Range thrust into an antiformal culmination during its emplacement (DeCelles and Coogan 2006). Early work by Christiansen (1952) and more recent work by Lawton et al.

(2007) demonstrated that the Canyon Range Conglomerate was deposited atop the Pavant thrust after thrusting contemporaneously with exhumation. Zircon (U/Th)/He ages from the Pavant–Nebo thrust sheets document exhumation and uplift of the thrust sheets between 102 and 96 Ma (Pujols et al. 2020). Using detrital zircon (U/Th)/He ages, they also found that the exhumation was concurrent with sediment dispersal eastward into the Cenomanian Dakota Formation, the temporally equivalent foredeep stratigraphic unit. Thus, the Pavant–Charleston–Nebo thrust system was active at about ~100 Ma and the Canyon Range Conglomerate is best interpreted as post-thrusting molasse.

Farther south in Utah, around and in Zion National Park (Fig. 11), a conglomeratic unit and an overlying smectitic mudstone unit were assigned to the Cedar Mountain Formation by Biek and Hylland (2007) and Hylland (2010). They obtained a single crystal $^{40}Ar/^{39}Ar$ sanidine age of 97.9 ± 0.5 Ma from an ash bed in the mudstone member, so correlated it with the Mussentuchit Member of the Cedar Mountain Formation of the western San Rafael Swell.

To the west, rocks related to the mid-Cretaceous thrust belt of the US Cordillera (Armstrong 1968), are known in the Cenomanian–Turonian Iron Springs Formation (Figs. 5 and 11), which consists of 800–1000 m of nonmarine conglomerate, sandstone, debris-flow breccia, mudstone, and limestone, with minor bentonite beds deposited on a fluvial N-NE sloping braidplain (Fillmore 1991). Zircons from a dacitic tuff intercalated with coarse talus breccias, conglomerates, and sandstones of the formation were recently dated by both laser ablation-inductively coupled plasma-mass spectrometry and chemical abrasion-thermal ionization mass spectrometry to be 100.18 ± 0.04 Ma (Quick et al. 2020).

In the Muddy Mountains east and northeast of Las Vegas (Fig. 11), Bohannon (1983) mapped and described rocks of the Willow Tank Formation and the White Member of Baseline Sandstone (Fig. 5), which he argued were both deposited during thrusting and overlain by the Red Member and Overton Conglomerate Member of the Baseline Sandstone. He reported that swamp and lake deposits of the Willow Tank Formation lie upon a gravel-covered unconformity on the Aztec Sandstone with up to 10 m of paleotopography on the basal contact (Reese 1989), and that the non-marine shallow-water deposits pass upwards into fluvial quartz arenite, minor conglomerate, and local talus breccias, which are tectonically overlain by the Summit-Willow Tank thrust in the southern part of the North Muddy Mountains. To the south, in the Valley of Fire, the Red Member and Overton Conglomerate interfinger and overstep the Summit-Willow Tank thrust fault. Bohannon (1983) also reported that the Muddy Mountain thrust, located west of the Summit-Willow Tank thrust, overrode at least part of the Overton Conglomerate. Carpenter (1989) documented a reverse clast stratigraphy within the Red and Overton Conglomerate members and noted that carbonate blocks up to 20 m within the Overton Member indicate deposition on alluvial fans close to the thrust front.

Bonde (2008) and Bonde et al. (2008, 2012) reported extensively on the fauna preserved within the Willow Tank Formation and noted the presence of tyrannosaurids, iguanodonts, turtles, and fossil dinosaur eggshells. Those fauna closely match fauna of the Mussentuchit Member of the Cedar Mountain Formation in central Utah, whereas fauna from the Aptian Newark Canyon Formation farther north in the Central Nevada thrust belt (Di Fiori et al. 2020) are closely allied with those of the Ruby Ranch Member of the Cedar Mountain Formation (Bonde et al. 2015), which support the concept of an Asian faunal influx into North America at about 100 Ma (Cifelli et al. (1997).

Decades ago, two K/Ar ages were determined on biotite from tuff beds in the Willow Tank Formation and yielded 98.6 and 98.4 Ma (Fleck 1970); whereas K/Ar analyses from biotite in the Baseline Sandstone produced ages of 95.8 and 93.1 Ma. More recently, Troyer et al. (2006) dated zircons from three ash beds of the Willow Tank Formation by SHRIMP RG U-Pb to be 101.6 ± 1 Ma to 99.9 ± 2 Ma; whereas Pape et al. (2011) reported that sanidine crystals collected from epiclastic units near the base and top of the Willow Tank Formation produced ages of 98.68 and 98.56 Ma, respectively.

On the western flank of Las Vegas valley, a conglomerate unit within Brownstone Basin (Fig. 5) sits structurally beneath the Red Spring thrust and contains cobbles and pebbles apparently derived from the Wheeler Pass thrust plate to the west (Axen 1987), as well as detrital zircons as young as 103–102 Ma (Wells 2016). Rocks within the Wheeler Pass thrust sheet itself, where exposed in the Spring Mountains (Fig. 5), contain evidence for exhumation during the Late Jurassic (Giallorenzo 2013), which perhaps reflects the Nevadan event; however, zircon (U–Th)/He thermochronology from the thrust sheet, where exposed in the Nopah Range to the southwest, shows that exhumation started there at ~100 Ma (Giallorenzo 2013).

In the southern Spring Mountains just southwest of Las Vegas (Page et al. 2005), non-marine sedimentary and volcaniclastic rocks of the Lavinia Wash sequence (Fig. 5), interpreted as synorogenic deposits by Carr (1980), lie structurally below the Contact thrust plate. A rhyolitic boulder in conglomerate of the Lavinia Wash sequence was dated at 98.0 Ma, and plagioclase from an ignimbrite in the sequence yielded a $^{40}Ar/^{39}Ar$ age of 99.0 ± 0.4 Ma (Fleck and Carr 1990).

In the Mescal Range to the southwest, a succession of 100.5 ± 2 Ma basaltic lavas and epiclastic rocks overlain by plagioclase porphyritic ignimbrites and lavas known as the Delfonte volcanics was detached, folded, and transported eastward on thrust faults (Fleck et al. 1994; Walker et al. 1995) prior to the emplacement of the 98–90 Ma Teutonia batholith (Fig. 5).

The thrust belt continues southward into the New York Mountains of California (Burchfiel and Davis 1977). There, highly strained metavolcanic rocks range in age from 98.4 to 97.6 Ma, whereas associated metasedimentary rocks of Sagamore Canyon (Fig. 5) have MDAs of 98 Ma (Wells 2016). The age of thrusting is constrained because the faults deform the volcanic rocks, but are cut by 90.4 ± 0.8 Ma Mid Hills monzogranite, which is one of several plutons of the 98–90 Ma Teutonia batholith (Beckerman et al. 1982; Miller et al. 2007; Haxel and Miller 2007; Wells 2016).

Sevier Foredeep in Canada

In the Canadian Cordillera, the Cretaceous of the Western Interior Basin contains Aptian to Albian clastic wedges equivalent to those in the western United States, and they are interpreted as a foredeep succession related to the Sevier orogeny, which started at 124–120 Ma (Currie 2002; Hildebrand 2013, 2014). These rocks, which sit unconformably upon Jurassic rocks, commonly have a basal conglomerate, the Cadomin Formation (Leckie and Cheel 1997; Leier and Gehrels 2011), much like the Buckhorn, Cloverly, Lakota, and Kootenai conglomerates, which unconformably overlie the Jurassic Morrison Formation and lateral equivalents of the US sector (Heller et al. 1986; Heller and Paola 1989). In Utah, the conglomerates are overlain by the dominantly non-marine Cedar Mountain and San Pitch formations (Lawton et al. 2010; Kirkland et al. 2016). In Canada, the basal conglomerates and sandstones do not extend as far east as their US counterparts, but instead were deposited by northward flowing rivers between alluvial fans on the west and escarpments to the east (Hayes et al. 1994). The clastic units grade upwards into finer-grained fluvial to marginal-marine, commonly deltaic, sandstones and shales of the Blairmore Group and farther to the east, northward flowing fluvial systems of the Mannville Group and restricted-marine Swan River Formation (Cycle 2 of Leckie and Smith 1992). The top of the succession throughout most of the basin is marked by an unconformity (Hayes et al. 1994).

Using mismatches in geology and robust paleomagnetism of Cordilleran rocks, Hildebrand (2013, 2014, 2015) argued that the western hinterland of the US Sevier belt is now located within the Canadian Cordillera, where it is known as the Omineca Belt (Monger et al. 1982). Scads of plutons (Fig. 5) ranging in age from 118–105 Ma intrude the Omineca belt (Hart et al. 2004) and are interpreted to represent post-collisional slab failure plutons emplaced into the upper-plate hinterland (Hildebrand and Whalen 2017). Middle Albian clastic rocks in the Canadian foreland contain a significant 108 Ma detrital zircon peak that Ross et al. (2005) suggested was formed from exhumation and weathering of plutons to the west. The slightly younger Hulcross Formation (Fig. 12), dominated by siltstone, shale, and sandstone, contains abundant bentonite and tonstein layers (Gibson 1992) and may represent extrusive phases of the post-collisional magmatism.

Joli Fou Seaway in Canada

Rocks of the successions in the Sevier foredeep in Canada are unconformably overlain by rocks of the Fort St. John and Colorado groups (Fig. 12), which Leckie and Smith (1992) termed Cycle 3. Overall, this succession is dominated by shale and represents a major transgression that allowed the Boreal and Tethyan oceans to flood the craton (Fig. 3) and form a continuous seaway known in Canada as the Joli Fou Sea and in the United States as the Kiowa-Skull Creek Sea (Leckie and Reinson 1993). Deposition of mudrocks in the seaway was interrupted by a period of relative drop in sea level within the basin, which led to the incision of fluvial channels and development of swamps and paleosol complexes found in the upper Boulder Creek Formation, the Paddy Member of the Peace River Formation, and farther east, the Viking, Bow Island, and Newcastle formations. These fluvial, non-marine units are in turn overlain by marine shales of the Shaftesbury and Westgate formations of the Canadian Plains and equivalents in the Foothills of Alberta, British Columbia, and the Northwest Territories (Fig. 12), which represent a second major basin-wide transgression, as once again the seaway grew to connect the Gulf of Mexico with the Boreal Sea (Leckie and Smith 1992; Leckie and Reinson 1993; Schröeder-Adams et al. 1996).

One of the major differences between the Canadian and US sectors of the trough is the much greater amount of latest Cretaceous–early Cenozoic shortening in the fold-thrust belt of Canada, which has destroyed, or at least masked, the western part of the basin there as exemplified by the isopach maps of Leckie et al. (1990, 1994) and Reinson et al. (1994). Thus, rocks of many formations, such as the Viking and Bow Island formations, generally considered temporally correlative with the Muddy and Newcastle sandstones of the US sector, are difficult to directly link with their American counterparts, despite overall similarities.

Boulder Creek–Paddy–Viking–Bow Island strata

Deposition of mud within the Joli Fou Seaway was interrupted by a relative drop of sea level, but instead of progressing from east to west as expected for a westward paleoslope, it appears to have passed from west to east similar to the relations documented in the western US where the more westerly units of the Muddy Sandstone are older than rocks of the lithologically similar Newcastle Sandstone located farther east (Fig. 4). We interpret the similarities in both US and Canadian successions to reflect the passing of a flexural bulge from west to east across the continental margin, such that the cratonic margin was uplifted, eroded, and locally incised, then pulled down below sea level again as it rode along the relatively starved outer slope towards the trench.

Although geochronology is sparse and proposed lithologic correlations require thorough testing, the Viking Formation appears to be correlative with the Muddy Formation of Wyoming. In Canada, a number of formations also appear more or less correlative, although not all workers agree (Reinson et al. 1994). According to their analysis, the Viking Formation, the Bow Island, the Paddy Member of the Peace River Formation, the Walton Creek Member of the Boulder Creek Formation, the Newcastle Sandstone of Manitoba, and the Crowsnest volcanics (Fig. 12) are all considered to be more or less broadly correlative, except that the volcanics occur above, rather than below, the sequence boundary common to the other units. More recent work, summarized by Roca et al. (2008), divided rocks of the late Albian–early Cenomanian into alloformations on the basis of regional unconformities as well as transgressive surfaces and found a southeastward spatial and temporal migration of uplift and erosion followed by subsidence and sedimentation, represented by the Walton Creek and Paddy successions in the west to the Joli Fou

Fig. 12. Stratigraphic correlation diagram for the relevant part of the Western Interior Basin in Canada. Largely from Bloch et al. (1993, 1999) and Schröder-Adams et al. (1996) with modifications from Stott (1982), Leckie et al. (1989), and Leckie and Reinson (1993).

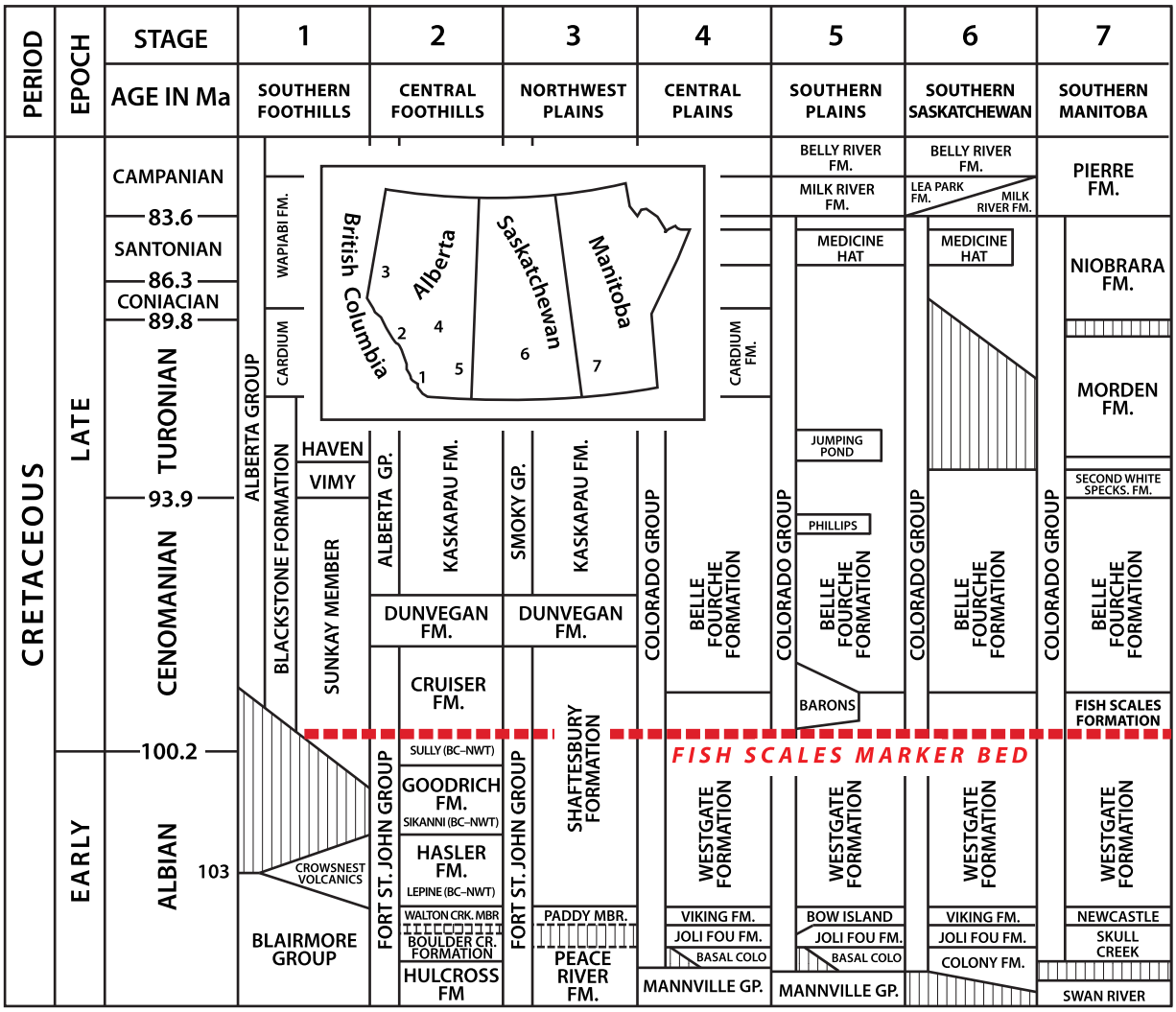

Formation and to the Viking Formation in the southeast (see their Fig. 28).

The initial drying of the trough seems to have started in the west with the upwards passage of the lower Boulder Creek rocks, which were dominated by marginal marine shoreface to foreshore sandstone and conglomerate, into strata of the mainly non-marine Walton Creek Member (Fig. 12), which contains channelized fluvial conglomerates and sandstones, coal seams, and abundant paleosols, including silica-rich forms known as ganisters (Leckie et al. 1989; Gibson 1992).

In northwestern Alberta and northeastern British Columbia, the Paddy Member of the Peace River Formation (Fig. 12) correlates with the Boulder Creek Formation and occurs in the area of the Peace River Arch, which subsided during the Albian (Leckie et al. 1990; Reinson et al. 1994; Roca et al. 2008; Plint et al. 2018). The eastward-thinning Paddy Member is lithologically variable and comprises a variety of fluvial channel, coastal plain, estuarine, and barrier island facies, that unconformably overlie and fill channels incised into the Caddie Member of the Peace River Formation and are overlain by marine mudstone of the Shaftesbury Formation, which contains the well-known Mowry equivalent Fish Scales unit (Fig. 12). Leckie et al. (1990), used data from 4500 wire logs plus 60 drill cores and local outcrops, to suggest that much of the Paddy Member consisted of debris deposited in a single broad shallow valley, tens of kilometers wide and hundreds long cut into previously deposited sediments. They also suggested that the incision of channels in the Paddy Member coincided with development of a paleosol complex in the Walton Creek Member in the Foothills at Monkman Pass (Fig. 5). To the north, the depositional edge of the Paddy Member occurs along a northeast trending line, which marks the northern limit of a sandy barrier island complex at least 350 km long and a northward facies change to interbedded marine siliciclastic rocks (Leckie et al. 1990; Plint et al. 2018). Other studies (Leckie and Singh 1991; Leckie and Reinson 1993) found that the top of the underlying Cadotte Member was incised by paleovalleys up

to 15 m deep, then onlapped and filled with rocks of the Paddy Member. A sample stratigraphic section is shown in Fig. 13 and described in detail by Leckie and Singh (1991). The section shares many similarities with those of the Muddy and Newcastle in the western United States, as well as the Bow River and Viking in Canada.

More recently, Plint et al. (2018) divided the Paddy Member into nine allomembers on the basis of flooding surfaces, and when traced to the west into alluvial facies, the surfaces seem to coincide with the base of alluvial or lacustrine mudstones that cap paleosol horizons, or with conglomerate and pebbly sandstone units that fill paleovalleys. The basal six allomembers are wedge shaped and onlap progressively eastward onto the eroded substrate, which formed a broad subaerial ridge that they suggest has characteristics of a forebulge, whereas three younger allomembers are sheetlike bodies that do not onlap, show little variation in thickness over ~300 km, blanket the ridge, and merge eastward and southeastward with deltaic rocks of the marine Pelican/Viking formations (Plint et al. 2018). A multigrain U-Pb discordia from zircons in a thin tuff layer in the Hulcross Formation, which lies beneath the Boulder Creek Formation (Fig. 12), gave an age of about 102.5 ± 2.5 Ma (Yanagi et al. 1988).

The uppermost Albian Viking Formation (Fig. 12) is a shale-encased sandstone unit that occurs in south-central Alberta and Saskatchewan and is correlated with the Bow Island Formation of southwestern Alberta, the Newcastle Sandstone in Manitoba, and parts of the Peace River Formation in northwestern Alberta (Stelck and Koke 1987; Leckie et al. 1994). The formation is 15–35 m thick over most of the Alberta plains, but it is thicker in southern Alberta where it merges with rocks of the Bow Island Formation. It overlies the shales of the Joli Fou Formation, in places gradationally, but in others, especially to the west and northwest, as well as in Saskatchewan, unconformably (Leckie et al. 1994). The formation is capped by conglomerate of a transgressive pebbly lag, which in turn, is overlain by black mudstones with thin lenses of very fine-grained sandstone of the Westgate Formation.

On the basis of more than 500 well logs and 153 cores, Boreen and Walker (1991) divided the rocks of the Viking Formation of the Alberta plains into five allomembers separated by four bounding discontinuities. Rocks of the Viking Formation sit disconformably on a pebbly lag atop Joli Fou shales, and the oldest two allomembers are composed of sheet-like, marine, upward-coarsening sequences of bioturbated mudstones and sandstones with several intercalated bentonites, all deposited beneath fairweather wave base (Drljepan 2018; Boreen and Walker 1991). A relative drop in sea level allowed non-marine rivers to cut channels 11–33 m deep in the older rocks during a lowstand in the middle of Viking deposition (Reinson et al. 1994). The channels are reminiscent of the incised valley systems cut during Muddy-Newcastle time in the western United States and, like those channels, were filled with finer grained, marginal marine sediments during the subsequent transgression. K-Ar dating of sanidine and biotite from bentonites collected from drill core in the Viking Formation east of Calgary (Tizzard and Lerbekmo 1975) yielded ages ranging from 105 to 94 Ma, but one 30 cm bed is widely traceable and interpreted to be about 100 Ma.

The stratigraphic equivalent to the Viking Formation in the southwestern Alberta Plains is known as the Bow Island Formation (Fig. 12), which Vorobieva (2000) divided into three informal members with the upper member assigned to the *Miliammina manitobensis* Zone with lesser fauna of the *Haplophragmoides gigas* Zone (Fig. 6), similar to shales above the Viking Formation (Tizzard and Lerbekmo 1975), the Paddy Member (Stelck and Leckie 1990), the Shell Creek Shale of the western United States (Eicher 1962), and more northerly locations, such as Sikanni Sandstone of northwestern British Columbia (Stelck 1975), and the Arctic Red Formation of the Peel Plateau (Thomson et al. 2011). Langenberg et al. (2000) reported the Bow Island Formation as dominantly marine, comprising immature sandstones, bentonite beds, and chert-pebble conglomerates, some amalgamated to 25 m thick, with the middle Bow Island Formation containing well-developed paleosols representing subaerial exposure as recorded in the middle of the Viking. They also reported that the rocks of the Bow Island Formation interfinger with rocks of the Bruin Creek Member of the Mill Creek Formation, which in turn are intercalated with volcanics of the Crowsnest Formation in the fold-thrust belt (Fig. 12).

Crowsnest Formation

Westward into the Foothills from the Alberta Plains, the typical upper Albian to lower Cenomanian marine and nonmarine units of the trough are generally represented in the fold-thrust belt of the southern Canadian Rockies by volcaniclastic to epiclastic strata of the Crowsnest Formation. Rocks of this formation commonly sit on, and interfinger with, a conspicuous conglomerate at the top of the Bruin Creek Member of the Mill Creek Formation (Blairmore Group; Fig. 12) and comprise up to 488 m of volcaniclastic and epiclastic sandstone consisting largely of sanidine, melanite garnet, and clinopyroxene crystal fragments, as well as conglomerate, breccia, and debris flows containing igneous clasts, some to 10 m in diameter (Peterson et al. 1997; Leckie and Burden 2001).

Rocks of the Bruin Creek Member overlie strata of the Blairmore Group in sharp, irregular basal contact with overlying westerly derived, coarse-grained, trough cross-bedded sandstone and (or) a laterally discontinuous volcanic-clast conglomerate (McDougall-Segur horizon) in beds 30 m thick and 3 km wide that Leckie and Burden (2001) considered to be lateral equivalents of the Crowsnest Formation. The volcanic clast conglomerates, locally auriferous (Leckie and Craw 1995), contain a variety of plutonic and volcanic clasts, dated by K-Ar to range from 173 to 113 Ma, with fewer chert and quartzite clasts (Norris et al. 1965). Leckie and Burden (2001) also report that the upper contact of the Crowsnest Formation is sharp with up to 37 m of relief beneath either 1–2.5 m of fine-grained sandstone or, more typically, black marine shale of the Blackstone Formation (Fig. 12).

Although Norris et al. (1965) considered many of the exposures of the Crowsnest Formation to contain primary volcanic rocks, Peterson et al. (1997) interpreted most of the

Fig. 13. Composite section illustrating relations of the Paddy Member of the Peace River Formation and its interpretation (modified from Leckie and Singh 1991). Note the emergent nature that led to the deposition and incision of the Cadotte Formation followed by the resubmergence and filling of the incised channels by estuarine and shallow marine sediments. The Walton Creek, Viking, and Bow Island formations in Canada, as well as the Muddy and Newcastle sandstones in the United States, have similar stratigraphic units and relations.

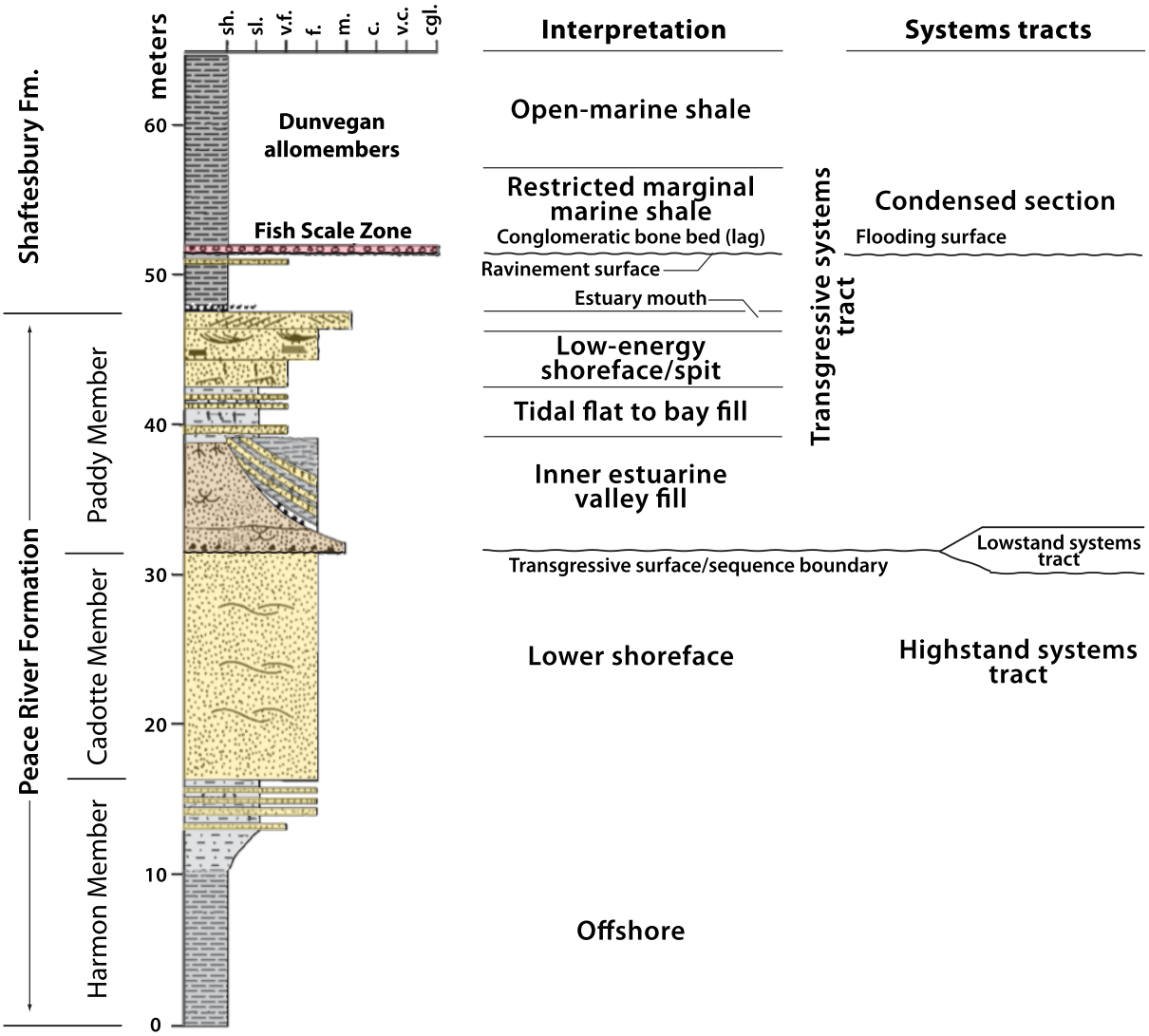

rocks to be epiclastic. They reported that some plane-bedded sandstones comprise grains of sanidine, garnet, and clinopyroxene, but that definitive evidence for a primary pyroclastic origin is lacking. A more recent study (Adair and Burwash 1996) used evidence such as plastically deformed volcanic fragments, charred wood, bedforms, and baked margins of clasts to indicate that many of the rocks in the formation were primary volcanic rocks, which originated as pyroclastic flows from collapsing eruption columns. Regardless of their origin, angular blocks and fragments include porphyritic analcime phonolites, analcite phonolite, trachyandesite, and trachyte (Peterson et al. 1997).

The age of the Crowsnest Formation has generally been considered to be close to 100 Ma on the basis of the paleontology above and below the formation, as well as a single sanidine $^{40}Ar/^{39}Ar$ age of 102 ± 0.5 Ma generated by Obradovich and reported in Leckie and Burden (2001), who found poorly preserved palynomorphs that they considered to possibly be Cenomanian. More recently, Pana et al. (2018*b*) analyzed U-Pb isotopes from melanite garnet xenocrysts in the lower Crowsnest Formation using isotope dilution–thermal ionization mass spectrometry, then averaged two analyses for a final result of 102.9 ± 1.1 Ma. They also dated titanite (U-Pb) from an alkaline sill also within the thrust belt, but located a few kilometers to the west and produced a crystallization age of 102.4 ± 0.5 Ma, within error of the age obtained from the xenocrystic melanite garnets in the Crowsnest Formation. Adair (1986, p. 141) noted that "melanite garnets identical

Fig. 14. Trace element discrimination plots (Hildebrand and Whalen 2017; Whalen and Hildebrand 2019) illustrating that rocks of the alkaline Crowsnest volcanics (Bowerman et al. 2006) plot in the slab failure fields as do 101.5–95 Ma bentonites from Wyoming (Bremer 2016), andesite clasts from the Frontier Formation of north-central Wyoming (Khandaker 1991), and for comparison, analyses from 8.5 to 0.2 Ma post-collisional magmatic rocks (55%–70% SiO_2) of Tuscany Province, Italy (from Peccerillo 2005), and late- to post-kinematic alkaline plutons of the Paleozoic Scandian orogeny in the Scottish Northern Highlands terrane (from Archibald et al. 2022).

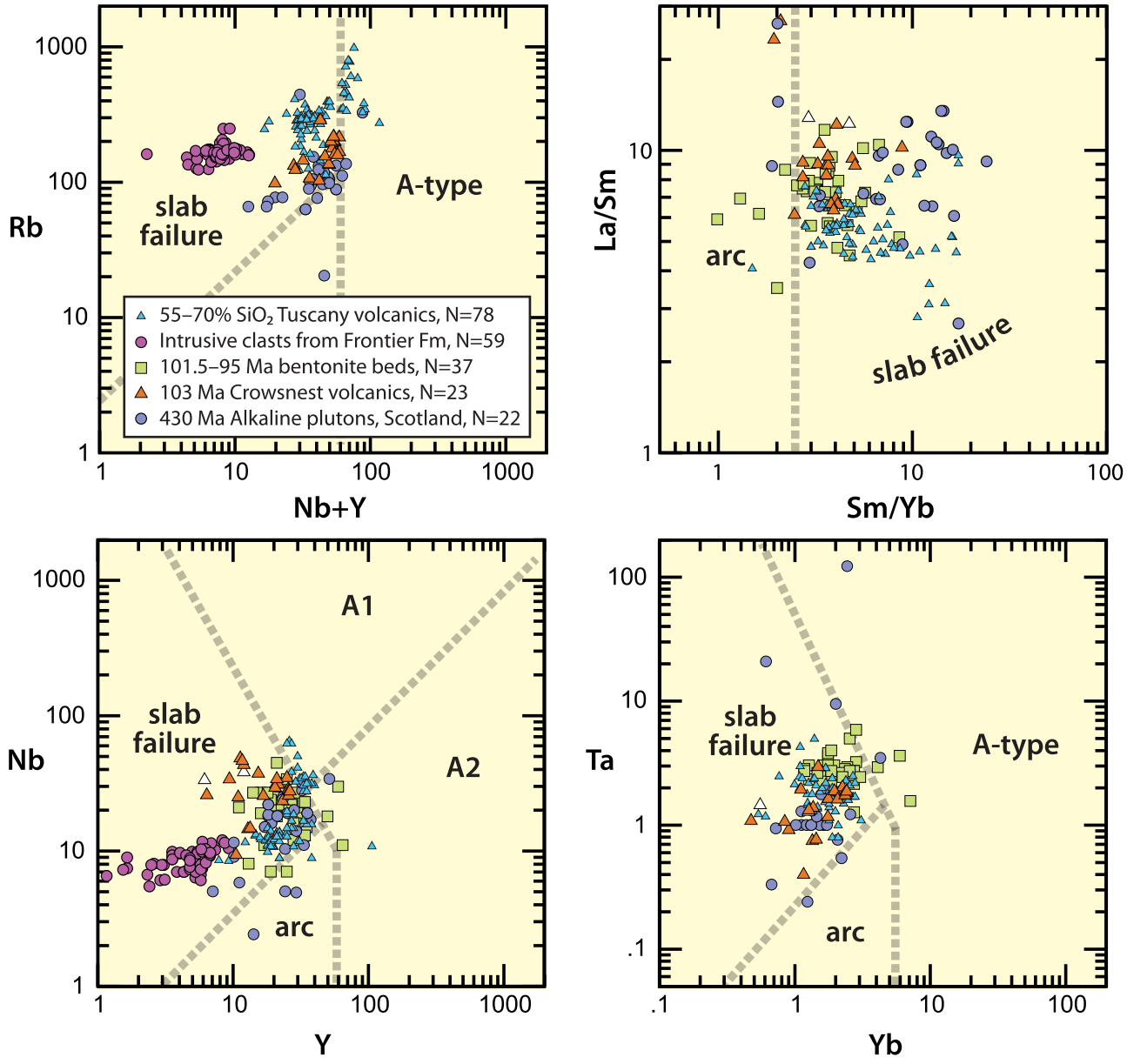

to those of the Crowsnest Formation are found consistently in the fine-grained sands and shales of the Viking Formation from the oil fields northwest of Calgary", which as discussed earlier, are interpreted to interfinger with rocks of the basal Crowsnest Formation. Ross et al. (2005) dated detrital zircons from the Bruin Creek Member and found nine zircons with ages between 107 and 102 Ma.

Geochemically, the rocks are high-K alkaline, do not contain normative nepheline or quartz, are depleted in high-field strength elements, lack Eu anomalies, are enriched in light rare earth elements and have flat heavy rare earth element profiles (Peterson et al. 1997; Bowerman et al. 2006). Initial $^{87}Sr/^{86}Sr$ values range from 0.704 to 0.706, and eNd_T ranges from −7 to −16 (Bowerman et al. 2006). We plotted geochemical data from the Crowsnest Formation on our discrimination diagrams, and most samples plot in the slab failure field (Fig. 14). The elevated initial $^{87}Sr/^{86}Sr$ and negative eNd_T values suggest interaction with subcratonic lithospheric mantle, not asthenosphere (Hildebrand et al. 2018).

Fig. 15. Sketch map showing the known localities of the endemic ammonite *Neogastroplites* spp. in the foothills belt of the Canadian Rockies and the Liard Plateau region (from Stott 1982). mp–Monkman Pass.

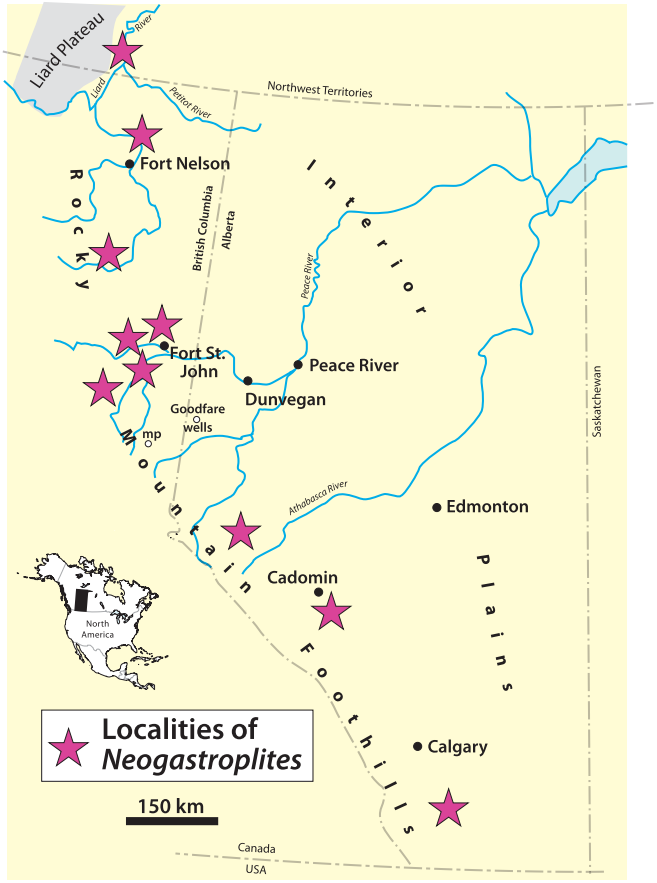

Fig. 16. Close-up view of block from Fish Scales Marker Bed exposed along Petitot River (Fig. 15) showing abundant fish scales on bedding surface. Rock hammer for scale.

Shaftesbury Formation and Fish Scales Marker Bed

The Fish Scale Marker Bed of the Shaftesbury Formation is widely recognized throughout the Western Interior Basin in Canada (Fig. 12). On the basis of lithology and the occurrence of *Neogastroplites* spp., most researchers correlate it with the Mowry Shale. The unit is typically radioactive and has the hallmarks of a condensed section (Leckie et al. 1992; Schröeder-Adams et al. 1996; Roca et al. 2008). Near Peace River, Alberta (Figs. 5 and 15), where it is well exposed in outcrop, Leckie et al. (1992) recognized three units within the Shaftesbury Formation: (1) a 13 m basal bioturbated shale unit devoid of fish remains, but with abundant foraminifera and dinoflagellates representing pelagic sedimentation in an offshore marine setting with a well-oxygenated water column; (2) a 1.5 m section of conglomerate, sandstone, siltstone, black shale, and bentonite holding abundant fish remains, sparse dinoflagellates, but no benthic foraminifera; and (3) an upper shale unit, 11 m thick, with some fish remains, minor foraminifera but only at the top, and moderate quantities of dinoflagellates.

The thin middle part of the formation represents the Fish Scale Marker Bed and according to Leckie et al. (1992), from which this section is adapted, is composite, with four distinct subdivisions. The lowermost 30 cm is in sharp contact with underlying shales and comprises finely interbedded non-burrowed shale, lenticular-graded or parallel-laminated siltstone, and very fine ripple-laminated lenses of sandstone with abundant fish scales, teeth, and probable coprolites, mostly within coarse siltstone and sandstone laminae. This unit is interpreted to represent distal storm deposits or density flows starved of sand, which apparently also carried some of the fish bones into the area. The fine laminations indicate no bioturbation and anoxic bottom conditions. This unit is overlain by 8 cm of phosphatic, fish-hash conglomerate containing fragments of scales and teeth to 1 cm (Fig. 16), scarce vertebrae of marine reptiles to 5 cm, and a conspicuous scarcity of extra-formational clasts. Leckie et al. (1992) interpret this unit as a lag deposit separating shallow water sediments below from deeper water deposits above (see Fig. 13).

Overlying the fish-hash conglomerate is just over 1 m of black shale holding abundant fish remains and a 20 cm bentonite bed. Tiny wisps of coarse siltstone and fine sandstone are interbedded with the shale, and the unit is not bioturbated. Fish debris, including scales, teeth, and their aggregates, likely coprolites, are concentrated in the silty and sandy laminae. The upper unit comprises 11 m of blocky weathering shale with only faint laminations and no bioturbation. Progressively decreasing amounts of fish debris upwards through the section suggested to Leckie et al. (1992) that the upper shale might represent an increase in a rate of sedimentation and so represent a progradational event, which was confirmed by overlying clinoforms that downlap onto the Fish Scale Marker Bed as shown in regional wireline cross sections (Bhattacharya 1994; Plint 2000; Plint et al. 2009).

In the Foothills of Alberta, the Hasler, Goodrich, and Cruiser formations are the equivalents of the Shaftesbury

Fig. 17. Outcrop in bank along Petitot River (Fig. 15) showing Fish Scales marker unit in the Sully Formation. The Fish Scales unit marks the transition from east-derived sediment below to west-derived sediment above. The Sully Formation is a stratigraphic equivalent of the Shaftesbury Formation in northwestern British Columbia and southwestern Northwest Territories (Stott 1982).

Formation (Fig. 12), whereas in the subsurface of the plains the muddy to silty Westgate Formation is correlative with the lower Shaftesbury (Bloch et al. 1993, 1999). In northeastern British Columbia and the southwesternmost corner of the Northwest Territories, the Lepine, Sikanni, and Sully formations are the correlative units (Fig. 17). Stott (1982), in his extensive overview of the stratigraphy of the Fort St. John Group in the Foothills of British Columbia and the northwestern Plains, compiled and reported many occurrences of *Neogastroplites* in the Shaftesbury Formation and all its equivalents in British Columbia and the Northwest Territories (Fig. 15). The ammonites undoubtably occurred in the basin to the east, but as the data come dominantly from drill holes there, they are not recognized. All of these correlative formations lie at least in part within the *Miliammina manitobensis* foraminiferal zone (Fig. 6).

The Fish Scales marker occurs in the central Foothills within the Cruiser Formation (Fig. 9), comprising ~300 m of thinly bedded and non-bioturbated marine shale, siltstone, and bentonite with sandy beds containing abundant fish scales near its base (Stelck 1962). He recorded the ammonites, *Neogastroplites americanus* and *Neogastroplites mclearni,* from the fish scale units and noted the correlation with the Mowry Shale. A second Fish Scale horizon occurs about 68 m higher in the section and thin bentonite beds about 15–20 cm thick increase in number throughout the upper portion of the formation (Stelck 1962).

In northeastern British Columbia and in the Liard River area of the Northwest Territories, Stott (1982) documented the occurrence of the Fish Scales unit in the Sully Formation (Fig. 12), which is a dark gray to black marine shale, 100–200 m thick, that is from west to east, sits on successively older sandstones of the Sikanni Formation, which contains *N. cornutus* and *N. muelleri*. Deposition on progressively older units to the east suggests that the older rocks dipped westward. The Fish Scale unit contains a silty argillaceous mudstone with abundant fish scales and bone fragments, along with associated bentonite beds, overlain by a gradational succession of sandstone and shale, where the contact is placed at the lower downlap surface of the overlying Dunvegan Formation (Fig. 17).

Dunvegan Formation

Lying stratigraphically above the Shaftesbury, Sully, and equivalent formations are rocks of the Dunvegan Formation (Fig. 12). Bhattacharya (1989) collected data from about 500 well logs and 130 cores to create isopach maps and detailed facies interpretations of the rocks, which form a southeastward prograding clastic wedge atop the Fish Scales Marker Bed (Bhattacharya and Walker 1991*a*, 1991*b*; Plint 2000; Plint et al. 2009).

The Shaftesbury shale unit above the Fish Scales Marker Bed is considered by Battacharya (1994) to be the basal unit of the southeasterly prograding Dunvegan clastic wedge because the bioturbated and rippled silty mudstones, generally lacking in fish parts, indicate deposition in brackish, prodeltaic, shallow-water conditions caused by southeastward progradation of the deltaic depositional system. Bhattacharya and Walker (1991*a*) subdivided the Dunvegan (Fig. 18) into seven allomembers separated from one another by transgressive, marine flooding surfaces that represent progradational cycles beginning with basal marine mudstones passing upwards through interbedded mudstones, siltstones, and sandstones into shallow, marine shoreline sandstones topped by non-marine facies such as coals and paleosols. The non-marine units thicken to the northwest. The southern continuation of the Dunvegan is the Blackstone Formation (Fig. 12), but most of the unit is truncated or obscured at the thrust belt to the west, so only the eastern muddy facies are preserved within the basin as documented by Plint (2000) and Plint et al. (2009), who, using more than 2300 well logs and >60 outcrop sections, traced the Fish Scales Member over 950 km southeast to the Blackstone Formation. They

Fig. 18. Regional cross section of Dunvegan Alloformation illustrating its wedge-shaped form and that its various allomembers (labeled G to C) downlap onto the planar surface of the Fish Scales unit (modified from Bhattacharya 1994). Correlation lines are interpreted to be chronostratigraphically significant surfaces. Location of section A to B is shown in the inset. Note that in the north facies trend more or less northerly, but to the south they are truncated by much younger Upper Cretaceous–Paleocene deformation in the Laramide fold-thrust belt (Fig. 5).

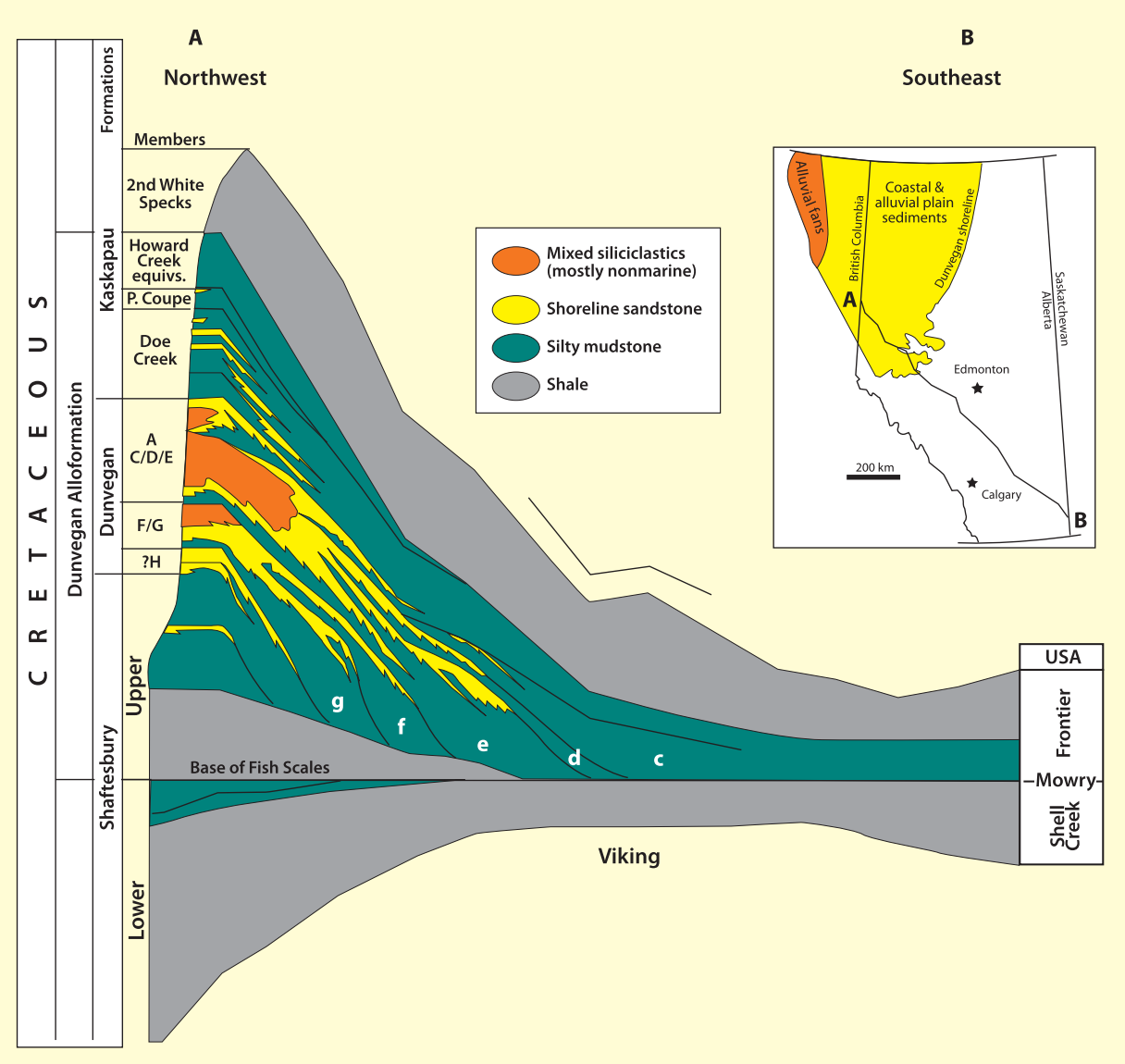

also documented that individual clinoforms of the prodelta mud-wedge in the Dunvegan Formation range from 80 km in the lower few allomembers; but progressively in the upper section they found progradational distances to be ~150, ~220, and ~250 km, with the upper allomembers, extending as 10–20 m thick tabular sheets for 400 km for allomember C and 800 km for allomember A at the Montana border (Fig. 19). Hay and Plint (2020) showed that the upper two allomembers of the formation preserved evidence of progressive drowning and had smaller and more linear delta-front sandstone bodies upsection, which suggested to them that more open-marine conditions were established over that interval.

Far to the east in Manitoba, rocks of the Belle Fourche Member of the Ashville Formation (also called Belle Fourche Formation), considered correlative with rocks atop the Fish Scale unit to the west (Fig. 12), are dominantly dark shales lacking in benthic foraminifera (Schröeder-Adams et al. 2001). They report that basal beds are not bioturbated and contain a 1-cm-thick bed of fish teeth, scales, and other debris, that coarsens upwards into bioturbated sandstones, shell beds, and additional bonebeds, some with vertebrate fossils. Apparently, the water column of the basin was stratified, with anoxia reaching into the photic zone as far east as its exposed margin in southern Canada, and remained starved for some time after deposition of the Fish Scales

Fig. 19. Diagram illustrating the geometry and shape of allomembers of the Dunvegan Formation (Plint et al. 2009) on a line from Fort St. John in the northwest to the US–Canada border in the SE. The top of the condensed Fish Scales unit is a downlap surface and represents a southeastward surface upon which successive younger clinoforms were deposited farther to the southeast. Plint et al. (2009) point out that the Fish Scales unit is a basin-wide deposit and marks the shutdown of deposition in the basin. Vertical exaggeration is about 1600.

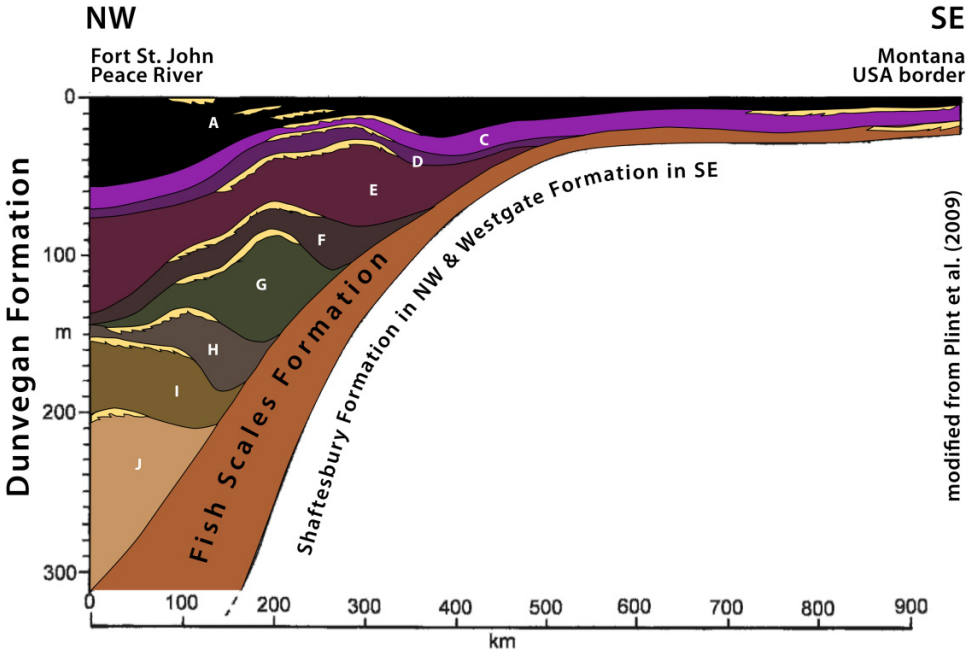

horizon, while clastic wedges prograded eastward across the basin.

Although bentonite beds are directly associated with the Fish Scales horizon and have been collected for dating, they remain unpublished; however, Plint (personal communication, 2021) reported the radiometric age as consistent with ages determined by Singer et al. (2021) for the Mowry Formation. A bentonite bed located to the south within dark marine mudstone of the Sunkay Member of the Blackstone Formation (Figs. 4 and 12), which was traced northward 350 km to the upper allomembers of the Dunvegan Formation (Tyagi et al. 2007), was dated by U-Pb on zircon to be 95.87 ± 0.10 Ma (Barker et al. 2011).

Buechmann (2013) studied detrital zircons in units above and below the Fish Scales Marker Bed (Fig. 20) and discovered a shift in provenance from dominantly Precambrian zircons (93%) below the bed in the Viking Formation to Paleozoic and Cretaceous in the Dunvegan Formation above the Fish Scale Marker. He interpreted the bulk of debris within the Viking Formation to have been derived from sources in the Canadian Shield with lesser quantities of Paleozoic rocks, perhaps largely cannibalized from incised paleovalleys cut into older rocks by pre-Viking erosion. Detrital zircons from the Dunvegan Formation (Fig. 20) are dominated by Mesozoic grains (69%) with prominent age peaks at 100, 101, and 102 Ma, which we infer to represent detritus shed from the rising hinterland to the west.

Peel Plateau—Great Bear Plain

Northeast and north of the Mackenzie Mountains, along the Hume River (Fig. 5) a sedimentary succession, about 2 km thick, sits unconformably upon a basement of Devonian sedimentary rocks and comprises a basal 20 m thick Albian transgressive sandstone, the Martin House Formation (Fig. 21), overlain by as many as 1000 m of Albian bioturbated, marine mudstones of the Arctic Red Formation, which contains a bentonite dated by U-Pb zircon as 107.0 ± 1.9 Ma (Thomson et al. 2011). Because strata of the Martin House Formation lie directly on Paleozoic basement, instead of Lower Cretaceous sedimentary rocks, field relationships are more straightforward than farther south.

Hadlari et al. (2014) indicate that the sandstones of the basal transgressive Martin House Formation are marginal marine and fine upwards, as well as westward, into offshore mudstones of the Arctic Red Formation, which reflect a westward-deepening basin. The Albian succession is capped by a pisolitic ironstone facies, holding rare wood fragments, unconformably overlain by mudstone and bentonite beds of the Cenomanian Slater River Formation, which is up to 500 m thick with a base composed of black carbonaceous shale and rare coal seams overlain by a 10 cm condensed section of nonbioturbated and radioactive mudstone with fish teeth, bones, and other organic material, but no foraminifera (Thomson et al. 2011). Gray mudstones with few foraminifera dominate the remainder of the Slater River Formation, but minor rippled sandstone beds occur towards the top, and the entire succession grades upwards through a transgressive peb-

Fig. 20. Detrital zircons of five samples from the Viking and Dunvegan formations collected and analyzed by Buechmann (2013) replotted as cumulative distribution and KDE (kernel density estimator) plots. The Viking is interpreted to be derived from the Canadian shield with lesser quantities of recycled zircons from the fold-thrust belt, whereas the zircons in the Dunvegan Formation were almost exclusively derived from the collisional hinterland to the west as reflected by the 100 Ma peaks. Curve labeled Great Bear Lake on plot of Viking 2 is from Hadlari et al. (2012) and illustrates zircons in Cambrian strata derived from the Wopmay orogen just south of Great Bear Lake. Plotted with detritalPy (Sharman et al. 2018).

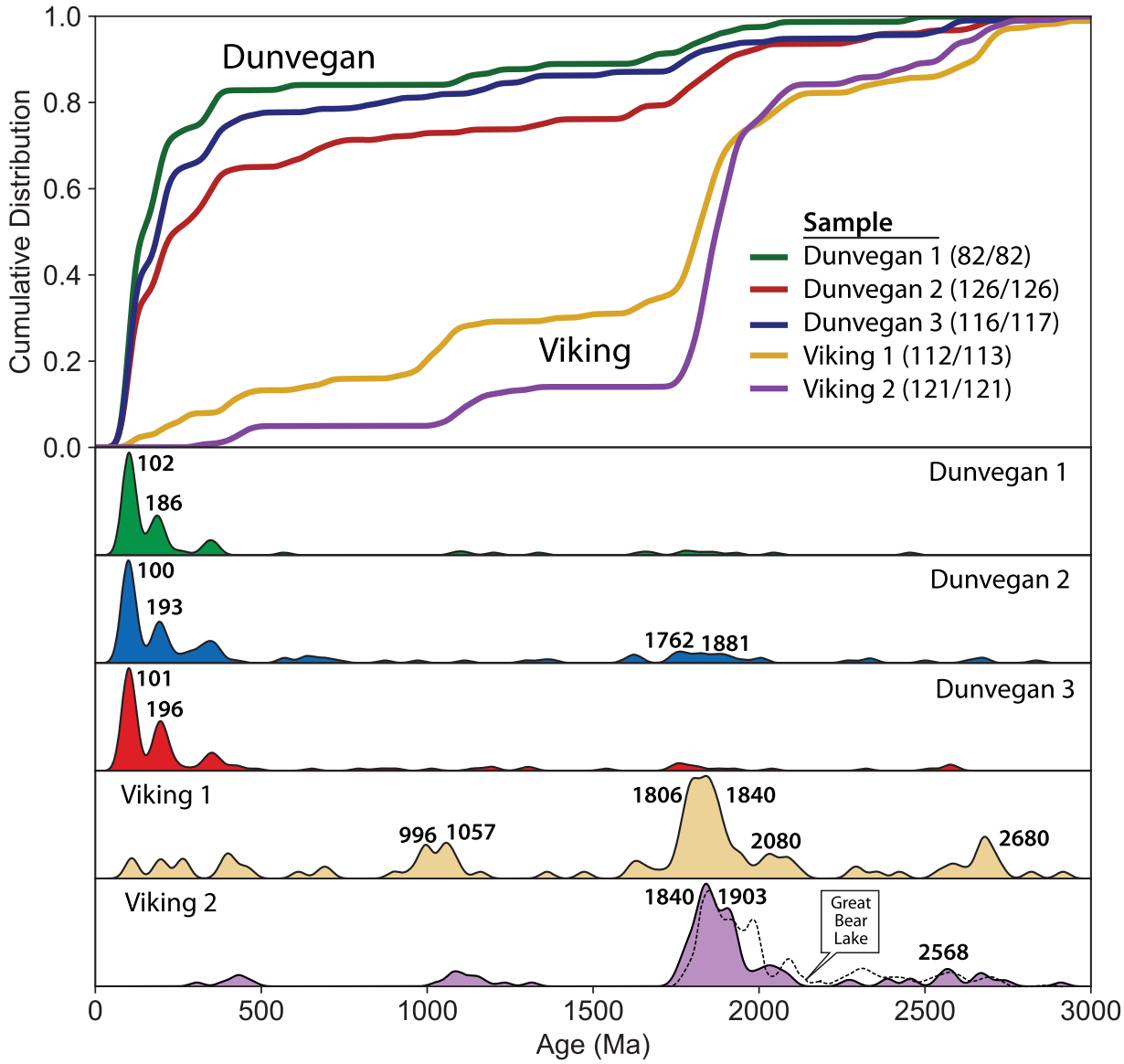

bly lag into 700 m of siliciclastic parasequences representing an easterly prograding clastic wedge of the Trevor Formation (Hadlari et al. 2014).

Ages of detrital zircons (Fig. 21) collected from the basal Martin House Formation are consistent with an easterly source in the Orosirian Wopmay orogen, whereas zircons from the Trevor Formation have a broader age range, similar to the Neoproterozoic to Mississippian rocks known in the Mackenzie Mountains, but also with a prominent, near-syndepositional peak at 93 Ma, similar in age to post-deformational plutons of the Selwyn Basin (Mair et al. 2006; Hadlari et al. 2014; Rasmussen 2013; Hildebrand and Whalen 2017).

Hadlari et al. (2014) interpreted the entire succession to have been deposited in an easterly migrating foredeep with the westerly prograding Albian sequence deposited on the eastern slope of the basin with sediment derived from the Shield to the east, whereas the Cenomanian section prograded towards the east and contains debris from the Mackenzie Mountains thrust belt and post-collisional plutons of Selwyn Basin (Fig. 22). In a general sense, we agree with this interpretation, except that we consider that the Albian section formed part of a Lower Cretaceous passive margin on the east side of the basin rather than in the younger foredeep trough. We note that the pisolitic ironstone beds at the top of the Albian succession are readily interpreted as soil horizons

Fig. 21. Stratigraphic section at Hume River (HR on Fig. 5) for mid-Cretaceous sedimentary rocks of the Peel Plateau, located just north of the Mackenzie Mountains showing the age probability curves of detrital zircons from pre-and post-Fish Scales units (modified from Hadlari et al. 2014). We interpret the Martin House and Arctic Red Formations as part of the west-facing passive margin of the 140–100 Ma seaway and were derived from the east. As the margin was pulled down into the west-dipping subduction zone, rocks of the margin were subaerially exposed on the peripheral bulge where a ferruginous paleosol complex developed. After passing over the bulge the region was resubmerged on the outer slope to the trench where the starved and anoxic Fish Scales unit of the Slater River Formation was deposited. Rocks of the overlying Trevor Formation were derived from the west and contain young detritus from post-collisional plutons in the hinterland.

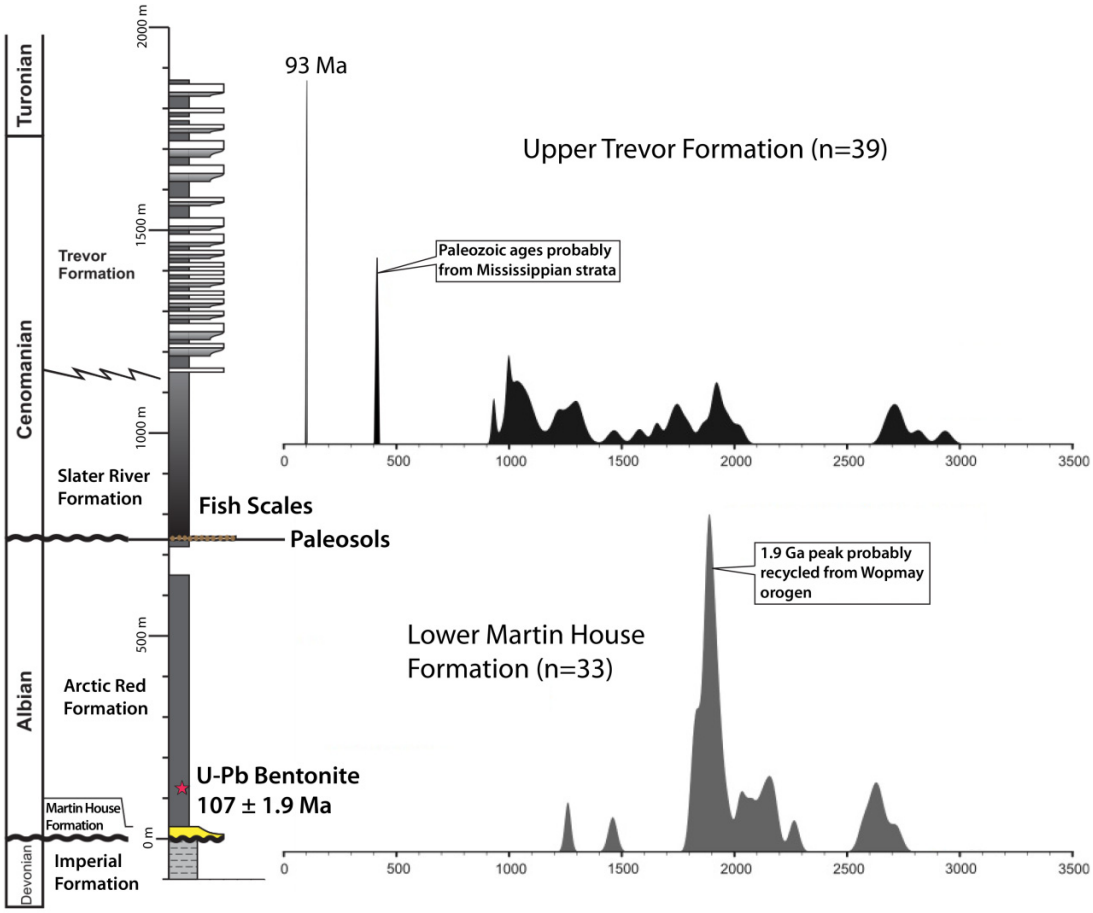

(Thomson et al. 2011) and that the unconformably overlying strata are recognized throughout the Western Interior Basin, where, as we have seen, they are known as the "fish debris marker" (Thomson et al. 2011), or Fish Scales Formation.

Whereas in a foredeep scenario, the easterly progradation of thrusts should result in a progressively deepening flexural basin to the east, the opposite occurred as the margin was uplifted, exposed, and eroded, before being buried by a condensed, anoxic interval. In our conception, the Albian succession was exposed when the passive margin rode over the outer swell (Jacobi 1981). The exposure generated the pisolitic soil horizons, which were investigated and described in detail by Thomson et al. (2011). Afterwards, the region subsided to form a restricted marginal marine to marshy environment that progressively deepened and is represented by the thin radioactive condensed horizon containing fish hash but no foraminifera, which Thomson et al. (2011, p. 281) interpreted to represent "an offshore marine environment … where sediment input to the system is minimal". The lack of sediment influx and inhospitable conditions for benthic life suggest to us that the area lay on the outer trench-slope, where sediment-starved conditions are typical. The overlying westerly derived siliciclastic rocks of the Trevor Formation represent orogenic debris shed from the hinterland.

Strata in Mexico, Arizona and New Mexico

A more complete geological record is preserved in northern Mexico and the southwestern United States (Fig. 23), where a pene-contemporaneous basin known as the Bisbee–Arperos seaway, or trough (see Martini et al. 2014) is well-exposed, relatively undeformed, and unconformably overlies pre-Nevadan Jurassic and Tithonian sedimentary and volcanic rocks of the Peñasquitos and Cucurpe formations, both deformed between about 145 and 139 Ma (Mauel et al. 2011; Kimbrough et al. 2014; Hildebrand and Whalen 2014, 2021*a*).

Fig. 22. Sketch map of part of the Selwyn Basin showing stratigraphic units, thrust faults, and 99–93 Ma plutons that postdate the thrust faults. Location of area shown on Fig. 5. From Murphy (1997).

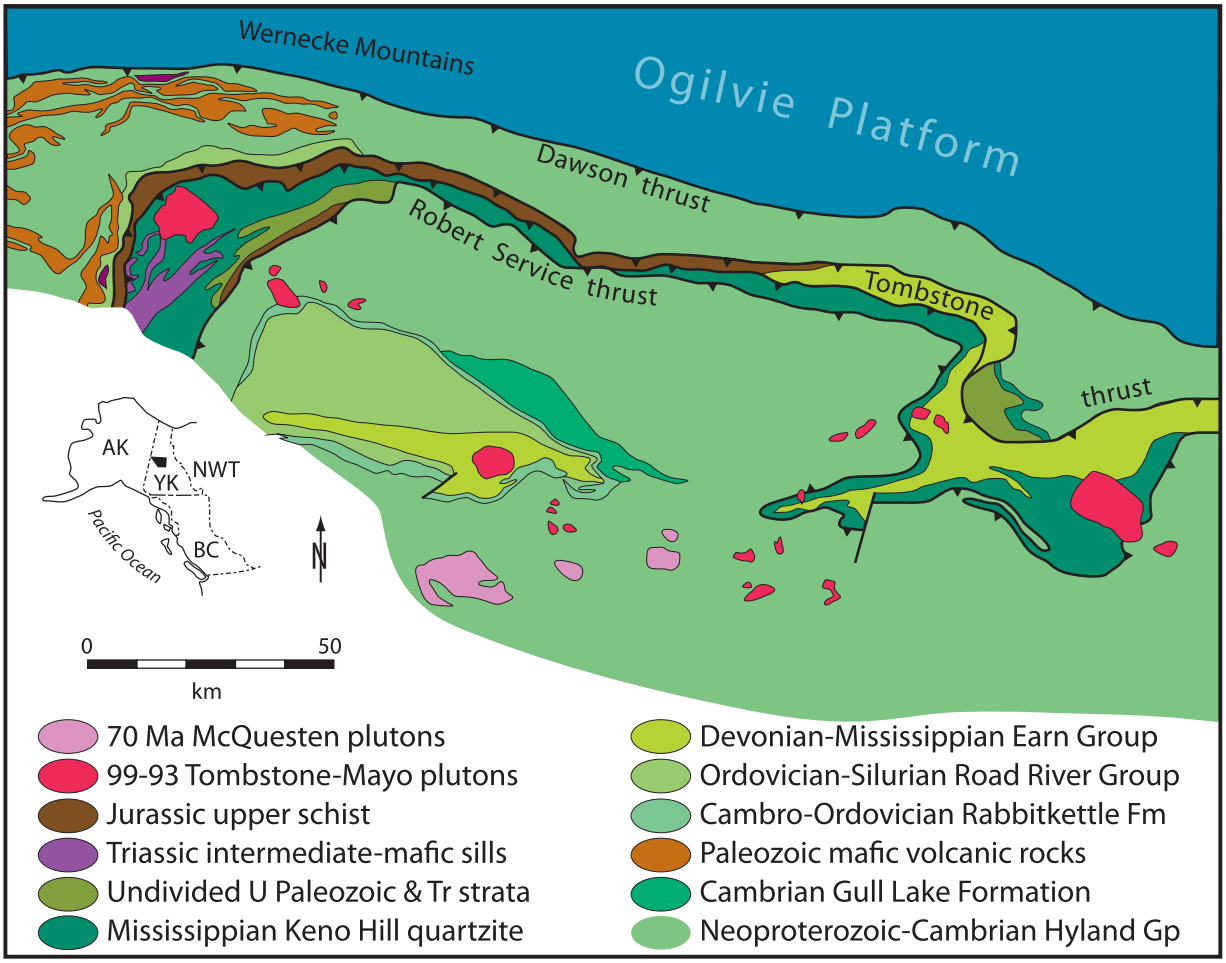

These units constrain the age of the pre-collisional seaway to be younger than about 140 Ma.

The eastern side of the trough is characterized by a west-facing Lower Cretaceous continental margin capped by a widespread carbonate platform/ramp, known as the Guerrero–Morelos platform in central-southern Mexico or Mural Formation of the Sonoran platform in Arizona and Sonora (Lawton et al. 2020*a*). During the late Albian, upward growth of the west-facing carbonate platform stopped, as marked by a disconformity atop massive bioclastic carbonate overlain by a few meters of well-laminated beds of detrital carbonate, breccia, condensed horizons rich in Late Albian faunal debris (Fig. 24), and capped by a thin interval of hemipelagic shale, itself passing up section into the extensive Cenomanian Mexcala flysch (Monod et al. 2000; Lawton et al. 2020*b*). U-Pb analyses of detrital zircons from the Mexcala flysch in central Mexico, just east of the suture (Lawton et al. 2015), yielded large age peaks at 97 and 95 Ma (Fig. 25).

To the north in the Bisbee Basin, the dominantly Albian Mural Limestone of the west-facing carbonate (Sonoran) platform/ramp (Fig. 23) was buried by at least 1500 m of westerly derived Cenomanian and Turonian fluvial and shallow marine siliciclastic rocks termed the Cintura Formation in Sonora and southeastern Arizona and in southwestern New Mexico, the Mojado Formation (Warzeski 1987; Jacques-Ayala 1995; González-León et al. 2008). Both are interpreted to have been deposited in a flexural foredeep by fluvial systems (Mack 1987; González-Léon and Jacques-Ayala 1988; Lawton et al. 2020*b*). The southwesternmost exposures of the Cintura Formation are in excess of 2000 m thick and are overlain gradationally by latest Albian–early Cenomanian fluvio-deltaic sandstone with sparse pebbles of quartzite and limestone and overthrust from the southwest by plutonic rocks (Jacques-Ayala 1992; Lawton et al. 2020*b*). In Sonora, the Cintura Formation is overlain by conglomerate and intercalated andesite of the Cocóspera Formation, the latter of which yielded a $^{40}Ar/^{39}Ar$ age of 93.3 ± 0.7 Ma (González-León et al. 2011). Lawton et al. (2020*b*) demonstrated the coeval nature of the west-facing, passive margin sequence of North America with the Alisitos arc of the Guerrero Superterrane to the west, established the temporal correlation between the Mojado and Cintura formations by U-Pb studies of detrital zircons and ash beds, inferred steep subsidence curves in the Sonora sector of the basin at ~100 Ma, and confirmed the consanguineous

Fig. 23. Sketch map illustrating key geological units of the Peninsular Ranges orogeny and Aptian–Albian volcano-sedimentary rocks of the Alisitos—Santiago Peak arc, various subterranes of the Guerrero superterrane, and Albian carbonate platforms, mostly located west of the younger Laramide suture and its related fold-and-thrust belt. The Peninsular Ranges batholith continues the length of Baja California, as indicated by a conspicuous aeromagnetic anomaly (Langenheim et al. 2014), but the batholith is buried by younger volcanic rocks south of the state line. Red dots represent drilled and dated core from La Posta plutons (Duque-Trujillo et al. 2015). Rocks of similar age and lithology to those of the Peninsular Ranges batholith crop out in Zihuatanejo (Centeno-García et al. 2011). Westward-facing Albian carbonate banks of the Sonora and Guerrero–Morelos platforms were pulled westward beneath rocks of the Guerrero superterrane at 100 Ma during closure of the Bisbee–Arperos seaway. We follow Hildebrand and Whalen (2014) and include the Cortes and Caborca terranes in Guerrero superterrane as they were thrust over the Sonoran shelf at ~100 Ma (Pubellier et al. 1995). Co–Concordia; MP–Mineral de Pozos; RG–Rio Grande; TT–Teloloapan thrust.

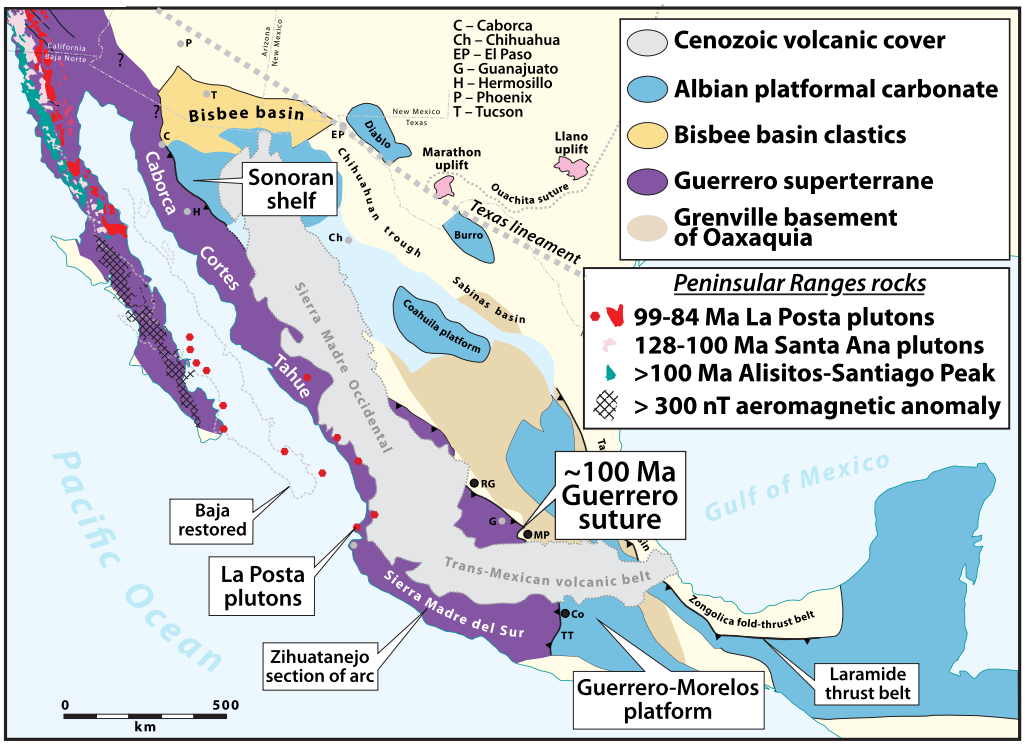

nature of the fluvial to marine foredeep system as far to the east as El Paso, Texas, and northeast to the Dakota Formation of the southeastern Colorado Plateau and Western Interior Basin (Fig. 26).

The lack of an Albian foredeep succession and related fold-thrust belt in southern Arizona and Mexico suggest that the Sevier collision, and thus, the Sevier colliding block, did not impact North America at this latitude. Likewise, the lack of similar features, discussed previously, on the Peel Plateau in northern Canada, constrain the northern extent of the incoming Sevier block and hence its overall length to about 2000 km.

The Peninsular Ranges orogeny

Hildebrand and Whalen (2021*a*, 2021*b*) expanded their earlier tectono-magmatic synthesis of the southwestern United States and Mexico (Hildebrand and Whalen 2014) to include the mid-Cretaceous geology of the Cordillera from southern Mexico to Alaska, which they interpreted to represent the closing of an oceanic trough, or basin, by westerly subduction at about 100 Ma, an event they termed the Peninsular Ranges orogeny. What follows is only a brief synopsis as the development of the orogen along the length of North America was described and discussed in the two most recent papers cited above.

The basin, or trough, was an ocean that formed after the Late Jurassic—Early Cretaceous Nevadan orogeny and associated post-collisional magmatism, when a long, linear sliver rifted from the western margin of the tectonic collage of previously accreted terranes then attached to the westernmost margin of North America. As originally suggested for the general case by Wilson (1968), the basin opened more or less along the Jurassic suture such that fragments of the collision ended up on both sides of the ocean basin (the subsequently named Wilson cycle). The trough was open for ~40 million years and during the Early Cretaceous a west-facing, passive-margin, sedimentary prism was deposited on its eastern margin (cratonic North America) whereas a well-developed, dominantly marine arc developed on the western fragment, or ribbon

Fig. 24. Detailed cross section of the uppermost few meters of the west-facing Guerrero–Morelos carbonate platform showing the rapid transition from carbonate shelf to orogenic deposits near Concordia, Estado de Guerrero. Hoffman (2012) presents an excellent overview of the process of platform foundering at the beginning of orogenesis. The figure is modified from Monod et al. (2000). (For location of Concordia, see Fig. 23.)

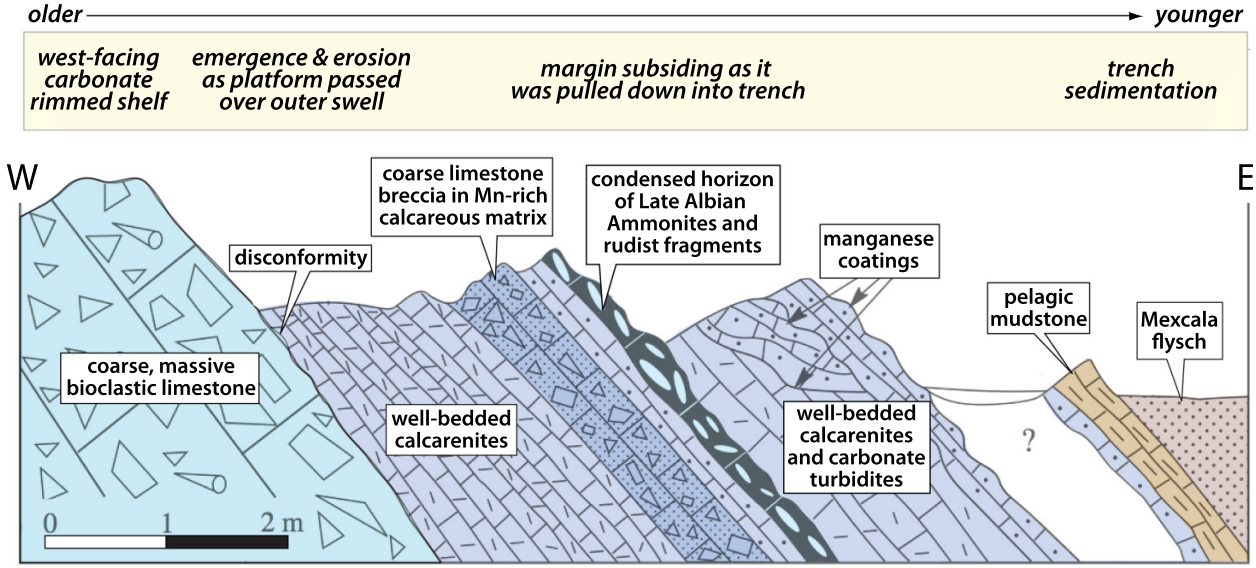

Fig. 25. Detrital zircon populations from four turbidite samples collected in central Mexico east of the suture between the Guerrero Superterrane and North America illustrating the dominant post-100 Ma peaks (from Lawton et al. 2015). (See Fig. 23 for locations: MP–Mineral de Pozos and RG–Rio Grande.) Plotted with detritalPy; Sharman et al. (2018).

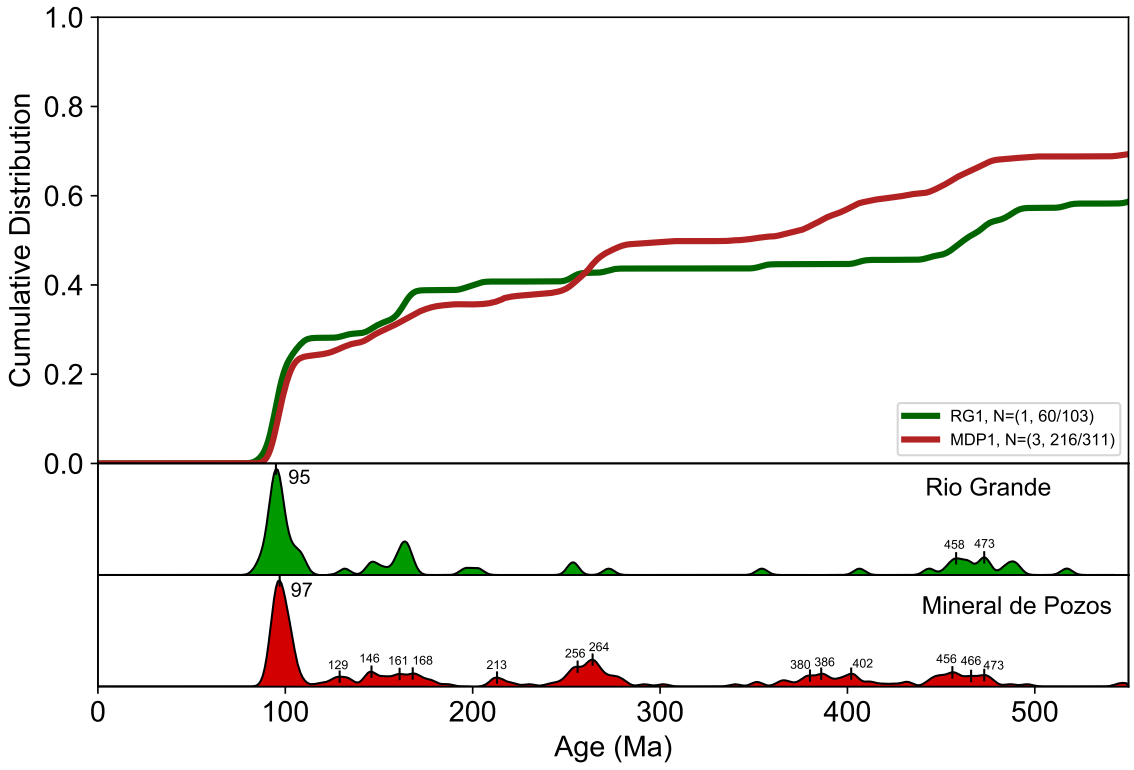

(Coney et al. 1980; Campa and Coney 1983; Tardy et al. 1994; Dickinson and Lawton 2001; Centeno-Garcia et al. 1993, 2008, 2011). The arc, known in southern California and Peninsular Mexico as the Alisitos–Santiago Peak arc, was active from about 130 Ma until ~100 Ma (Hildebrand and Whalen 2014).

As described above, platformal-carbonate rocks of the westerly facing passive margin in Mexico are disconformably over-

Fig. 26. Stratigraphic correlations from Bootheel area of southwestern New Mexico (Fig. 5) northeast to eastern Colorado Plateau at San Ysidro, illustrating detrital zircon maximum depositional ages, and tuff ages of Mojado Formation and stratigraphic equivalents modified from Lawton et al. (2020*b*). The Mojado Formation is the more easterly correlative of the Cintura Formation in Arizona and Sonora, which is the clastic wedge that sits atop the west-facing Mural carbonate platform of the Bisbee Basin. Location of sections and line are shown in Fig. 5.

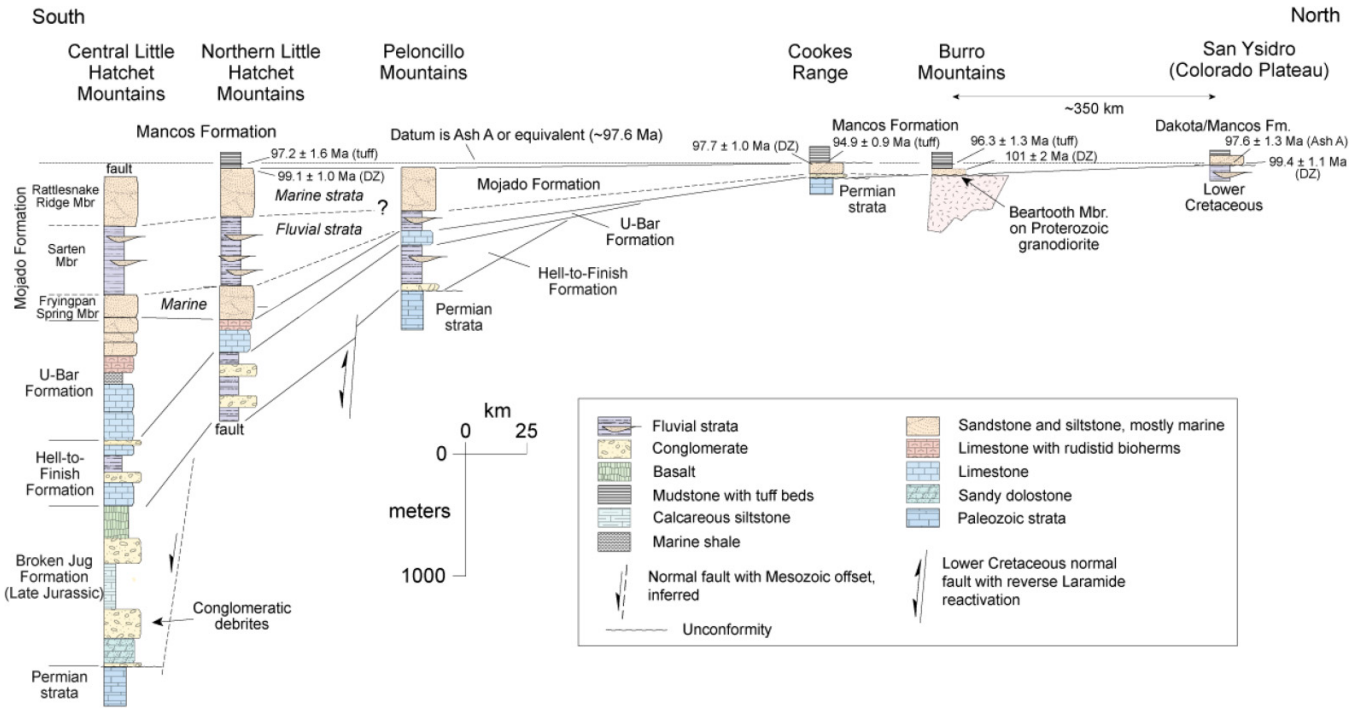

lain by a few meters of transported carbonate and condensed horizons rich in Late Albian faunal debris (Fig. 24) capped by hemipelagic shale and Cenomanian Mexcala flysch containing 97–95 Ma detrital zircons (Fig. 25) similar in age to those of the Frontier and Dunvegan formations to the north. The disconformity, as well as the rapid tectonic subsidence and burial of the carbonate platform by hemipelite and orogenic flysch, is readily explained by a collision, during which transport of a platform over the outer swell to a trench, where it was eroded (Jacobi 1981). Then, as the platform was pulled into the trench, it was covered by a thin veneer of hemipelagic mud deposited on the starved outer-trench slope, only to be overwhelmed by trench-fill turbidites upon arrival in the trench axis (see Sinclair 1997; Hoffman 2012; Sabbatino et al. 2021). These rocks were detached and scraped off their cratonic basement, accreted to the upper plate as part of the accretionary prism, and then transported eastwards over the craton.

The post-100 Ma detrital zircons in the orogenic flysch were most plausibly derived from the suite of 99–86 Ma La Posta plutons (Fig. 23), which were emplaced into the collisional hinterland located west of the foredeep (Hildebrand and Whalen 2014). The plutons postdate ~100 Ma deformation of the Alisitos–Santiago Peak arc and its basement of Guerrero superterrane, as well as the drowning and burial of the west-facing upper Albian carbonate platform perched on the western margin of North America (Hildebrand and Whalen 2014). The La Posta plutons intrude as far west as the Santiago Peak–Alisitos arc, but predominantly outcrop just to the east of it (Fig. 23), and have long been recognized to differ in age, trace element and isotope content, opaque mineralogy, depth of emplacement, and crustal thickness from the Alisitis-Santiago Peak arc rocks (Gastil et al. 1975, 1990; Silver et al. 1979; Gromet and Silver 1987; Silver and Chappell 1988; Kimbrough et al. 2001; Tulloch and Kimbrough 2003). We compiled modern geochemical data from both the Alisitos–Santiago Peak arc rocks and the post-100 Ma La Posta plutons and found consistent major and minor geochemical differences between the two suites (Hildebrand and Whalen 2014). For example, most rocks of the La Posta plutonic suite contained 60%–70% SiO_2 whereas the arc suite displayed a continuous range from basalt to rhyolite. Relative to the arc rocks, members of the La Posta suite are generally more enriched in incompatible elements, Na, and Nb, but are depleted in Y and Yb. We exploited the differences between the pre- and post-collisional suites to develop several discrimination diagrams (Fig. 27) that distinguish arc from failed slab rocks, and then tested them using Cenozoic suites (Hildebrand et al. 2018), before applying the discriminants to other Cordilleran batholiths in western North America, where we found similar rocks and relations northward through the Cordillera to Alaska (Hildebrand and Whalen 2017; Whalen and Hildebrand 2019; Hildebrand and Whalen 2021*a*, 2021*b*). More recently, these discrimi-

Fig. 27. Volcanic and plutonic samples with SiO_2 > 60% from the Peninsular Ranges batholith plotted on five discrimination diagrams modified from Hildebrand and Whalen (2014, 2017) and Whalen and Hildebrand (2019). Santiago Peak–Alisitos arc rocks are 130–100 Ma, whereas the post-collisional La Posta suite is 100–86 Ma. The Nb vs. Y and Ta vs. Yb discrimination diagrams were modified from Pearce et al. (1984) by addition of fields for post-collisional and arc plutons based empirically on samples from the Peninsular Ranges batholith. Alisitos volcanic arc data are from Morris et al. (2019).

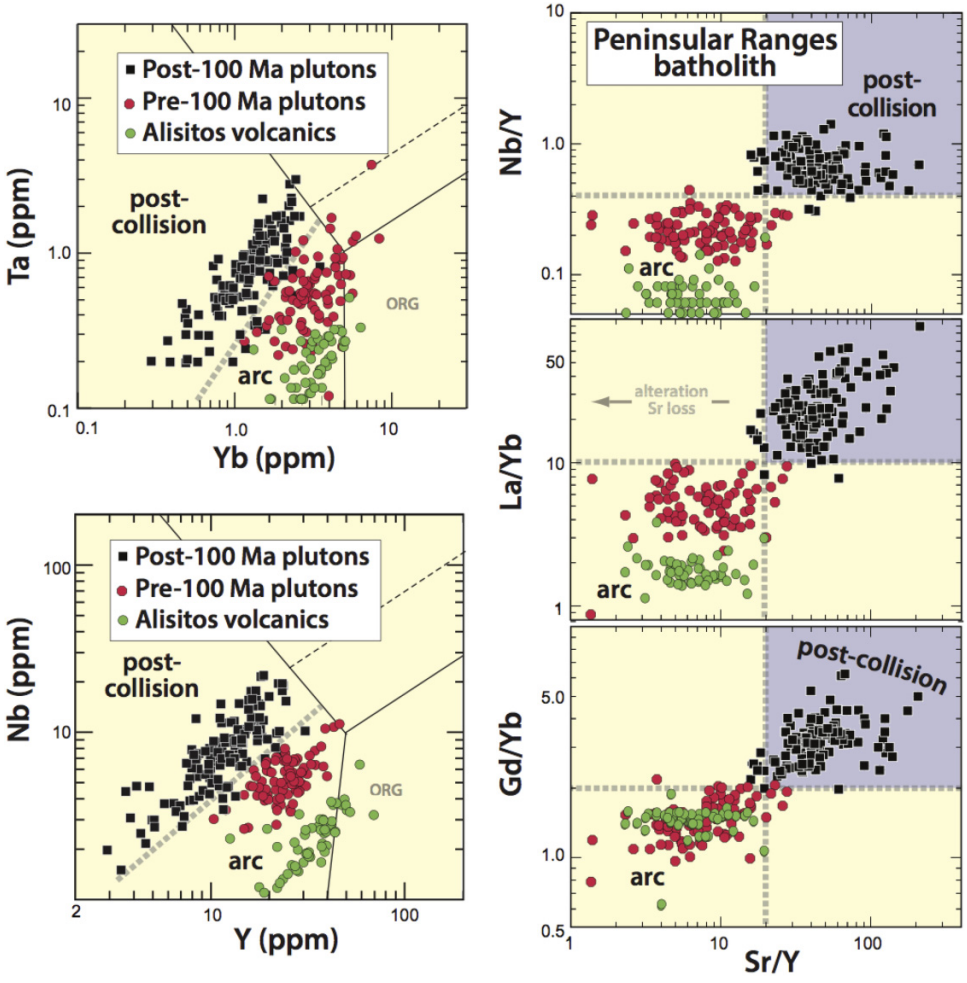

nation diagrams have been applied elsewhere to discriminate arc from failed slab rocks (e.g., Archibald and Murphy 2021; Dostal and Jutras 2021; Gianni and Navarrete 2022).

Understanding the age of collision is important not only for resolving the origin of plutons in the hinterland (Hildebrand and Whalen 2017) but also because the debris eroded from them during uplift and exhumation can be used to demonstrate that specific depocenters or even entire basins can be properly recognized as post-collisional. For example, Kimbrough et al. (2001) demonstrated that the La Posta plutons of Peninsular and Southern California closely postdated a period of contractional deformation, were deep-seated, and emplaced during rapid uplift/exhumation on the basis of debris, including 99–92 Ma zircons, shed rapidly westward from the rising hinterland into what they assumed was a forearc basin represented by rocks of the Valle Group. However, as we demonstrated, subduction was westward beneath the Alisitos–Santiago Peak arc, and so the Valle Group was deposited west of the thickened collision zone and not in a pre-collisional forearc setting. In fact, similarly preserved fragments along strike, such as the Valle and eastern Great Valley groups, the Hornbrook of the eastern Klamaths, the Ochoco Group of Oregon, the Cascade River schist, lower Nanaimo Group, Queen Charlotte Group, and the McHugh complex—all of which contain abundant 100–90 Ma detrital zircons—combine to suggest that the westerly basin, or sea, was continuous from the Baja Peninsula to Alaska and was partially filled after the collision in a retro-collisional setting, not in a forearc (Hildebrand and Whalen 2021*a*, 2021*b*).

In another case, researchers working in central Mexico argued that the Arperos sector of the basin closed during the lower Cretaceous (Martini et al. 2013) rather than at about 100 Ma as we suggested (Hildebrand and Whalen 2014). They cited a location in the complex thrust stack of the Sierra de Guanajuato (Fig. 23) where a ~50 m-thick Aptian–Albian carbonate unit, known as the La Perlita Formation, unconformably overlies a basal conglomerate deposited on greenschist-grade, isoclinally folded, Tithonian–

Berriasian metasedimentary rocks (Chiodi et al. 1988; Quintero-Legorreta 1992; Martini et al. 2011), so inferred that the rocks of the La Perlita Formation were deposited after collision. However, elsewhere in the Sierra they noted several thrust sheets carrying younger volcanic and related epiclastic successions such as the westerly derived Teloloapan and Arperos formations and the easterly derived, siliciclastic Cuestecita Formation, which all have the youngest detrital zircon peaks ranging mainly from 133 to 116 Ma, consistent with ages of the Alisitos–Santiago Peak arc built on Guerrero superterrane (Talavera-Mendoza et al. 2007; Martini et al. 2011), as well as upper Aptian–upper Albian platform facies to the east on the North American side of the basin (Lawton et al. 2004). These observations suggest that the Tithonian–Berriasian successions in the Sierra de Guanajuato are correlative with the more northerly Cucurpe and Peñasquitos successions, both deformed between about 145 and 139 Ma (Mauel et al. 2011; Kimbrough et al. 2014; Hildebrand and Whalen 2014, 2021*a*), and *then* overlain by rocks of the Bisbee–Arperos basin, much in the way the older deformed successions of the Sierra de Guanajuato were overlain by conglomeratic and carbonate rocks of the Albian La Perlita Formation. Thus, we see no conflict between areas, and the stratigraphy constrains the age of the seaway to be younger than about 140 Ma with terminal collision at about 100 Ma. This is consistent with the geology farther south in the Zihuatanejo area (Fig. 23), where 250 m of Albian carbonate of the Ixtapa Formation was uplifted, eroded, and unconformably overlain by 2–10 m of carbonate-clast conglomerate and breccia capped by >2000 m of molasse: red volcaniclastic sandstone, conglomerate, and shale, containing samples with detrital zircon peaks of 123, 109, 106, 99, 97, and 94 Ma (Martini et al. 2010; Martini and Ferrari 2011; Centeno-Garcia et al. 2011), which represent both pre-collisional arc and post-collisional plutons of the La Posta suite.

Although dismembered and translated during younger tectonic events, the rocks and their temporal relations as found in the southwestern North American sector (Fig. 28) are readily recognized and correlated northward along the entire Cordillera from southern Mexico to Alaska and constitute the Peninsular Ranges orogeny (Hildebrand and Whalen 2021*a*, 2021*b*). The continent-long parallelism between the structural axis of the orogen, coupled with the post-collisional basin to the west of the collision zone, suggests to us that rocks within the mid-Cretaceous succession of the Western Interior Basin were not deposited in a retro-arc foreland basin developed above an easterly dipping oceanic slab (Dickinson 1970), but instead may have formed as a collisional foredeep related to westerly subduction and collision of the Peninsular Ranges composite terrane with North America during the ~100 Ma Peninsular Ranges orogeny (Fig. 28). With the timing of the collision to the west reasonably well-constrained, along with numerous dated bentonite beds and detailed studies of detrital zircons from many stratigraphic units within the Western Interior basin, it seemed timely to ask: How does the stratigraphy, sedimentology, and volcanism of the basin fit with the mid-Cretaceous geology of the Peninsular Ranges orogeny?

Discussion

During our study of the Cenomanian–Turonian stratigraphy of the Western Interior Basin, we recognized three distinct sectors of the basin: central, northern, and southern. The northern sector is represented by the succession on the Peel Plateau of Boreal Canada; the southern sector extends from southern Mexico to southern Arizona; and the central sector lies between the two.

In northern Canada and Arizona–Mexico, we interpret foredeep sediments of the Peninsular Ranges orogeny to sit disconformably atop Cretaceous passive margin sedimentary successions, which themselves sit unconformably upon cratonic North America basement (Hildebrand and Whalen 2021*a*, 2021*b*). In both regions, relations are straightforward: a west-facing marine platform was uplifted, eroded, and then promptly submerged, creating a succession that we interpret to reflect the migration of a forebulge (see Crampton and Allen 1995). In Mexico and southern Arizona, the platform was capped by Albian carbonate as it was located in a warm, southerly climate, whereas in the northern Canadian Peel Plateau, the margin was muddy, as befits its northern Boreal connection and location during the Cenomanian–Turonian (Kauffman and Caldwell 1993; Kent and Irving 2010).

In the successions of southern Mexico, the top of the carbonate platform was disconformably overlain by 2 m of channelized calcarenites and calcareous turbidites, themselves overlain by a condensed horizon containing an abundance of closely packed Late Albian ammonites and rudist fragments covered by an Mn-rich, dark-red to black, shaley coating (Monod et al. 2000), likely formed in an anoxic environment (Fig. 24). The carbonates were covered by less than a meter of pelagic mudstone then buried by Cenomanian Mexcala flysch, which contains 97–95 Ma detrital zircons derived from post-collisional La Posta plutons (Lawton et al. 2015) emplaced into the orogenic hinterland farther west. Although Mendoza and Suástegui (2000) considered that the carbonate succession represents an upper-plate patch reef, it constitutes part of an extensive thrust panel of upper Aptian–Albian platformal carbonate, so we interpreted (Hildebrand and Whalen 2021*a*) the overall sedimentary succession above the disconformity, which consists of (1) shallow- to deep-water carbonate deposition on the margin; (2) hemipelagic mud; and (3) deep water siliciclastic turbidites, to represent superposition of lateral facies changes as the migrating margin was pulled downwards into the trench. Overall, it constitutes a typical lower-plate foreland basin sequence (Sinclair 1997).

On the Peel Plateau of Boreal Canada (Fig. 5), a west-facing mid- to upper-Albian marine siliciclastic margin (Fig. 21) was uplifted and sufficiently exposed to develop a paleosol complex comprising pisoidal ironstones containing sparse wood fragments, then submerged and buried initially by black carbonaceous shale with thin, but rare, coal beds, overlain by a 10 cm thick condensed section of radioactive, dark-black mudrock containing fish teeth, bone and organic material, but no benthic foraminifera, passing upwards into the Lower Cenomanian Fish Scales marker, also devoid of foraminifera (Thomson et al. 2011). Overlying Cenomanian–Turonian oro-

Fig. 28. Similarities along strike within the Peninsular Ranges orogen, from Mexico to Alaska, of major sedimentological, magmatic, and tectonic packages arranged from west to east, along with their age constraints, where known. Note the coeval nature of most units along strike, which are comparable to the along-strike stratigraphic continuity found in units of the Western Interior Basin over the same N-S distance. Modified from Hildebrand and Whalen (2021*a*).

West → East

North ↑ South

Location	Western retroarc debris 99-83 Ma	Arc terrane 130-100 Ma	Syn-arc basin 140-100 Ma	Age of Collision	Post-collision plutonism 99-84 Ma
Mainland Alaska	McHugh complex	133-98 Ma Chisana	Kahiltna	103-97 Ma	94-88 Ma Tok-Tetlin Gardiner Crk. ?
Insular Alaska	Queen Charlotte Group	Muir-Chichagof suite & Gravina	Gravina	105-95 Ma	95-90 Ma Moth Bay & many others
Coast Plutonic belt, BC	Nainaimo Group	Gambier Group Firvale & Desire plutonic suites	Gambier Group	101-97 Ma	Ecstall & many others 99-85 Ma
Cascades	Cascade River Skagit gneiss ?	Chiwaukum schist	Nooksack	108-96 Ma	Many plutons 96-89 Ma
Idaho & Montana	Ochoco Basin (Oregon)	Little Goose Hazard Creek 120-108 Ma	unknown	100-91 Ma	Atlanta lobe Payette-Rat Cr. 98-84 Ma
Nevada/UT	unknown	King Lear 125-123 Ma	Newark Canyon ?	101-96 Ma	Many plutons 98-84 Ma
Sierra Nevada	Eastern Great Valley Group	western arc terrane & Cinko Lake arc	Cinko Lake trough	103-98 Ma	Sierran Crest 99-84 Ma
Mojave Desert	unknown	Delfonte volcanics 100.5±2 Ma	not recognized	100.5-98 Ma	Teutonia & others 98-85 Ma
Peninsular Ranges Mexico & USA	Valle Gp	128-100 Ma Santiago Peak & Alisitos	Bisbee-Arperos trough	103-98 Ma	La Posta 99-84 Ma

genic deposits of the Trevor Formation, which were derived from the west and contain abundant detrital zircons between 100 and 90 Ma (Hadlari et al. 2014), presumably derived from 99 to 93 Ma post-deformational plutons to the southwest in the Selwyn basin (Figs. 5 and 22). This sector represents a siliciclastic, more northerly version of a typical foreland basin (Sinclair 1997).

Between the Arizona–Mexican and northern Canadian sectors, the western part of North America was earlier affected by the Sevier orogeny (Fig. 29), which involved 124–105 Ma thrusting and development of a foredeep trough (Lawton et al. 2010; Yonkee and Weil 2015; DeCelles and Coogan 2006), so the overall stratigraphic succession is different there. Nevertheless, the relations within the sector are similar to those both north and south in that pre-existing Albian sedimentary rocks were uplifted and exposed just prior to 100 Ma, subaerially exposed, after which they were incised by fluvial systems; then rapidly buried by neritic successions, commonly deposited in paleovalleys eroded in mid-Cretaceous sandstone. These successions fine upwards into mudstone and a condensed, anoxic section containing abundant faunal debris, overlain the length of the basin by Cenomanian

Fig. 29. Cartoon view of western North America just before ~124 Ma collision illustrating arrival of the Sevier upper plate. Its collision with North America was followed at ~100 Ma by the arrival of another ribbon, this one carrying the Santiago Peak–Alisitos arc, during the Peninsular Ranges orogeny.

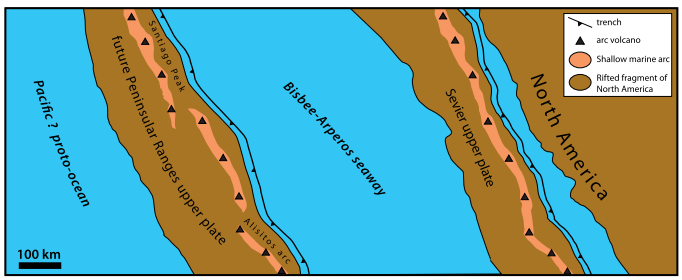

clastic wedges, such as the Dunvegan, Frontier, and Mexcala, which contain 97–93 Ma detrital zircons (Figs. 7, 20, 21, and 25).

In all three sectors, the post-unconformity, neritic succession fines upward into mudstones that, in turn, pass upwards into a condensed anoxic section termed either the Fish Scales Formation or the Mowry Shale, each of which contains abundant fish scales, teeth, and disarticulated bones. In most sectors, the condensed section is accompanied by abundant bentonite beds and an endemic gastroplitine ammonite fauna, which collectively provide excellent age control. Nearly everywhere in the basin atop the condensed, bentonite-rich zone, there are easterly prograding clastic wedges, such as the Trevor, Dunvegan, Frontier, Cintura, and Mexcala units, each of which contains abundant detrital zircons with ages between 99 and 90 Ma, indicating that the wedges represent post-collisional molasse.

The overall sequence sitting atop a regional, eastward-migrating disconformity of (1) shallow-water sediments fining progressively upwards into (2) condensed hemipelagite, overlain by (3) orogenic debris derived from the rising hinterland is typical of the sedimentation in active collisional foredeeps (Crampton and Allen 1995: Sinclair 1997; DeCelles 2012; Sabbatino et al. 2020, 2021). Although the overall mid-Cretaceous stratigraphy is convincing and fits the timing known from the Peninsular Ranges orogeny (Hildebrand and Whalen 2021*a*, 2021*b*), the following additional points support our stratigraphic argument that the overall Cenomanian–Turonian succession within the basin better fits a collisional foredeep setting than the more widely accepted retro-arc basin scenario.

First, sedimentation within the basin was remarkably consistent, both across and along its length, as well as temporally, which collectively requires a plate-scale explanation, not one related to displacement, loading, and flexure on individual thrust faults. This problem is especially acute because researchers have demonstrated that thrust timing, shortening, and hence loading, in the fold-thrust belt varied along strike (Price and Sears 2000; DeCelles and Coogan 2006).

Second, the width of the basin is simply too large, some 1500 km, to be explained by lithospheric flexure generated by a thrust load to the west or to rise of sea level (Beaumont et al. 1993). This led some workers to speculate that a slab of cold oceanic lithosphere dipped eastward beneath the craton, which, along with sea level rise, pulled the surface downward to create a basin that could be as wide as 1500 km (Mitrovica et al. 1989). How a shallowly dipping slab can exist when cratonic lithosphere is thick remains unresolved. Also, arc magmatism appears to have ceased at 100 Ma (Hildebrand and Whalen 2021*a*, 2021*b*) coincident with drowning of the North American passive margin and its burial by orogenic clastics.

The eastward migration of the peripheral bulge from near the thrust front to the Dakotas, some 650 km to the east, is too broad to be caused by loading of thrust faults in the fold-thrust belt, especially given that sedimentation in the basin was sparse at that time. Following passage of the bulge, this area of the basin was closer to the thrust belt, yet received only limited sedimentary input, which is inconsistent with thickening, loading, exhumation, and emergence in the thrust belt to the west.

Where the westerly derived clastic wedges have been studied in great detail, such as the distal regions of the Dunvegan clastic wedge, individual prodeltaic clinoforms are documented to have prograded across the anoxic Fish Scales unit for up to 800 km, demonstrating the essentially featureless, low gradient, and isochronous nature of the Fish Scales–Mowry horizon (Bhattacharya 1994; Plint et al. 2009). A similar result was found by Byers and Larson (1979), who used bentonite datum planes to document that the Frontier–Mowry contact was isochronous and dipped very gently eastward over the width of the basin. It is difficult to reconcile these observations with a retro-arc setting where the basin was caused by a thick thrust stack located to the west, as in that case the basinal floor should dip westward towards the load, not eastward as observed. This observation is better understood to represent the rebound of the collisional hinterland once slab break-off freed the cratonic lip from the oceanic slab pulling it down.

Where not extremely altered, trace element geochemistry of the Upper Cretaceous bentonites suggests that they are not arc magmas, but instead, post-collisional slab break-off magmas (Fig. 14). Compositions of volcanic rocks of the Crowsnest Formation also support a break-off origin, as early post-collisional magmatism is commonly alkaline.

All these relations are better explained by attempted westward subduction of the North American craton, which led to the entire western edge of the craton dipping to the west as it was pulled into the trench. After the forebulge on the margin was uplifted and subsided beneath the wave base, the basin floor dipped westward, but very gently. By deposition of the Fish Scales unit, the floor of the basin was reversed again to dip ever so slightly eastward, the opposite direction from that expected for loading by thrust sheets to the west. It appears that exhumation in the hinterland was not fully underway until deposition of the Frontier and related clastic wedges.

If correct, then the Mowry–Fish Scales succession records the syn- to early post-collisional time interval, and because it is isochronous and occurs both across and over the length of the entire basin, it is unlikely that the basin was the product of dynamic topography, other than some initial subsidence related to the vertical sinking of the detached slab. It is more likely that, because the basin sits almost entirely east of the North American cratonic hingeline, the effective elastic thickness of the North American craton, which is a measure of its flexural rigidity (Turcotte 1979; Flück et al. 2003), was likely in excess of 100 km, perhaps even 150–200 km (Tesauro et al. 2015), consistent with other Precambrian cratons (Zuber et al. 1989; Hansen et al. 2009). This is because the thermal regime primarily controls the flexural rigidity, except perhaps close to the hingeline, where there may have been some local ductile necking during creation of the older passive margin. Other potential modifications, such as heating from extension and magmatism within the United States and Mexican Basin and Range, as well as those of the Rio Grande Rift, are all much younger than the age of the ~100 Ma Peninsular Ranges orogeny (Fig. 30), so it is reasonable to infer a typical cratonic thickness for the area. If elastic thickness is ~125 km, typical for Precambrian cratonic lithosphere, Flück et al. (2003) calculated that the flexural wavelength would be nearly 1100 km and would increase propor-

Fig. 30. Effective elastic thickness (*Te*) of the lithosphere in kilometers for two different models of North America modified from Tesauro et al. (2015). We suggest that during the Cretaceous the region east of the US hingeline had a thicker, more typical cratonic *Te* than at present. The thickness was likely much diminished during the Cenozoic by extension and magmatism.

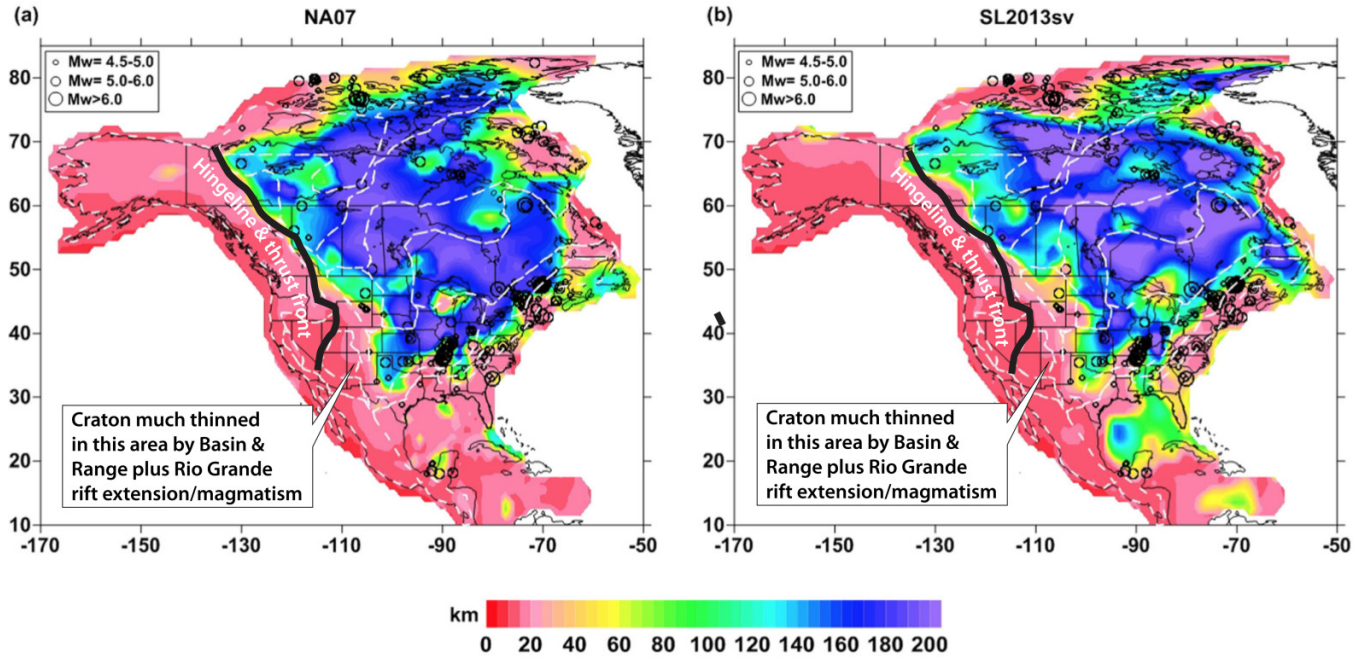

tionally with a thicker elastic thickness. This calculation is consistent with the distance from the thrust belt to the Black Hills, which is about 600 km, approximately half the flexural wavelength. Therefore, we favor flexural bending of the cratonic lithosphere as it entered the trench, augmented by local isostatic subsidence along the western margin caused by the bulk of the thrust stack and related post-collisional sediments sitting on the lithosphere.

The downward flexure of the cratonic or oceanic lithosphere into a trench is accompanied by the generation and migration of an adjacent peripheral bulge, or lithospheric upwarp, located seaward of the trench (Section 3–17: Turcotte and Schubert 1982). The uplift causes stratigraphic condensation and commonly a forebulge unconformity. Within the Western Interior Basin, where temporal constraints are documented, such as the Wyoming–Dakota transect of the basin (Fig. 4), exposure and incision of the sedimentary succession due to relative sea level fall occurred earlier to the west in Wyoming than in South Dakota, which is the reverse of that expected for a basin that shoaled to the east. Our preferred explanation is that the eastward migration and passage of the peripheral bulge progressively elevated a sector of the basin above sea level (such that it could be eroded), only for it to rapidly subside below sea level rather promptly after passage (Crampton and Allen 1995). The sector that rode up and over the bulge then lay on the outer slope to the trench, which is, in many places, a region characterized by low sedimentation rates of mostly pelagic sediment (see Harris 2011; Heirtzler 1974 for an example). Within the US sector of the Western Interior Basin, the emergent Muddy and Newcastle sandstones likely relate to the passage of the peripheral bulge (Fig. 31), whereas the overlying and partly coeval Shell Creek Shale consists of shale, fine sandstone, siltstone, and bentonites deposited on the outer slope to the trench, located some distance to the west. As the flexural bulge migrated eastward into the craton, its wavelength likely increased proportionately with a thicker elastic thickness as it encountered older, thicker, and more rigid cratonic lithosphere (Flück et al. 2003), causing it to progressively widen and decrease in amplitude, dampening its topographic and stratigraphic expression and rendering it more difficult to recognize.

Within the shaley units that sit atop the neritic-facies rocks deposited on the western flank of the migrating flexural bulge, the presence of bentonites might reflect ash erupted from an arc approaching from the west, but in the case of the upper Shell Creek and the Mowry shales, the bentonites have compositions more consistent with post-collisional slab failure magmas than arc magmas, as do volcanic rocks of the Crowsnest Formation in Canada (Fig. 14). The volcanics and associated sills are the only known magmatic rocks other than bentonites within the predominantly sedimentary succession, and so without an extensive data set of ages along strike we cannot tell if break-off was diachronous as we expect, or merely leaked magmas locally. In either case, the age of the unit relative to the basinal bentonites could be documented more precisely by obtaining high-quality $^{40}Ar/^{39}Ar$ sanidine ages from the volcanic rocks.

Within the Canadian sector of the Western Interior Basin, reliable radiometric ages from bentonites are scarce (Fig. 4). However, the lithological similarities between the Canadian and US sectors and their successions attest to similar origins.

Fig. 31. Idealized eastward migrating peripheral bulges in Canada and the United States.

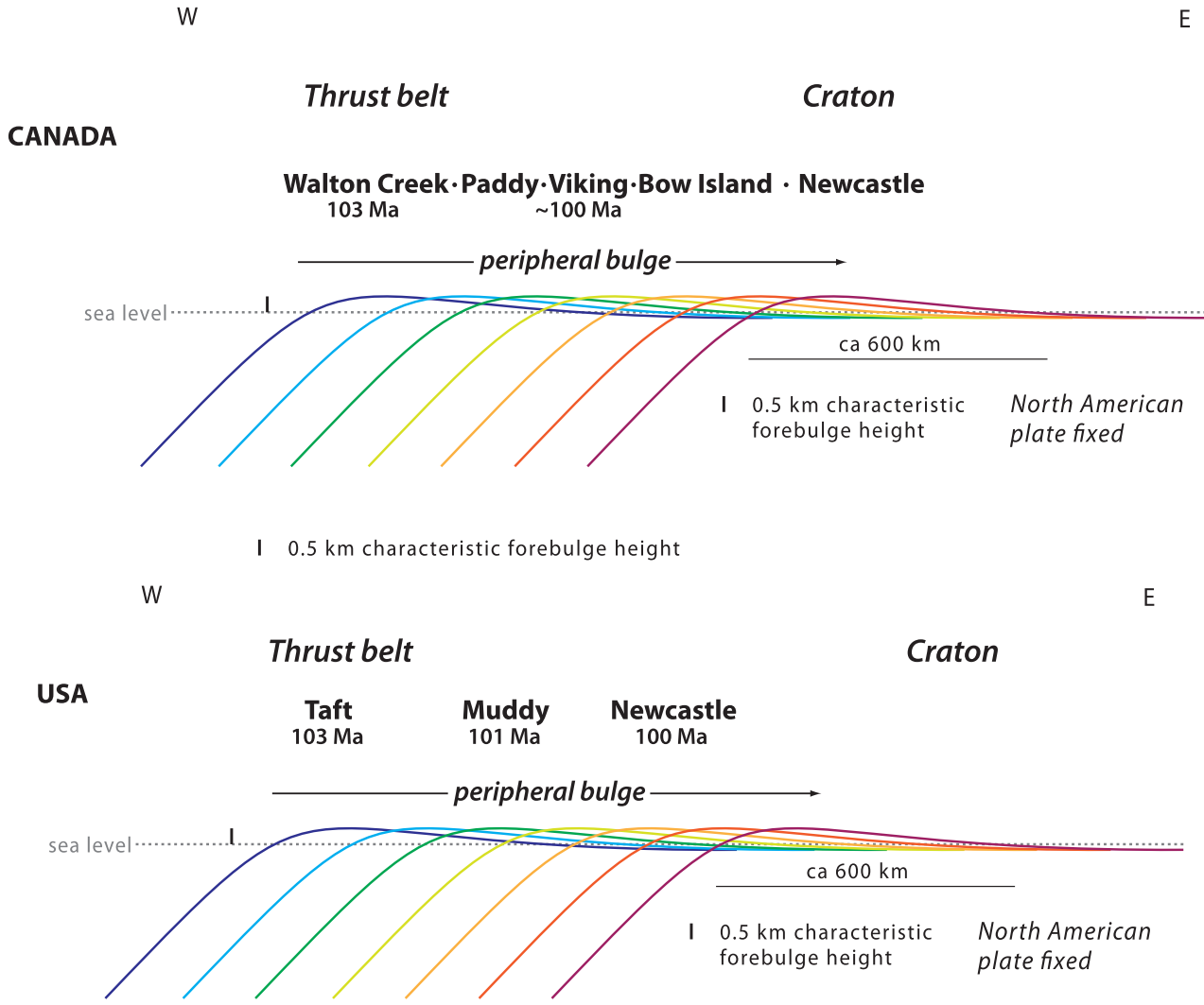

For example, basinal rock packages within the Fort St. John and Colorado Groups (Fig. 31), such as the Walton Creek, Paddy, Viking, and Bow Island successions, all exhibit erosion, soil horizons, fluvial incision, and deposition of neritic facies prior to re-submergence and deposition of overlying shales, including the Fish Scales unit, prior to being overwhelmed by westerly derived clastic wedges, such as the Dunvegan or Frontier with their abundant post-100 Ma detrital zircons.

Isopachs of the lower part of the Shaftesbury Formation, that is, the post Viking–Bow Island and pre-Fish Scales shale unit (Fig. 5), yield insight into potential processes. First, note the approximately logarithmic westward slope over the western 500 km of isopachs, which range from over 500 m in the west to about 40 m in the east. As the Fish Scales unit is essentially isochronous, the thickness of the basal shale under it should reflect the slope of the surface beneath it and provide a minimum for the available accommodation space. The logarithmic nature of the thickness variations suggests the bending, and likely rollback of the subjacent basement, as the oceanic lithosphere steepened and was pulled downward into the trench to the west. It is difficult to relate the bending to isostatic load as there was no commensurate deposit of coarse clastic debris that might signify the emergence of a thrust stack to the west. Instead, the area was exposed subaerially during the immediately underlying Viking–Bow River interval, but rapidly subsided, a scenario consistent with the eastward migration of a peripheral bulge through the area (see also Roca et al. 2008; Fig. 28). The migration could be tested and refined by systematically dating bentonites within the Viking–Bow River interval of the basin by $^{40}Ar/^{39}Ar$ to ascertain if the outer swell migrated eastward at about the same rate as that in the United States. (See Sabbatino et al. 2020, 2021, for a well-dated example from the Apennine collisional orogen.) Nevertheless, on the basis of the foregoing, we consider that the foredeep to the Peninsular Ranges orogeny displays the effects of the passage of the peripheral bulge along its entire length from southern Mexico to northern Canada and affected both pre-existing carbonate and clastic margins as well as older orogenic deposits related to the Sevier orogeny in the central sector of North America.

In our collisional model, slab break-off must have occurred rather widely by upper Shell Creek time as the number of bentonites increases up section into the Mowry, where they dominate the succession. The starved nature of the Mowry–Fish Scales may represent the time when break-off was underway, but that exhumation of the hinterland had not started, or at least was still insufficiently emergent to flood the basin with sediment.

Models designed to observe surface deformation resulting from slab break-off indicate that after break-off, the detached part of the slab sinks vertically into the mantle, which creates flow within the viscous mantle that pulls the overlying lithosphere downward (Buiter et al. 2002; Chatelain et al. 1992). As the lithospheric slab sinks farther, the suction and downward pull are reduced. Presumably, this would delay surface uplift and exhumation such that sediment flux into the basin would be dramatically retarded and reduced. This process could create the somewhat short-lived sediment-starved sequence with a high flux of ash and an anoxic hypolimnion as observed for the Fish Scales–Mowry succession. This is consistent with the model of Plint et al. (2009), who argued that the basin-wide Fish Scales Formation was a downlap surface and represents a sedimentological hiatus of up to 2 Myr. It was during this hiatus that the slope of the basin was reversed from west dipping to east dipping, such that eventually the first prodeltaic muds of the Dunvegan and Frontier clastic wedges began to prograde eastward over the Mowry and Fish Scale units on the shallowly dipping basin floor.

Although we are attracted to the concept of additional subsidence due to slab break-off, it might only represent one component, or may not even be necessary to explain the lack of coarse detritus. A modern example of an accretionary prism in front of a starved and underfilled oceanic trough, but one in which the slab apparently has not failed yet, occurs in the Timor Trough, the 3 km deep trench south of the island of Timor, which represents an uplifted portion of the accretionary prism between Australia and the Banda arc. There, as noted by Harris (2011), the island of Timor is quite dry, with only a 4-month rainy season which provides the bulk of the 1.3 m annual precipitation. Due to the long dry period, and the consequent lack of vegetation, the amount of clastic sediment transported from the mountains to the coast as cobbly to pebbly debris by braided streams is huge: about 60% of the annual discharge of the Ganges/Brahmaputra River system of the Indian subcontinent (Cecil et al. 2003). As documented by DSDP 262, none of the coarse sediment reaches the adjacent Timor trough to the south, where only pelagic nanooze was found to overlie the Australian carbonate platform (Heirtzler 1974). Apparently, the coarse debris is trapped in submarine piggy-back thrust basins on Timor and unable to escape southward into the trench (Harris, personal communication, 2021). As southern North America was located near 30° N latitude during the mid-Cretaceous (Kent and Irving 2010), its western margin would have been relatively dry, perhaps with seasonal rainfall not very different than today. Thus, in the case of western North America, the combination of topography, seasonal climate, lack of vegetation, coupled with break-off-induced subsidence might have led to an especially starved basin.

One of the more interesting outcomes from our study of the Peninsular Ranges orogeny is the recognition that a new terrestrial faunal assemblage with Asian affinities (tyrannosaurids, hadrosaurids, pachycephalosaurs, snakes, anocid turtles, and marsupials) arrived in North America at about 100 Ma, the time of accretion of the Peninsular Ranges composite terrane, which suggests that the two events might be related. Cifelli et al. (1997) indicate that the new fauna are the oldest dinosaur fauna with representatives of each family characteristic of the remainder of the Late Cretaceous in North America. The bulk of the fauna was initially discovered in the Mussentuchit Member of the Cedar Mountain Formation of central Utah, where the unit was deposited along the terrestrial southern margin of the Mowry Sea (Fig. 3), which allowed newly arrived fauna to migrate into eastern North America. Similar faunal assemblages were found west of the seaway in the Blackleaf Formation of Montana and the Willow Tank Formation of southern Nevada as discussed previously. Some paleontologists (Cifelli et al. 1997; Kirkland et al. 1997, 1999) suggested that the introduction of the new taxa wiped out the previous inhabitants to dominate North America for the remainder of the Cretaceous. As the Canada Basin was still open at 100 Ma (Grantz et al. 2011), it is unlikely that there was a direct Asian–North American connection as sometimes hypothesized (Kirkland and Madsen 2007; Samson 2009); instead, it is more likely that the fauna arrived on the Peninsular Ranges composite terrane and spread throughout eastern North America following the collision. Overall, the paleontological findings support our collisional model for the 100 Ma Peninsular Ranges orogeny.

Summary

1. The tripartite succession of mid-Cretaceous stratigraphic units within the Western Interior Basin lies disconformably upon older rocks and is readily interpreted in terms of a collisional foredeep between the North American craton and the Peninsular Ranges composite terrane (Fig. 32). Upper Albian sediments were derived from the east, whereas Cenomanian–Turonian clastic wedges were westerly derived.
2. The earliest sign of collision was the eastward migration of the peripheral bulge from west to east along the western edge of cratonic North America (T1 and T2: Fig. 32) just before it was pulled down into the trench. Rocks in the western United States related to the uplift, erosion, and re-submergence of the margin during migration of the bulge were the Muddy and Newcastle sandstones, which range in age from 101 to 99.5 Ma. Equivalent strata in the Canadian sector include the Bruin Creek, Bow Island, Viking, Peace River, and Sikanni successions, but radiometric dating is scarce.
3. Thin, but westward-thickening, units of dark shale, such as the Shell Creek Shale in the United States and the Sully, Westgate, and Shaftesbury in Canada, were deposited on the starved outer slope of the trench between about 100 and 99 Ma (T3: Fig. 32). Bentonite beds are more common up section.

Fig. 32. Our model for development of the mid-Cretaceous Western Interior Basin as a collisional foredeep.

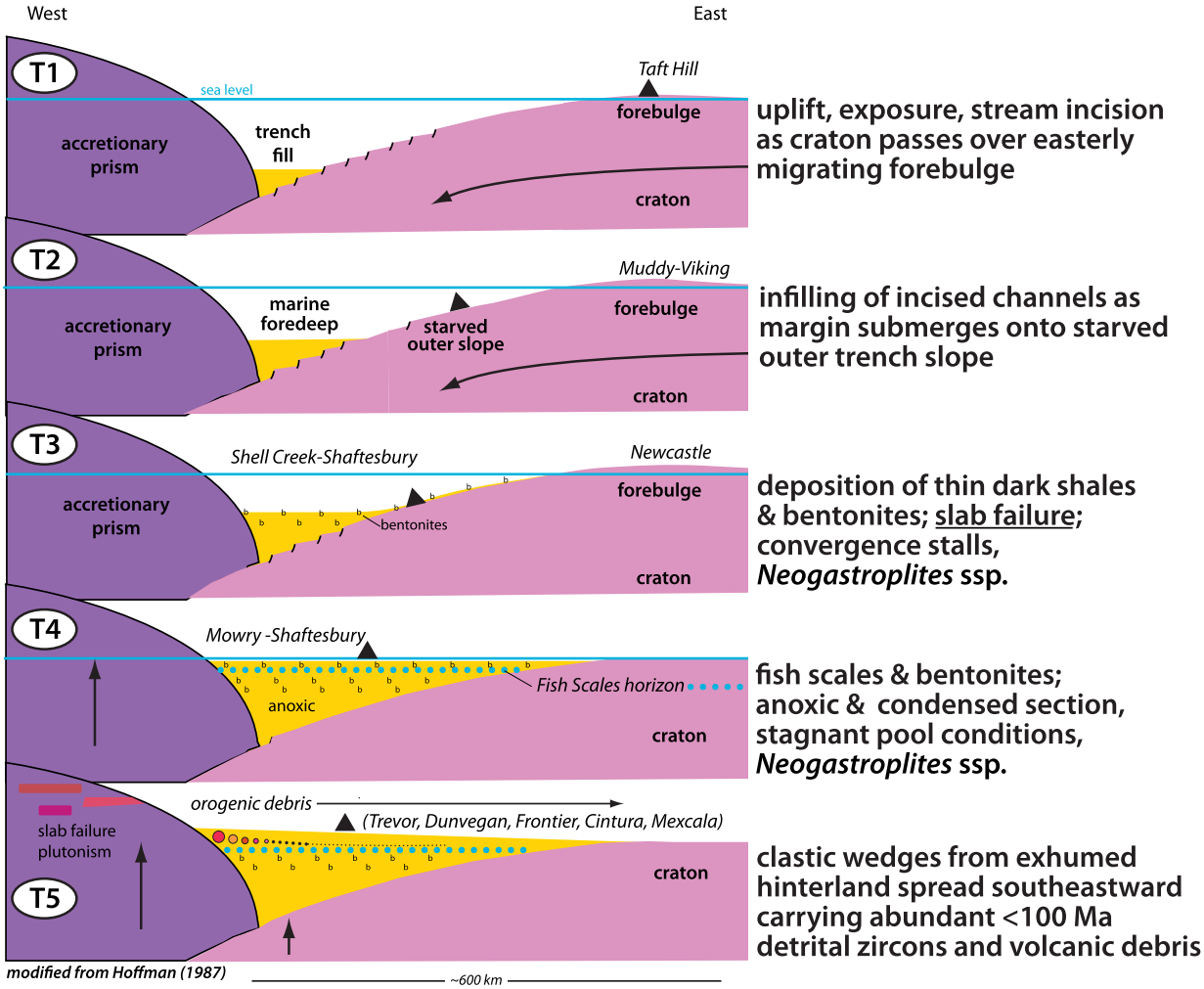

4. The dark shales are overlain by a condensed and anoxic, black-shale section, rich in fish debris and numerous beds of bentonite and porcellanite, known as the Mowry Shale in the United States and the Fish Scales Formation in Canada (T4: Fig. 32). In the United States, these rocks were deposited between about 99 and 97.5 Ma. The Shell Creek–Mowry–Fish Scales units contain five species of endemic ammonites (*Neogastroplites* ssp.), which reflect its restricted nature.
5. Bentonites deposited in marine environments are commonly altered, and their origin is difficult to decipher. However by using relatively immobile high-field strength and rare earth elements, those effects are minimized. We found that the intercalated bentonites have trace element compositions more typical of the failed slab, not arc, magmatism. This suggests that slab failure took place just before, or during, deposition of the Mowry–Fish Scales units, consistent with slightly older ages for the alkaline Crowsnest volcanics in the southern Canadian foothills.
6. Starting at about 97.5 Ma, the Mowry–Fish Scales unit was overlain by westerly derived, and easterly to southeasterly prograding, clastic wedges (T5: Fig. 32), which contained igneous clasts and abundant detrital zircons younger than 100 Ma derived from post-collisional magmatic rocks in the hinterland. These delta-front wedges included, from north to south, the Trevor, Dunvegan, Frontier, Cintura–Mojado, and Mexcala successions (Fig. 33).
7. Single delta-face clinoforms 10 m thick at the base of the clastic wedges can be traced for 800 km sitting directly on the Fish Scales unit, which, along with the evidence outlined above, indicates that the Mowry–Fish Scales represents an isochronous unit deposited on a very gently dipping eastward slope and that its upper surface might represent ~2 Myr of non-deposition. This precludes extensive thickening, uplift, and subaerial emergence of the thrust stack to the west during deposition of the Mowry–Fish Scales succession.
8. The Mowry–Fish Scales succession records the syn- to post-collisional time interval and represents the reversal of slope from westerly to easterly within the basin.
9. The presence of the Mowry–Fish Scales units over the entire width and length of the basin rules out generation by dynamic topography caused by a gently eastward-dipping slab, as there was no broadening of the basin

Fig. 33. Approximate locations of five deltas that transported material from the hinterland of the Peninsular Ranges orogen into the trough on the basis of stratigraphy and detrital zircon suites during the Middle to Late Cenomanian.

at that time. Instead, it is more likely that, because the basin sat almost entirely east of the hingeline, it was probably built on Precambrian cratonic lithosphere with an effective elastic thickness (*Te*) of more than 100 km (and perhaps even 150 km), the basin had a long wavelength and so was broad and shallow, with a narrow westernmost isostatic sector loaded by thrusts and coarse sediment.

10. Recognizing that the Cenomanian to Turonian sedimentary succession within the Western Interior Basin can be interpreted as a collisional foredeep, developed during the Peninsular Ranges orogeny, is consistent with the presence of a westerly facing passive margin setting atop North America, both in the south, where the platform was capped by a carbonate bank, and farther north in Canada, where it was a clastic margin.
11. The seemingly pene-contemporaneous break-off of the lower North American plate from northernmost Canada to southern Mexico suggests that the plate boundaries were not irregular with large and identifiable promontories, but fundamentally linear. Within the limits of the geochronology, which for the North American Cordillera are at reconnaissance level compared to the Alpine and Apennine belts, there was no obvious lateral migration of subsidence and uplift as seen in collision zones where lateral migration of slab detachment has been recognized, such as the Apennines (van der Meulen et al. 1998, 1999). Thus, it appears that break-off may have occurred rapidly over thousands of kilometers. More detailed studies, especially dating and improving the correlation of regionally abundant bentonite beds may refine this concept considerably.
12. The accretion of the Peninsular Ranges composite terrane at ~100 Ma was more likely to have led to arrival of vertebrates from Asia and their subsequent dispersal throughout North America, than their arrival by an unrecognized polar route.

Acknowledgements

This work relies heavily on the exquisite geochronology of Brad Singer, as well as detailed work by countless sedimentologists and petroleum geologists over many decades. Although our knowledge of the Cordillera is only at a reconnaissance level by Alpine standards, we are nevertheless amazed that we could discover a previously unrecognized Cretaceous orogenic belt and hope that our success, or lack of it, depending on one's viewpoint, will suggest new avenues to explore and ideas to test.

We received insightful and supportive comments on early drafts of the manuscript by Bob Hatcher, Paul Hoffman, and Paul Link. Late night discussions on Cordilleran tectonics throughout the pandemic with Basil Tikoff were always interesting and informative. Suggestions during discussion with Josh Bonde helped expand our understanding of the 100 Ma faunal introduction. Reviews by Tim Lawton and an anonymous reviewer were very useful, as were detailed editorial comments by Brendan Murphy. As usual, this study relied entirely on personal funding.

Article information

History dates

Received: 10 August 2022
Accepted: 19 September 2022
Accepted manuscript online: 27 September 2022
Version of record online: 23 December 2022

Copyright

Data availability

All data are in cited publications and associated online files.

Author information

Author ORCIDs

Robert S. Hildebrand https://orcid.org/0000-0001-5870-1342

Author contributions

Conceptualization: RSH
Formal analysis: RSH, JBW
Investigation: RSH, JPB
Methodology: RSH, JPB, JBW
Project administration: RSH
Writing – original draft: RSH
Writing – review & editing: RSH, JPB, JBW
Validation: JPB
Data curation, Resources: JBW

Competing interests

The authors declare there are no competing interests

References

Adair, R., and Burwash, R.A. 1996. Evidence for pyroclastic emplacement of the Crowsnest Formation, Canadian Journal of Earth Sciences, **33**: 715–728. doi:10.1139/e96-055.

Adair, R.N. 1986. The pyroclastic rocks of the Crowsnest Formation, Alberta. M.S. thesis, University of Alberta, Edmonton, AB, 196p.

Aitken, J.D. 1989. The Sauk Sequence — Cambrian to Lower Ordovician miogeocline and platform Western Canada Sedimentary Basin: a case history. *Edited by* B.D. Ricketts Canadian Society of Petroleum Geologists, Calgary. pp. 105–119.

Anderson, A.D., and Kowallis, B.J. 2005. Storm deposited fish debris in the Cretaceous Mowry Shale near Vernal, Utah. *In* Uinta Mountain Geology. *Edited by* C.M. Dehler, J.L. Pederson, D.A. Sprinkel and B.J. Kowallis Utah Geological Association Publication 33, pp. 125–130.

Archibald, D.B., and Murphy, J.B. 2021. A slab failure origin for the Donegal composite batholith, Ireland, as indicated by trace-element geochemistry, *In* Pannotia to Pangaea: Neoproterozoic and Paleozoic orogenic cycles in the circum-Atlantic region. *Edited by* J.B. Murphy, R.A. Strachan and C. Quesada. Geological Society of London, Special Publication 503, pp. 347–370. doi:10.1144/SP503.

Archibald, D.B., Murphy, J.B., Fowler, M., Strachan, R.A., and Hildebrand, R.S. 2022. Testing petrogenetic models for contemporaneous mafic and felsic-intermediate magmatism within the 'Newer Granite' suite of the Scottish and Irish Caledonides. *In* New developments in the Appalachian-Caledonian-Variscan orogen. *Edited by* Y.D. Kuiper, J.B. Murphy, R.D. Nance, R.A. Strachan and M.D. Thompson. Geological Society of America Special Paper 554. The Geological Society of America, Boulder, CO. pp. 375–400. doi:10.1130/2021.2554(15).

Armstrong, F.C., and Oriel, S.S. 1965. Tectonic development of Idaho-Wyoming thrust belt. American Association of Petroleum Geologists Bulletin, **49**: 1847–1866.

Armstrong, R.L. 1968. Sevier orogenic belt in Nevada and Utah. Geological Society of America Bulletin, **79:** 429–458. doi:10.1130/0016-7606(1968)79[429:SOBINA]2.0.CO;2.

Arnott, R.W.C. 1988. Regressive-transgressive couplets of the Bootlegger Sandstone (Cretaceous), north-central Montana – the possible influence of the Sweetgrass Arch, sequences, stratigraphy, sedimentology: surface and subsurface. *Edited by* D.P. James and D.A. Leckie. Canadian Society of Petroleum Geologists Memoir 15. Canadian Society of Petroleum Geologists, Calgary, AB. pp. 255–260.

Avrahami, H.M., Gates, T.A., Heckert, A.B., Makovicky, P.J., and Zanno, L.E. 2018. A new microvertebrate assemblage from the Mussentuchit Member, Cedar Mountain Formation: insights into the paleobiodiversity and paleobiogeography of early Late Cretaceous ecosystems in western North America. PeerJ, **6**: e5883. doi:10.7717/peerj.5883.

Axen, G.J. 1987. The keystone and red spring thrust faults in the La Madre Mountain area, eastern Spring Mountains, Nevada. *In* Centennial field guide. *Edited by* M.L. Hill. Geological Society of America, North American Geology, Vol. 1. pp. 57–60.

Bally, A.W., Gordy, P.L., and Stewart, G.A. 1966. Structure, seismic data, and orogenic evolution of southern Canadian Rocky Mountains. Bulletin of Canadian Petroleum Geology, **14:** 337–381.

Barclay, R.S., Rioux, M., Meyer, L.B., Bowring, S.A., Johnson, K.R., and Miller, I.M. 2015. High precision U–Pb zircon geochronology for Cenomanian Dakota Formation floras in Utah. Cretaceous Research, **52**: 213–237. doi:10.1016/j.cretres.2014.08.006.

Barker, I., Moser, D., Kamo, S., and Plint, A.G. 2011. High-precision TIMS U-Pb zircon dating of two transcontinental bentonites: Cenomanian stage, western Canada foreland basin. Canadian Journal of Earth Sciences, **48**: 543–556. doi:10.1139/E10-042.

Beaumont, C. 1981. Foreland basins. Geophysical Journal International, **65**: 291–329. doi:10.1111/j.1365-246X.1981.tb02715.x.

Beaumont, C., Quinlan, G., and Stockmal, G.S. 1993. The evolution of the Western Interior Basin: causes, consequences and unsolved problems. *In* Evolution of the Western Interior Basin. *Edited by* W.G. Caldwell and E.G. Kauffman. Geological Association of Canada, Special Paper 39. Geological Association of Canada, St. John's, NL. pp. 97–117.

Beckerman, G.M., Robinson, J.P., and Anderson, J.L. 1982. The Teutonia batholith: a large intrusive complex of Jurassic and Cretaceous age in the eastern Mojave Desert, California. *In* Mesozoic–Cenozoic tectonic evolution of the Colorado River region, California, Arizona, and Nevada. *Edited by* E.G. Frost and D.L. Martin. Cordilleran Publishers, San Diego, CA. pp. 205–220.

Benyon, C., Leier, A., Leckie, D.A., Webb, A., Hubbard, S.M., and Gehrels, G. 2014. Provenance of the Cretaceous Athabasca Oil Sands, Canada: implications for continental-scale sediment transport. Journal of Sedimentary Research, **84**: 136–143, doi:10.2110/jsr.2014.16.

Bhattacharya, J.P. 1989. Allostratigraphy and river- and wave-dominated depositional systems of the Upper Cretaceous Dunvegan Formation, Alberta. Unpublished Ph.D. dissertation, McMaster University, Hamilton, ON, 588p.

Bhattacharya, J.P. 1994. Chapter 22 – Cretaceous Dunvegan Formation of the western Canada sedimentary basin. *In* Geological Atlas of the Western Canadian sedimentary basin. *Compiled by* G.D. Mossop and I. Shetson. Canadian Society of Petroleum Geologists and Alberta Research Council, Calgary, AB. pp. 365–373.

Bhattacharya, J.P., and Walker, R.G. 1991a. Allostratigraphic subdivisions of the Upper Cretaceous Dunvegan, Shaftesbury, and Kaskapau formations in the northwestern Alberta subsurface. Bulletin of Canadian Petroleum Geology, **39**: 145–164.

Bhattacharya, J.P., and Walker, R.G. 1991b. River- and wave-dominated depositional systems of the Upper Cretaceous Dunvegan Formation, northwestern Alberta. Bulletin of Canadian Petroleum Geology, **39**: 165–191.

Bhattacharya, J.P., and Willis, B.J. 2001. Lowstand deltas in the Frontier Formation, Powder River Basin, Wyoming: implications for sequence stratigraphic models. American Association of Petroleum Geologists Bulletin, **85**: 261–294.

Biek, R.F., and Hylland, M.D. 2007. Geologic map of the Cogswell Point Quadrangle, Washington, Kane, and Iron counties, Utah. Utah Geological Survey Map 221, two plates, scale 1:24,000. Utah Geological Survey, Salt Lake City, UT.

Blakey, R.C. 2014. Paleogeography and paleotectonics of the Western Interior Seaway, Jurassic-Cretaceous of North America. AAPG Search and Discovery Article 30392.

Bloch, J., Schröder-Adams, C., Leckie, D.A., McIntyre, D.J., Craig, J., and Staniland, M. 1993. Revised stratigraphy of the Lower Colorado Group (Albian to Turonian), Western Canada. Bulletin of Canadian Petroleum Geology, **41**: 325–348.

Bloch, J.D., Schröder-Adams, C.J., Leckie, D.A., Craig, J., and McIntyre, D.J. 1999. Sedimentology, micropaleontology, geochemistry and hydrocarbon potential of shale from the Cretaceous Lower Colorado Group in western Canada. Geological Survey of Canada Bulletin **531**: 185p.

Bohannon, R.G. 1983. Mesozoic and Cenozoic tectonic development of the Muddy, North Muddy, and northern Black Mountains, Clark County, Nevada. *In* Tectonic and stratigraphic studies in the Eastern Great Basin. *Edited by* D.M. Miller, V.R. Todd and K.A. Howard. Geological Society of America Memoir 157. Geological Society of America, Boulder, CO. pp. 125–148. doi:10.1130/MEM157-p125.

Bonde, J. W., Varricchio, D.J., Jackson, F.D., Loope, D.B., and Shirk., A.M. 2008. Dinosaurs and dunes! Sedimentology and paleontology of the Mesozoic in the Valley of Fire State Park. *In* Field guide to plutons, volcanoes, faults, reefs, dinosaurs, and possible glaciation in selected areas of Arizona, California, and Nevada. *Edited by* E.M. Duebendorfer

and E.I. Smith. Geological Society of America Field Guide 11. Geological Society of America, Boulder, CO. pp. 249–262.

Bonde, J.W. 2008. Paleoecology and taphonomy of the Willow Tank Formation (Albian), Southern Nevada. M.Sc. thesis, Montana State University Bozeman, MT, 96p.

Bonde, J.W., Hilton, R.P., Jackson, F.D., and Druschke, P.A. 2015. Fauna of the Newark Canyon Formation (Lower Cretaceous), east-central Nevada. *In* Geological Society of Nevada Symposium. Geological Society of Nevada, Reno, NV. pp. 139–150.

Bonde, J.W., Varricchio, D.J., Bryant, G., and Jackson, F.D. 2012. Mesozoic vertebrate paleontology of Valley of Fire State Park, Clark County, Nevada. *In* Field Guide for the 71st Annual Meeting of the Society of Vertebrate Paleontology. *Edited by* J.W. Bonde and A.R.C. Milner. Nevada State Museum Paleontological Paper Number 1. Nevada Department of Tourism and Cultural Affairs. Division of Museums and History, Carson City, NV. pp. 108–126.

Boreen, T., and Walker, R.G. 1991. Definition of allomembers and their facies assemblages in the Viking Formation, Willesden Green area, Alberta. Bulletin of Canadian Petroleum Geology, **38**: 123–144.

Bowerman, M., Christianson, A., Creaser, R.A., and Luth, R.W. 2006. A petrological and geochemical study of the volcanic rocks of the Crowsnest Formation, southwestern Alberta, and of the Howell Creek suite, British Columbia. Canadian Journal of Earth Sciences, **43**: 1621–1637. doi:10.1139/e06-037.

Bremer, J.M. 2016. Stratigraphy and sedimentology of the Cretaceous Mowry Shale in the northern Bighorn Basin of Wyoming: implications for unconventional resource exploration and development, M.S. thesis, University of Nebraska, Lincoln, NE. 55p.

Britt, B.B., Burton, D., Greenhalgh, B.W., Kowallis, B.J., Christiansen, E., and Chure, D.J. 2007. Detrital zircon ages for the basal Cedar Mountain Formation (Early Cretaceous) near Moab, and Dinosaur National Monument, Utah. Geological Society of America Abstracts with Programs, **39**(5): 16.

Buechmann, D.L. 2013. Provenance, detrital zircon U-Pb geochronology, and tectonic significance of middle Cretaceous sandstones from the Alberta foreland basin. MS thesis, University of Houston, Houston, TX. 87p.

Buiter, S.J.H., Govers, R., and Wortel, M.J.R. 2002. Two-dimensional simulations of surface deformation caused by slab detachment. Tectonophysics, **354**: 195–210. doi:10.1016/S0040-1951(02)00336-0.

Burchfiel, B.C., and Davis, G.A. 1977. Geology of the Sagamore Canyon-Slaughterhouse Spring area. New York Mountains, California. Geological Society of America Bulletin. **88**: 1623–1640. doi:10.1130/0016-7606(1977)88⟨1623:GOTSCS⟩2.0.CO;2.

Burgess, P.M., and Moresi, L. 1999. Modelling rates and distribution of subsidence due to dynamic topography over subducting slabs: Is it possible to identify dynamic topography from ancient strata? Basin Research, **11**: 305–314. doi:10.1046/j.1365-2117.1999.00102.x.

Burtner, R.L., and Nigrini, A. 1994. Thermochronology of the Idaho-Wyoming thrust belt during the Sevier orogeny. American Association of Petroleum Geologists Bulletin. **78**: 1613–1636.

Byers, C.W., and Larson, D.W. 1979. Paleoenvironments of Mowry Shale (Lower Cretaceous), western and central Wyoming. American Association of Petroleum Geologists Bulletin, **63**: 354–375.

Campa, M.F., and Coney, P.J. 1983. Tectono-stratigraphic terranes and mineral resource distributions in Mexico. Canadian Journal of Earth Sciences, **20**: 1040–1051. doi:10.1139/e83-094.

Cant, D.J., and Stockmal, G.S. 1989. The Alberta foreland basin: relationship between stratigraphy and Cordilleran terrane-accretion events. Canadian Journal of Earth Sciences, **26**: 1964–1975. doi:10.1139/e89-166.

Carpenter, D.G. 1989. Geology of the North Muddy Mountains, Clark county, Nevada and regional structural synthesis: fold-thrust and basin-range in southern Nevada, southwest Utah and northwest Arizona. MS Thesis Oregon State University, Corvallis, OR. 139p.

Carpenter, K. 2014. Where the sea meets the land—the unresolved Dakota problem in Utah. *In* Geology of Utah's far south. *Edited by* J.S. MacLean, R.F. Biek and J.E. Huntoon. Utah Geological Association Publication 43. Utah Geological Association, Salt Lake City, UT. pp. 357–372.

Carr, M.D. 1980. Upper Jurassic to Lower Cretaceous (?) synorogenic sedimentary rocks in the southern Spring Mountains. Geology, **8**: 385–389. doi:10.1130/0091-7613(1980)8⟨385:UJTLCS⟩2.0.CO;2.

Carrapa, B., DeCelles, P.G., and Romero, M. 2019. Early inception of the Laramide orogeny in southwestern Montana and northern Wyoming: implications for models of flat-slab subduction. Journal of Geophysical Research, Solid Earth, **124**: 2102–2123. doi:10.1029/2018JB016888.

Catuneanu, O., Sweet, A.R., and Miall, A.D. 2000. Reciprocal stratigraphy of the Campanian–Paleocene western interior of North America. Sedimentary Geology, **134**: 235–255. doi:10.1016/S0037-0738(00)00045-2.

Cecil, C.B., Dulong, F.T., Harris, R.A., Cobb, J.C., Gluskoter, H.G., and Nuroho, H. 2003. Observations on climate and sediment discharge in selected tropical rivers, Indonesia. *In* Climate controls on stratigraphy. *Edited by* C.B. Cecil and T. Edgar. Society of Sedimentary Geology, Special Publication 77. Society of Sedimentary Geology, Tulsa, OK. pp. 29–50.

Cecil, M.R., Gehrels, G.E., Rusmore, M.E., Woodsworth, G.J., Stowell, H.H., Yokelson, I.N. et al. 2021. Mantle control on magmatic flare-ups in the southern Coast Mountains batholith, British Columbia. Geosphere. **17**: 2027–2041. doi:10.1130 /GES02361.1.

Centeno-García, E., Busby, C., Busby, M., and Gehrels, G. 2011. Evolution of the Guerrero composite terrane along the Mexican margin, from extensional fringing arc to contractional continental arc. Geological Society of America Bulletin, **123**: 1776–1797. doi:10.1130/B30057.1.

Centeno-García, E., Guerrero-Suastegui, M., and Talavera-Mendoza, O. 2008. The Guerrero composite terrane of western Mexico: collision and subsequent rifting in a supra-subduction zone. *In* Formation and applications of the sedimentary record in arc collision zones. *Edited by* A.E. Draut, P.D. Clift and D.W. Scholl. Geological Society of America Special Paper 436. Geological Society of America, Boulder, CO. pp. 279–308. doi:10.1130/2008.2436(13).

Centeno-García, E., Ruíz, J., Coney, P.J., Patchett, P.J., and Ortega-Gutiérrez, F. 1993. Geology of the Guerrero terrane and its role in the tectonic evolution of the southern North America Cordillera from new geochemical data. Geology, **21**: 419–422. doi:10.1130/0091-7613(1993)021%3c0419:GTOMIR%3e2.3.CO;2.

Chatelain, J., Molnar, P., Prévot, R., and Sacks, B. 1992. Detachment of part of the downgoing slab and uplift of the New Hebrides (Vanuatu) islands. Geophysical Research Letters, **19**: 1507–1510. doi:10.1029/92GL01389.

Chiodi, M., Monod, O., Busnardo, R., Gaspard, D., Sánchez, A., and Yta, M. 1988. Une descordance anté-Albienne daté par una faune d'Ammonites et de Brachiopods de type Téthysien au Mexique central. Geobios, **21**: 125–135. doi:10.1016/S0016-6995(88)80014-7.

Christiansen, F.N. 1952. Structure and stratigraphy of the Canyon Range, central Utah. Geological Society of America Bulletin, **63**: 717–740.

Cifelli, R.L., Kirkland, J.I., Weil, A., Deinos, A.R., and Kowallis, B.J. 1997. High-precision $^{40}Ar/^{39}Ar$ geochronology and the advent of North America's Late Cretaceous terrestrial fauna. Proceedings of the National Academy of Sciences of the United States of America, **94**: 11163–11167. doi:10.1073/pnas.94.21.11163.

Cifelli, R.L., Nydam, R.L., Gardner, J.D., Weil, A., Eaton, J.G., Kirkland, J.I., and Madsen, S.K. 1999. Medial Cretaceous vertebrates from the Cedar Mountain Formation, Emery County, Utah: the Mussentuchit local fauna. *In* Vertebrate paleontology in Utah. *Edited by* D.D. Gillette. Utah Geological Survey Miscellaneous Publication 99-1. Utah Geological Survey, Salt Lake City, UT. pp. 219–242.

Cobban, W.A., and Kennedy, W.J. 1989. The ammonite *Metengonoceras* Hyatt, 1903, from the Mowry Shale (Cretaceous) of Montana and Wyoming. United States Geological Survey Bulletin 1787-L, 22p.

Cobban, W.A., and Larson, N.L. 1997. Marine upper Cretaceous rocks and their ammonite record along the northern flank of the Black Hills uplift, Montana, Wyoming, and South Dakota. Rocky Mountain Geology, **32**: 27–35.

Cobban, W.A., and Reeside, J.B. 1952. Correlation of the Cretaceous formations of the Western Interior of the United States. Geological Society of America Bulletin, **63**: 1011–1044. doi:10.1130/0016-7606(1952)63%5b1011:COTCFO%5d2.0.CO;2.

Cobban, W.A., Erdmann, C.E., Lemke, R.W., and Maughan, E.K. 1976. Type sections and stratigraphy of the members of the Blackleaf and Marias River formations (Cretaceous) of the Sweetgrass Arch, Montana. U.S. Geological Survey Professional Paper 974. U.S. Geological Survey, Reston, VA. 71p. doi:10.3133/pp974.

Coleman, D.S., and Glazner, A.F. 1998. The Sierra Crest magmatic event: rapid formation of juvenile crust during the Late Cretaceous in California. *In* Integrated earth and environmental evolution of the southwestern United States: The Clarence A. Hall Jr. volume. *Edited by* W.G. Ernst and C.A. Nelson. Bellwether Publishing for the Geological Society of America, Columbia, MD. pp. 253–272.

Coney, P.J. 1981. Accretionary tectonics in western North America. *In* Relations of tectonics to ore deposits in the southern Cordillera. *Edited by* W.R. Dickinson and W.D. Payne. Arizona Geological Society Digest, **14**: 23–37.

Coney, P.J., Jones, D.L., and Monger, J.W.H. 1980. Cordilleran suspect terranes. Nature, **288**: 329–333. doi:10.1038/288329a0.

Crampton, S.L., and Allen, P.A. 1995. Recognition of flexural forebulge unconformities in the geologic record. American Association of Petroleum Geologists Bulletin, **79**: 1495–1514.

Currie, B.S. 1998. Upper Jurassic–Lower Cretaceous Morrison and Cedar Mountain formations, NE Utah–NW Colorado: relationships between nonmarine deposition and early Cordilleran foreland-basin development. Journal of Sedimentary Research, **68**: 632–652. doi:10.2110 /jsr.68.632.

Currie, B.S. 2002. Structural configuration of the Early Cretaceous Cordilleran foreland-basin system and Sevier thrust belt, Utah and Colorado. The Journal of Geology, **110**: 697–718. doi:10.1086/342626.

Curry, W.H., III. 1962. Depositional environments in central Wyoming during the early Cretaceous. *In* Symposium on Early Cretaceous rocks of Wyoming and adjacent areas: 17th Annual Field Conference Guidebook. Wyoming Geological Association, Casper, WY. pp. 118–123.

Darton, N.H. 1904. Comparison of the stratigraphy of the Black Hills, Bighorn Mountains, and Rocky Mountain Front Range. Geological Society of America Bulletin, **15**: 379–448.

DeCelles, P.G. 2004. Late Jurassic to Eocene evolution of the Cordilleran thrust belt and foreland basin system, western USA. American Journal of Science, **304**: 105–168. doi:10.2475/ajs.304.2.105.

DeCelles, P.G. 2012. Foreland basin systems revisited: variations in response to tectonic settings. *In* Tectonics of sedimentary basins: recent advances. *Edited by* C. Busby, A. Azor and A. Pérez. Blackwell Publishing Ltd., Chichester, UK, pp. 405–426.

DeCelles, P.G., and Cavazza, W. 1999. A comparison of fluvial megafans in the Cordilleran (Late Cretaceous) and modern Himalayan foreland basin systems. Geological Society of America Bulletin, **111**: 1315–1334. doi:10.1130/0016-7606(1999)111⟨1315:ACOFMI⟩2.3.CO;2.

DeCelles, P.G., and Coogan, J.C. 2006. Regional structure and kinematic history of the Sevier fold-and-thrust belt, central Utah. Geological Society of America Bulletin, **118**: 841–864. doi:10.1130/B25759.1.

DeCelles, P.G., and Currie, B.S. 1996. Long-term sediment accumulation in the middle Jurassic–early Eocene Cordilleran retroarc foreland basin system. Geology, **24**: 591–594. doi:10.1130/0091-7613(1996)024⟨0591:LTSAIT⟩2.3.CO;2.

DeCelles, P.G., Ducea, M.N., Kapp, P., and Zandt, G. 2009. Cyclicity in Cordilleran orogenic systems. Nature Geoscience, **2**: 251–257. doi:10.1038/ngeo469.

Di Fiori, R.V., Long, S.P., Fetrow, A.C., Snell, K.E., Bonde, J.W., and Vervoort, J. 2020. Syn-contractional deposition of the Cretaceous Newark Canyon Formation, Diamond Mountains, Nevada: implications for strain partitioning within the U.S. Cordillera. Geosphere, **16**: 546–566. doi:10.1130/GES02168.1.

Dickinson, W.R. 1970. Global tectonics. Science, **168**: 1250–1259. doi:10.1126/science.168.3936.1250.

Dickinson, W.R., and Lawton, T.F. 2001. Carboniferous to Cretaceous assembly and fragmentation of Mexico. Geological Society of America Bulletin, **113**: 1142–1160. doi:10.1130/0016-7606(2001)113⟨1142:CTCAAF⟩2.0.CO;2.

Dickinson, W.R., Klute, M.A., Hayes, M.J., Janecke, S.U., Lundin, E.R., McKittrick, M.A., and Olivares, M.D. 1988. Paleogeographic and paleotectonic setting of Laramide sedimentary basins in the central Rocky Mountain region. Geological Society of America Bulletin, **100**: 1023–1039. doi:10.1130/0016-7606(1988)100⟨1023:PAPSOL⟩2.3.CO;2.

Doelling, H.H., and Kuehne, P.A. 2013. Geologic map of the Short Canyon quadrangle, Emery County, Utah. Utah Geological Survey Map 255DM, two plates, scale 1:24,000.Utah Geological Survey, Salt Lake City, UT. 31p.

Dolson, J.C., Muller, D., Evetts, M.J., and Stein, J.A. 1991. Regional paleotopographic trends and production, Muddy Sandstone (Lower Cretaceous), central and northern Rocky Mountains. American Association of Petroleum Geologists Bulletin, **75**: 409–435.

Dostal, J., and Jutras, P. 2021. Tectonic and petrogenetic settings of the Eocene Challis-Kamloops volcanic belt of western Canada and the northwestern United States. International Geology Review. **64**(18): 2565–2583. doi:10.1080/00206814.2021.1992800.

Dresser, H.W. 1974. Muddy sandstone–Wind River basin. Earth Science Bulletin, **7**: 5–70.

Drljepan, M. 2018. Allostratigraphy of the Viking and Joli Fou formations, the Lower Colorado Group (Upper Albian), central Alberta and Saskatchewan, Western Canada foreland basin. Ph.D. dissertation, The University of Western Ontario, London, ON. 221p.

DuBois, D.P. 1982. Tectonic framework of basement thrust terrane, northern Tendoy Range, southwest Montana. *In* Geologic studies of the Cordilleran thrust belt. *Edited by* R.B. Powers. Rocky Mountain Association of Geologists. Denver, CO. pp. 145–158.

Ducea, M.N. 2002. Constraints on the bulk composition and root foundering rates of continental arcs: a California arc perspective. Journal of Geophysical Research. **107**: 2304. doi:10.1029/2001JB000 643.

Ducea, M.N., and Barton, M.D. 2007. Igniting flare-up events in Cordilleran arcs. Geology, **35**: 1047–1050. doi:10.1130/G23898A.1.

Ducea, M.N., Paterson, S.R., and DeCelles, P.G. 2015. High-volume magmatic events in subduction systems. Elements. **11**: 99–104. doi:10.2113/gselements.11.2.99.

Duque-Trujillo, J., Ferrari, L., Orozco-Esquivel, T., López-Martínez, M., Lonsdale, P. Bryan, S.E., et al. 2015. Timing of rifting in the southern Gulf of California and its conjugate margins: insights from the plutonic record. Geological Society of America Bulletin, **127**: 702–736. doi:10.1130/B31008.1.

Dyman, T.S., and Nichols, D.J. 1988. Stratigraphy of mid-Cretaceous Blackleaf and lower part of the Frontier formations in parts of Beaverhead and Madison counties, Montana. United States Geological Survey Bulletin 1773. United States Geological Survey, Denver, CO. 31p.

Dyman, T.S., and Tysdal, R.G. 1998. Stratigraphy and depositional environment of nonmarine facies of Frontier Formation, eastern Pioneer Mountains, southwestern Montana. The Mountain Geologist. **35**: 115–125.

Dyman, T.S., Porter, K.W., Tysdal, R.G., Cobban, W.A., and Obradovich, J.D. 2000. Late Albian Blackleaf and Thermopolis-Muddy sequence in southwestern Montana and correlation with time-equivalent strata in west-central Montana. *In* Montana Geological Society 50th Anniversary Symposium, **Volume I**: Montana Geological Society, Billings, MT. pp. 65–81.

Eicher, D.L. 1958. The Thermopolis Shale in eastern Wyoming. *In* Powder River Basin of Wyoming; 13th Annual Field Conference guidebook. Wyoming Geological Association, Casper, WY. pp. 79–83.

Eicher, D.L. 1962. Biostratigraphy of the Thermopolis, Muddy, and Shell Creek formations. *In* 17th Annual Field Conference Guidebook. Wyoming Geological Association, Casper, WY. pp. 72–93.

Enkin, R.J. 2006. Paleomagnetism and the case for Baja British Columbia. *In* Paleogeography of the North American Cordillera: Evidence for and against large-scale displacements. *Edited by* J.W. Haggart, R.J. Enkin and J.W.H. Monger. Geological Association of Canada Special Paper 46. Geological Association of Canada, St. John's, NL. pp. 233–254.

Fillmore, R.P. 1991. Tectonic influence on sedimentation in the southern Sevier foreland Iron Springs Formation (Upper Cretaceous), southwestern Utah. *In* Stratigraphy, depositional environments, and sedimentary tectonics of the western margin, Cretaceous Western Interior Seaway. *Edited by* J.D. Nations and J.G. Eaton. Geological Society of America Special Paper 260. Geological Society of America, Boulder, CO. pp. 9–25.

Finn, T.M. 2021. Stratigraphic cross sections of the Mowry Shale and associated strata in the Wind River Basin, Wyoming. United States Geological Survey, Scientific Investigations Map 3476. United States Geological Survey, Denver, CO. 14p.

Finzel, E.S. 2014. Detrital zircons from Cretaceous midcontinent strata reveal an Appalachian Mountains-Cordilleran foreland basin connection. Lithosphere, **6:** 378–382. doi:10.1130/L400.1.

Finzel, E.S. 2017. Detrital zircon microtextures and U-Pb geochronology of Upper Jurassic to Paleocene strata in the distal North Ameri-

can Cordillera foreland basin. Tectonics, **36**: 1295–1316. doi:10.1002/2017TC004549.1295.

Fleck, R.J. 1970. Tectonic style, magnitude, and age of deformation in the Sevier orogenic belt in southern Nevada and eastern California. Geological Society of America Bulletin, **81**: 1705–1720. doi:10.1130/0016-7606(1970)81[1705:TSMAAO]2.0.CO;2.

Fleck, R.J., and Carr, M.D. 1990. The age of the Keystone thrust: laser-fusion $^{40}Ar/^{39}Ar$ dating of foreland basin deposits, southern Spring Mountains, Nevada. Tectonics **9**: 467–476. doi:10.1029/TC009i003p00467.

Fleck, R.J., Mattinson, J.M., Busby, C.J., Carr, M.D., Davis, G.A., and Burchfiel, B.C. 1994. Isotopic complexities and the age of the Delfonte volcanic rocks, eastern Mescal Range, southeastern California: stratigraphic and tectonics implications. Geological Society of America Bulletin, **106**: 1242–1253. doi:10.1130/0016-7606(1994)106⟨1242:ICATAO⟩2.3.CO;2.

Flück, P., Hyndman, R.D., and Lowe, C. 2003. Effective elastic thickness *Te* of the lithosphere in western Canada. Journal of Geophysical Research, **108**: 2430. doi:10.1029/2002JB002201.

Fuentes, F., DeCelles, P.G., Constenius, K.N., and Gehrels, G.E. 2011. Evolution of the Cordilleran foreland basin system in northwestern Montana, USA. Geological Society of America Bulletin, **123**: 507–533. doi:10.1130/B30204.1.

Gardner, J.D., and Cifelli, R.L. 1999. A primitive snake from the mid-Cretaceous of Utah, USA—the geologically oldest snake from the New World. Special Papers in Palaeontology, **60**: 87–100.

Garrison, J.R., Brinkman, D., Nichols, D.J., Layer, P., Burge, D., and Thayn, D. 2007. A multidisciplinary study of the Lower Cretaceous Cedar Mountain Formation, Mussentuchit Wash, Utah: a determination of the paleoenvironment and paleoecology of the *Eolambia caroljonesa* dinosaur quarry. Cretaceous Research, **28**: 461–494. doi:10.1016/j.cretres.2006.07.007.

Gastil, R.G., Diamond, J., Knaack, C., Walawender, M., Marshall, M., Boyles, C., et al. 1990. The problem of the magnetite/ilmenite boundary in Southern and Baja California. *In* The nature and origin of Cordilleran magmatism. *Edited by* J.L. Anderson. Geological Society of America Memoir 174. Geological Society of America, Boulder, CO. pp. 19–32. doi:10.1130/MEM174-p19.

Gastil, R.G., Phillips, R.P., and Allison, E.C. 1975. Reconnaissance geology of the state of Baja California: Geological Society of America Memoir 140. Geological Society of America, Boulder, CO. 201p. doi:10.1130/MEM140-p1.

Gentry, A., Yonkee, W.A., Wells, M.L., and Balgord, E.A. 2018. Resolving the history of early fault slip and foreland basin evolution along the Wyoming salient of the Sevier fold-and-thrust belt: integrating detrital zircon geochronology, provenance modeling, and subsidence analysis. *In* Tectonics, sedimentary basins, and provenance: A celebration of William R. Dickinson's career. *Edited by* R.V. Ingersoll, T.F. Lawton and S.A. Graham. Geological Society of America Special Paper 540. Geological Society of America, Boulder, CO. pp. 509–545. doi:10.1130/2018.2540(23).

Giallorenzo, M. 2013. Application of (U-Th)/He and $^{40}Ar/^{39}Ar$ thermochronology to the age of thrust faulting in the Sevier orogenic belt. Unpublished Ph.D. dissertation. University of Nevada, Las Vegas, NV. 281p.

Gianni, G.M., and Navarrete, C.R. 2022. Catastrophic slab loss in southwestern Pangea preserved in the mantle and igneous record. Nature Communication, **13**, 698. doi:10.1038/s41467-022-28290-z.

Gibson, D.W. 1992. Stratigraphy and sedimentology of the Lower Cretaceous Hulcross and Boulder Creek formations, northeastern British Columbia. Geological Survey of Canada Bulletin 440. Geological Survey of Canada, Ottawa, ON. 105p.

Gladwin, K., and Johnston, S.T. 2006. Mid-Cretaceous pinning of accreted terranes to miogeoclinal assemblages in the northern Cordillera: irreconcilable with paleomagnetic data. *In* Paleogeography of the North American Cordillera: Evidence for and against Large-Scale Displacements. *Edited by* J.W. Haggart, R.J. Enkin and J.W.H. Monger. Geological Association of Canada Special Paper 46. Geological Association of Canada, St. John's, NL. pp. 299–306.

González-Léon, C., and Jacques-Ayala, C. 1988. Estratigrafía de las rocas cretácicas del área de Cerro de Oro, Sonora central. Boletín de Departmento de Universidad Sonora, **5**: 1–23.

González-León, C., Solari, L., Solé, J., Ducea, M.N., Lawton, T.F., Bernal, J.P., et al. Stratigraphy, geochronology, and geochemistry of the Laramide magmatic arc in north-central Sonora, Mexico. Geosphere, **7**: 1392–1418. doi:10.1130/GES00679.1.

González-León, C.M., Scott, R.W., Löser, H., Lawton, T.F., Robert, E., and Valencia, V.A. 2008. Upper Aptian–Lower Albian Mural Formation: stratigraphy, biostratigraphy and depositional cycles on the Sonoran shelf, northern México. Cretaceous Research, **29**: 249–266. doi:10.1016/j.cretres.2007.06.001.

Grantz, A., Hart, P.E., and Childers, V.A. 2011. Geology and tectonic development of the Amerasia and Canada basins, Arctic Ocean, *In* Arctic petroleum geology. *Edited by* A.M. Spencer, A.F. Embry, D.L. Gautier, A.V. Stoupakova and K. Sorensen. Geological Society of London Memoir 35. Geological Society, London. pp. 771–799. doi:10.1144/M35.50.Memoirs35.

Greenhalgh, B.W. 2006. A stratigraphic and geochronologic analysis of the Morrison Formation/Cedar Mountain Formation boundary, Utah. MS thesis, Brigham Young University, Provo, UT. 61p.

Greenhalgh, B.W., and Britt, B.B. 2007. Stratigraphy and sedimentology of the Morrison–Cedar Mountain Formation boundary, east-central Utah. *In* Central Utah—Diverse geology of a diverse landscape. *Edited by* G.C. Willis, M.D. Hylland, D.L. Clark and T.C. Chidsey, Jr. Utah Geological Association Publication 36. Utah Geological Association, Salt Lake City, UT. pp. 81–100.

Gries, R. 1983. North-south compression of Rocky Mountain foreland structures. *In* Mountain foreland basins and uplifts. *Edited by* J.D. Lowell, R. Gries and R. Denver. Rocky Mountain Association of Geologists, Denver, CO. pp. 9–32.

Gromet, L.P., and Silver, L.T. 1987. REE variations across the Peninsular Ranges batholith: implications for batholithic petrogenesis and crustal growth in magmatic arcs. Journal of Petrology, **28**: 75–125. doi:10.1093/petrology/28.1.75.

Gurnis, M. 1992. Rapid continental subsidence following the initiation and evolution of subduction. Science, **255**: 1556–1558. doi:10.1126/science.255.5051.1556.

Gustason, E.R. 1988. Depositional and tectonic history of the lower Cretaceous Muddy Sandstone, Lazy B Field, Powder River Basin, Wyoming. *In* Eastern Powder River Basin - Black Hills. Wyoming Geological Association, 39th Annual Field Conference Guidebook. Wyoming Geological Association, Casper, WY. pp. 129–146.

Hadlari, T., Davis, W.J., Dewing, K., Heaman, L.M., Lemieux, Y., Ootes, L., et al. 2012. Two detrital zircon signatures for the Cambrian passive margin of northern Laurentia highlighted by new U-Pb results from northern Canada. Geological Society of America Bulletin. **124**: 1155–1168. doi:10.1130/B30530.1.

Hadlari, T., Maclean, B.C., Galloway, J.M., Sweet, A.R., White, J.M., Thomson, D., et al. 2014. The flexural margin, the foredeep, and the orogenic margin of a northern Cordilleran foreland basin: Cretaceous tectonostratigraphy and detrital zircon provenance, northwestern Canada. Marine and Petroleum Geology, **57**: 173–186. doi:10.1016/j.marpetgeo.2014.05.019.

Hamlin, H. S. 1996. Frontier Formation stratigraphy on the Moxa arch, Green River Basin, Wyoming. The Mountain Geologist, **33**: 35–44.

Hannon, J.S. 2020. Reconstructing the generation, evolution, and migration of arc magmatism using the whole-rock geochemistry of bentonites: a case study from the Cretaceous Idaho-Farallon arc system. Ph.D. Dissertation, University of Cincinnati, Cincinnati, OH. 189p.

Hannon, J.S., Huff, W.D., and Sturmer, D.M. 2019. Geochemical relationships in Cretaceous bentonites as inferred from linear discriminant analysis: Sedimentary Geology, **390**: 1–14. doi:10.1016/j.sedgeo.2019.07.001.

Hansen, S.E., Nyblade, A.A., and Julia, J. 2009. Estimates of crustal and lithospheric thicknesses in sub-Saharan Africa from S-wave receiver functions. South African Journal of Geology, **112**: 229–240. doi:10.2113/gssajg.112.3-4.229.

Harris, R. 2011. The nature of the Banda arc–continent collision in the Timor region. *In* Arc continent collision. *Edited by* D. Brown and P.D. Ryan. Frontiers in earth sciences, Springer Verlag, Berlin, pp. 163–211.

Hart, C.J.R., Goldfarb, R.J., Lewis, L.L., and Mair, J.L. 2004. The northern Cordillera mid-Cretaceous plutonic province: ilmenite/magnetite-series granitoids and intrusion-related mineralisation. Resource Geology, **54**: 253–280. doi:10.1111/j.1751-3928.2004.tb00206.x.

Haxel, G.B., and Miller, D.M. 2007. Mesozoic rocks. *In* Geology and mineral resources of the East Mojave National Scenic Area, San Bernardino County, California. *Edited by* T.G. Theodore. United States Geological Survey Bulletin, 2160. United States Geological Survey, Denver, CO. pp.59–66.

Hay, M.J., and Plint, A.G. 2020. High-frequency sequences within a retrogradational deltaic succession: upper Cenomanian Dunvegan Formation, Western Canada foreland basin. Depositional Record, **6**: 524–551. doi:10.1002/dep2.114.

Hayes, B.J.R., Christopher, J.E., Rosenthal, L., Los, G., McKercher, B., Minken, D., et al. 1994. Chapter 19 – Cretaceous Mannville Group of the Western Sedimentary basin. *In* Geological atlas of the western Canadian sedimentary basin. *Compiled by* G.D. Mossop and I. Shetson. Canadian Society of Petroleum Geologists and Alberta Research Council, Calgary, AB. pp.317–334.

Heirtzler, J.R. 1974. Site 262. *In* initial reports of the Deep-Sea Drilling Project; Fremantle, Australia to Fremantle, Australia; November-December 1972: site reports. Initial Reports of the Deep-Sea Drilling Project. **27**: 193–278.

Heller, P.L., and Paola, C. 1989. The paradox of lower Cretaceous gravels and the initiation of thrusting in the Sevier orogenic belt, United States Western Interior. Geological Society of America Bulletin, **101**: 864–875. doi:10.1130/0016-7606(1989)101⟨0864:TPOLCG⟩2.3.CO;2.

Heller, P.L., Bowler, S.S., Chambers, H.P., Coogan, J.C., Hagen, E.S., Shuster, M.W., et al. 1986. Time of initial thrusting in the Sevier orogenic belt, Idaho-Wyoming and Utah. Geology, **14**: 388–391. doi:10.1130/0091-7613(1986)14⟨388:TOITIT⟩2.0.CO;2.

Heller, P.L., Ducker, K., and McMillan, M.E. 2003. Post-Paleozoic alluvial gravel transport as evidence of continental tilting in the U.S. Cordillera. Geological Society of America Bulletin, **115**: 1122–1132. doi:10.1130/B25219.1.

Helwig, J. 1974. Eugeosynclinal basement and a collage concept of orogenic belts. *In* Modern and ancient geosynclinal sedimentation. *Edited by* R.H. Dott, Jr. and R.H. Shaver. SEPM Special Publication 19. SEPM, Tulsa, OK. pp. 359–376.

Hildebrand, R.S. 2013. Mesozoic assembly of the North American Cordillera. Geological Society of America Special Paper 495. Geological Society of America, Boulder, CO. 169p. doi:10.1130/2013.2495.

Hildebrand, R.S. 2014. Geology, mantle tomography, and inclination corrected paleogeographic trajectories support westward subduction during Cretaceous orogenesis in the North American Cordillera. Geoscience Canada, **41**: 207–224. doi:10.12789/geocanj.2014.41.032.

Hildebrand, R.S. 2015. Dismemberment and northward migration of the Cordilleran orogen: Baja-BC resolved. GSA Today, **25**: 4–11. doi:10.1130/GSATG255A.1.

Hildebrand, R.S., and Whalen, J.B. 2014. Arc and slab-failure magmatism in Cordilleran batholiths II—The Cretaceous Peninsular Ranges batholith of Southern and Baja California. Geoscience Canada, **41**: 399–458. doi:10.12789/geocanj.2014.41.059.

Hildebrand, R.S., and Whalen, J.B. 2017. The tectonic setting and origin of Cretaceous batholiths within the North American Cordillera: the case for slab failure magmatism and its significance for crustal growth. Geological Society of America Special Paper 532. Geological Society of America, Boulder, CO. 113p.

Hildebrand, R.S., and Whalen, J.B. 2021a. The mid-Cretaceous Peninsular Ranges orogeny: a new slant on Cordilleran tectonics? I: Mexico to Nevada. Canadian Journal of Earth Sciences, **58**: 670–696. doi:10.1139/cjes-2020-0154.

Hildebrand, R.S., and Whalen, J.B. 2021b. The mid-Cretaceous Peninsular Ranges orogeny: a new slant on Cordilleran tectonics? II: northern United States and Canada. Canadian Journal of Earth Sciences, **58**: 697–719. doi:10.1139/cjes-2021-0006.

Hildebrand, R.S., Whalen, J.B., and Bowring, S.A. 2018. Resolving the crustal composition paradox by 3.8 billion years of slab failure magmatism and collisional recycling of continental crust. Tectonophysics, **734-735**: 69–88. doi:10.1016/j.tecto.2018.04.001.

Hoffman, P.F. 2012. The Tooth of time: how do passive margins become active? Geoscience Canada, **39**: 67–73.

Hunt, G.J., Lawton, T.F., and Kirkland, J.I. 2011. Detrital zircon U-Pb geochronological provenance of lower Cretaceous strata, foreland basin, Utah. *In* Sevier thrust belt—northern and central Utah and adjacent areas. *Edited by* D.A. Sprinkel, W.A. Yonkee and T.C. Chidsey. Utah Geological Association Publication 40. Utah Geological Association, Salt Lake City, UT. pp. 193–211.

Husson, L., Bernet, M., Guillot, S., Huyghe, P., Mugnier, J-L., Replumaz, A., et al. 2014. Dynamic ups and downs of the Himalaya. Geology, **42**: 839–842. doi:10.1130/G36049.1.

Hutsky, A.J., Fielding, C.R., Hurd, T.J., and Kittinger Clark, C. 2012. Sedimentology and stratigraphy of the upper Cretaceous (Cenomanian) Frontier Formation, northeast Bighorn Basin, Wyoming, USA. The Mountain Geologist, **49**: 77–98.

Hylland, M.D. 2010. Geologic map of the Clear Creek Mountain Quadrangle, Kane County, Utah. Utah Geological Survey Map 245, two plates, scale 1:24,000. Utah Geological Survey, Salt Lake City, UT.

Jacobi, R.D. 1981. Peripheral bulge – a causal mechanism for the lower/middle Ordovician unconformity along the western margin of the northern Appalachians. Earth and Planetary Science Letters, **56**: 245–251. doi:10.1016/0012-821X(81)90131-X.

Jacques-Ayala, C. 1992. Stratigraphy of the lower Cretaceous Cintura Formation, Sierra el Chanate, northwestern Sonora, Mexico. Universidad Nacional Autónoma de México, Instituto de Geologia Revista, **10**: 129–136.

Jacques-Ayala, C. 1995. Paleogeography and provenance of the lower Cretaceous Bisbee Group in the Caborca-Santa Ana area, northwestern Sonora. *In* Studies on the Mesozoic of Sonora and adjacent areas. *Edited by* C. Jacques-Ayala, C.M. González-León and J. Roldán-Quintana. Geological Society of America Special Paper 301. Geological Society of America, Boulder, CO. pp. 79–98. doi:10.1130/0-8137-2301-9.79.

Jamieson, R.A., and Beaumont, C. 1988. Orogeny and metamorphism: a model for deformation and pressure-temperature-time paths with applications to the central and southern Appalachians. Tectonics, **7**: 417–445. doi:10.1029/TC007i003p00417.

Joeckel, R.M., Ludvigson, G.A., Möller, A., Hotton, C.L., Suarez, M.B., Suarez, C.A., et al. 2020. Chronostratigraphy and terrestrial palaeoclimatology of Berriasian–Hauterivian strata of the Cedar Mountain Formation, Utah, USA. *In* Cretaceous climate events and short-term sea-level changes. *Edited by* M. Wagreich, M. B. Hart, B. Sames and I.O. Yilmaz. Geological Society of London, Special Publication 498. Geological Society of London, London. doi:10.1144/SP498-2018-133.SP49875.

Jordan, T.E. 1981. Thrust loads and foreland basin evolution, Cretaceous, western United States. AAPG Bulletin, **65**: 2506–2520.

Kauffman, E.G. 1977. Geological and biological overview: Western Interior Cretaceous basin. The Mountain Geologist, **14**: 75–99.

Kauffman, E.G., and Caldwell, W.G.E. 1993. The Western Interior basin in space and time. *In* Evolution of the Western Interior Basin. *Edited by* W.G.E. Caldwell and E.G. Kauffman. Geological Association of Canada Special Paper 39. Geological Association of Canada, St. John's, NL. pp. 1–30.

Kent, D.V., and Irving, E. 2010. Influence of inclination error in sedimentary rocks on the Triassic and Jurassic apparent pole wander path for North America and implications for Cordilleran tectonics. Journal of Geophysical Research, **115**: doi:10.1029/2009JB007205.

Khandaker, N.I. 1991. Tectonosedimentologic significance of the upper Cretaceous Frontier Formation, north-central Wyoming. Ph.D. dissertation. Iowa State University, Ames, IA, 251p.

Kimbrough, D.L., Abbott, P.L., Balch, D.C., Bartling, S.H., Grove, M., Mahoney, J.B., and Donohue, R.F. 2014. Upper Jurassic Peñasquitos Formation—forearc basin western wall rock of the Peninsular Ranges batholith. *In* Peninsular Ranges batholith, Baja California and Southern California. *Edited by* D.M. Morton and F.K. Miller. Geological Society of America Memoir 211. Geological Society of America, Boulder, CO. pp. 625–643. doi:10.1130/2014.1211(19).

Kimbrough, D.L., Smith, D.P., Mahoney, J.B., Moore, T.E., Grove, M., Gastil, R.G., et al. 2001. Forearc-basin sedimentary response to rapid late Cretaceous batholith emplacement in the Peninsular Ranges of southern and Baja California. Geology, **29**: 491–494. doi:10.1130/0091-7613(2001)029%3c0491:FBSRTR%3e2.0.CO;2.

Kirkland, J.I., and Madsen, S.K. 2007. The lower Cretaceous Cedar Mountain Formation, eastern Utah:—the view up an always interesting learning curve. *In* Field guide to geological excursions in southern Utah. *Edited by* W.R. Lund. Geological Society of America Rocky Mountain Section 2007 Annual Meeting, Grand Junction Geological Society,

and Utah Geological Association Publication 35, Salt Lake City, UT, pp. 1–108. Compact disc.

Kirkland, J.I., Britt, B.B., Burge, D.L., Carpenter, K., Cifelli, R., DeCourten, F., et al. 1997. Lower to middle Cretaceous dinosaur faunas of the central Colorado Plateau—a key to understanding 35 million years of tectonics, sedimentology, evolution, and biogeography. Brigham Young University Geology Studies, **42 (pt. II)**: 69–103.

Kirkland, J.I., Cifelli, R., Britt, B.B., Burge, D.L., DeCourten, F., Eaton, J., and Parrish, J.M. 1999. Distribution of vertebrate faunas in the Cedar Mountain Formation, east-central Utah. *In* Vertebrate paleontology in Utah. *Edited by* D.D. Gillette. Utah Geological Survey Miscellaneous Publication 99-1. Utah Geological Survey, Salt Lake City, UT. pp. 201–217.

Kirkland, J.I., Suarez, M., Suarez, C., and Hunt-Foster, R. 2016. The Lower Cretaceous in east-central Utah—the Cedar Mountain Formation and its bounding strata. Geology of the Intermountain West, **3**: 101–228. doi:10.31711/giw.v3.pp101-228.

Kirschbaum, M.A., and Mercier, T.J. 2013. Controls on the deposition and preservation of the Cretaceous Mowry Shale and Frontier Formation and equivalents, Rocky Mountain region, Colorado, Utah, and Wyoming. AAPG Bulletin, **97**: 899–921. doi:10.1306/10011212090.

Kirschbaum, M.A., and Roberts, L.N.R. 2005. Stratigraphic framework of the Cretaceous Mowry Shale, Frontier Formation and adjacent units, southwestern Wyoming province, Wyoming, Colorado, and Utah. *In* Petroleum systems and geologic assessment of oil and gas in the southwestern Wyoming province: Wyoming, Colorado, and Utah. U.S. Geological Survey Digital Data Series DDS–69–D. Denver, CO. 31p.

Kowallis, B.J., Britt, B.B., Greenhalgh, B.W., and Spinkel, D.A. 2007. New U-Pb zircon ages from an ash bed in the Brushy Basin Member of the Morrison Formation near Hanksville, Utah. *In* Central Utah—Diverse geology of a diverse landscape. *Edited by* G.C. Willis, M.D. Hylland, D.L. Clark and T.C. Chidsey, Jr. Utah Geological Association Publication 36. Utah Geological Association, Salt Lake City. pp. 75–80.

Kowallis, B.J., Christiansen, E.H., Deino, A.L., Peterson, F., Turner, C.E., Kunk, M.J., and Obradovich, J.D. 1998. The age of the Morrison Formation. Modern Geology, **22**: 235–260.

Krumenacker, L.J. 2010. Chronostratigraphy and paleontology of the mid-Cretaceous Wayan Formation of eastern Idaho, with a description of the first *Oryctodromeus* specimens from Idaho. Unpublished MSc thesis, Brigham Young University, Provo, UT. 88p.

Lackey, J.S., Valley, J.W., Chen, J.H., and Stockli, D.F. 2008. Dynamic magma systems, crustal recycling, and alteration in the central Sierra Nevada batholith: the oxygen isotope record. Journal of Petrology, **49**: 1397–1426. doi:10.1093/petrology/egn030.

Langenberg, C.W., Hein, F.J., Bieber, K., Losert, J., Berhane, H., and Cotterill, D.K. 2000. Regional geology of the upper Blairmore Group and Bow Island Formation: a subsurface study in southwestern Alberta. Alberta Energy and Utilities Board, Alberta Geological Survey, Earth Sciences Report 2000-6. Alberta Geological Survey, Edmonton, AB. 68p.

Langenheim, V.E., Jachens, R.C., and Aiken, C. 2014. Geophysical framework of the Peninsular Ranges batholith—implications for tectonic evolution and neotectonics. *In* Peninsular Ranges batholith, Baja California and Southern California. *Edited by* D.M. Morton and F.K. Miller. Geological Society of America Memoir 211. Geological Society of America, Boulder, CO. pp. 1–20. doi:10.1130/2014.1211(01).

Larson, K.P., Price, R.A., and Archibald, D.A. 2006. Tectonic implications of $^{40}Ar/^{39}Ar$ muscovite dates from the Mt. Haley stock and Lussier River stock, near Fort Steele, British Columbia. Canadian Journal of Earth Sciences, **43**: 1673–1684. doi:10.1139/e06-048.

Lawton, T.F., Amato, J.M., Machin, S.E.K., Gilbert, J.C., and Lucas, S.G. 2020b. Transition from Late Jurassic rifting to middle Cretaceous dynamic foreland, southwestern U.S. and northwestern Mexico. Geological Society of America Bulletin, **132**: 2489–2516. doi:10.1130/B35433.1.

Lawton, T.F., González-León, C.M., Lucas, S.G., and Scott, R.W. 2004. Stratigraphy and sedimentology of the Upper Aptian–Upper Albian Mural limestone (Bisbee Group) in northern Sonora, Cretaceous Research, **25**: 43–60. doi:10.1016/j.cretres.2003.09.003.

Lawton, T.F., Hunt, G.J., and Gehrels, G.E. 2010. Detrital zircon record of thrust belt unroofing in Lower Cretaceous synorogenic conglomerates, central Utah. Geology, **38**: 463–466. doi:10.1130/G30684.1.

Lawton, T.F., Pindell, J., Beltran-Triviño, A., Juárez-Arriaga, E., Molina-Garza, R., and Stockli, D. 2015. Late Cretaceous-Paleogene foreland sediment-dispersal systems in northern and eastern Mexico: Interpretations from preliminary detrital-zircon analysis. AAPG Search and Discovery Article #30423. American Association of Petroleum Geologists, Tulsa, OK.

Lawton, T.F., Sierra-Rojas, M.I., and Martens, U. 2020a. Stratigraphic correlation chart of Carboniferous–Paleogene rocks of Mexico, adjacent southwestern United States, Central America, and Colombia. *In* Southern and Central Mexico: Basement Framework, Tectonic Evolution, and Provenance of Mesozoic–Cenozoic Basins. *Edited by* U. Martens and R.S. Molina Garza. Geological Society of America Special Paper 546. Geological Society of America, Boulder, CO. pp. 115–142. doi:10.1130/2020.2546(05).

Lawton, T.F., Sprinkel, D.A., and Waanders, G.L. 2007. The Cretaceous Canyon Range Conglomerate, central Utah—stratigraphy, structure and significance. *In* Central Utah—diverse geology of a dynamic landscape. *Edited by* G.C. Willis, M.D. Hylland, D.L. Clark and T.C. Chidsey, Jr. Utah Geological Association Publication 36. Utah Geological Association, Salt Lake City, UT. pp.101–122.

Leckie, D.A., and Burden, E.T. 2001. Stratigraphy, sedimentology and palynology of the Cretaceous (Albian) Beaver Mines, Mill Creek and Crowsnest formations (Blairmore Group) of southwestern Alberta. Geological Survey of Canada Bulletin **563**: 103p.

Leckie, D.A., and Cheel, R.J. 1997. Sedimentology and depositional history of Lower Cretaceous coarse-grained clastics, southwest Alberta and southeast British Columbia. Bulletin of Canadian Petroleum Geology, **45**: 1–24.

Leckie, D.A., and Craw, D. 1995. Westerly derived early Cretaceous gold paleoplacers in the Western Canada foreland basin, southwestern Alberta: tectonic and economic implications. Canadian Journal of Earth Sciences, **32**: 1079–1092. doi:10.1139/e95-090.

Leckie, D.A., and Reinson, G.E. 1993. Effects of middle to late Albian sea-level fluctuations in the Cretaceous interior seaway, Western Canada. *In* Evolution of the Western Interior Basin. *Edited by* W.G.E. Caldwell and E.G. Kauffman. Geological Association of Canada, Special Paper 39. Geological Association of Canada, St. John's, NL. pp. 151–175.

Leckie, D.A., and Singh, C. 1991. Estuarine deposits of the Albian Paddy Member (Peace River Formation) and lowermost Shaftesbury Formation, Alberta, Canada. Journal of Sedimentary Petrology, **61**: 825–849.

Leckie, D.A., and Smith, D.G. 1992. Regional setting, evolution, and depositional cycles of the western Canada foreland basin. *In* Foreland basins and fold belts. *Edited by* R.W. MacQueen and D.A. Leckie. American Association of Petroleum Geologists Memoir 55. American Association of Petroleum, Tulsa, OK. pp. 9–46.

Leckie, D.A., Bhattacharya, J.P., Bloch, J., Gilboy, C.F., and Norris, B. 1994. Chapter 20 – Cretaceous Colorado/Alberta Group of the western Canada sedimentary basin. *In* Geological atlas of the western Canadian sedimentary basin. *Compiled by* G.D. Mossop and I. Shetson. Canadian Society of Petroleum Geologists and Alberta Research Council, Calgary, AB. pp. 335–352.

Leckie, D.A., Fox, C., and Tornacai, C. 1989. Multiple paleosols of the Late Albian Boulder Creek Formation, British Columbia, Canada. Sedimentology, **36**: 307–323. doi:10.1111/j.1365-3091.1989.tb00609.x.

Leckie, D.A., Singh, C., Bloch, J., Wilson, M., and Wall, J.H. 1992. An anoxic event at the Albian-Cenomanian boundary: the Fish Scale marker bed, northern Alberta, Canada. Palaeogeography, Palaeoclimatology, Palaeoecology, **92**: 139–166. doi:10.1016/0031-0182(92)90139-V.

Leckie, D.A., Staniland, M.R., and Hayes, B.J. 1990. Regional maps of the Albian Peace River and lower Shaftesbury formations on the Peace River arch, northwestern Alberta and northeastern British Columbia. Bulletin of Canadian Petroleum Geology, **38A**: 176–189.

LeFever, R.D., and McCloskey, G.G. 1995. Depositional history of the Newcastle Formation (Lower Cretaceous), Williston Basin, north Dakota, south Dakota and eastern Montana. *In* Seventh International Williston Basin Symposium, July 23, 1995. *Edited by* L.D.V. Hunter and R.A. Schalla. Montana Geological Society, Billings, MT. pp. 411–416.

Leier, A.L., and Gehrels, G.E. 2011. Continental-scale detrital zircon provenance signatures in Lower Cretaceous strata, western North America. Geology, **39**: 399–402. doi:10.1130/G31762.1.

Li, Z., and Aschoff, J. 2022. Constraining the effects of dynamic topography on the development of Late Cretaceous Cordilleran foreland

basin, western United States. Geological Society of America Bulletin. **134**(1-2): 446–462. doi:10.1130/B35838.1.134446.

Lichtner, D.T., Toner, R.N., Wrage, J.M., and Lynds, R.M. 2020. Upper Cretaceous strata in the Powder River Basin: formation tops database, structure and thickness contour maps, and associated well data. Wyoming Geological Survey Open File Report 2020-9. Wyoming Geological Survey, Casper, WY. 50p.

Liu, S., Nummedal, D., and Gurnis, M. 2014. Dynamic versus flexural controls of late Cretaceous Western Interior Basin, USA. Earth and Planetary Science Letters, **389**: 221–229. doi:10.1016/j.epsl.2014.01.006.

Liu, S., Nummedal, D., Yin, P., and Luo, H. 2005. Linkage of Sevier thrusting episodes and Late Cretaceous foreland basin megasequences across southern Wyoming (USA). Basin Research, **17**: 487–506. doi:10.1111/j.1365-2117.2005.00277.x.

Logan, J. 2002. Intrusion-related mineral occurrences of the Cretaceous Bayonne magmatic belt, southeast British Columbia. British Columbia Geological Survey, Geoscience Map 2001-1, scale 1:500,000. British Columbia Geological Survey, Victoria, BC.

Ludvigson, G.A., Joeckel, R.M., González, L.A., Gulbranson, E.L., Rasbury, E.T., Hunt, G.J., et al. 2010. Correlation of Aptian–Albian carbon isotope excursions in continental strata of the Cretaceous foreland basin, eastern Utah, U.S.A. Journal of Sedimentary Research, **80**: 955–974. doi:10.2110/jsr.2010.086.

M'Gonigle, J.W., and Dover, J.H. 1992. Geologic map of the Kemmerer 30′ × 60′ quadrangle, Lincoln, Uinta, and Sweetwater counties, Wyoming. United States Geological Survey Geologic Investigations Map I-2079, scale 1:100,000. United States Geological Survey, Denver, CO.

Mack, G.H. 1987. Mid-Cretaceous (Late Albian) change from rift to retroarc foreland basin in southwestern New Mexico. Geological Society of America Bulletin, **98**: 507–514. doi:10.1130/0016-7606(1987)98⟨507:MLACFR⟩2.0.CO;2.

Mair, J.L., Hart, C.J.R., and Stephens, J.R. 2006. Deformation history of the northwestern Selwyn basin, Yukon, Canada: implications for orogen evolution and mid-Cretaceous magmatism. Geological Society of America Bulletin, **118**: 304–323. doi:10.1130/B25763.1.

Martini, M., and Ferrari, L. 2011. Style and chronology of the Late Cretaceous shortening in the Zihuatanejo area (south-western Mexico): implications for the timing of the Mexican Laramide deformation. Geosphere, **7**: 1469–1479. doi:10.1130/GES00743.1.

Martini, M., Ferrari, L., López-Martínez, M., and Valencia, V. 2010. Stratigraphic redefinition of the Zihuatanejo area, southwestern Mexico. Revista Mexicana de Ciencias Geológicas, **27**: 412–430.

Martini, M., Mori, L., Solari, L., and Centeno-García, E. 2011. Sandstone provenance of the Arperos basin (Sierra de Guanajuato, central Mexico): Late Jurassic–Early Cretaceous back-arc spreading as the foundation of the Guerrero terrane. The Journal of Geology, **119**: 597–617. doi:10.1086/661989.

Martini, M., Solari, L., and Camprubí, A. 2013. Kinematics of the Guerrero terrane accretion in the Sierra de Guanajuato, central Mexico: new insights for the structural evolution of arc–continent collisional zones. International Geology Review, **55**: 574–589. doi:10.1080/00206814.2012.729361.

Martini, M., Solari, L., and Lopez-Martínez, M. 2014. Correlating the Arperos basin from Guanajuato, central Mexico, to Santo Tomás, southern Mexico: implications for the paleogeography and origin of the Guerrero terrane. Geosphere, **10**: 1385–1401. doi:10.1130/GES01055.1.

Mauel, D.J., Lawton, T.F., González-Léon, C., Iriondo, A., and Amato, J.M. 2011. Stratigraphy and age of upper Jurassic strata in north-central Sonora, Mexico: southwestern Laurentian record of crustal extension and tectonic transition. Geosphere, **7**: 390–414. doi:10.1130/GES00600.1.

May, S.R., Gray, G.G., Summa, L.I., Stewart, N.R., Gehrels, G.E., and Pecha, M.E. 2013a. Detrital zircon geochronology from Cenomanian–Coniacian strata in the Bighorn Basin, Wyoming, U.S.A.: implications for stratigraphic correlation and paleogeography. Rocky Mountain Geology, **48**: 41–61. doi:10.2113/gsrocky.48.1.41.

May, S.R., Gray, G.G., Summa, L.L., Stewart, N.R., Gehrels, G.E., and Pecha, M.E. 2013b. Detrital zircon geochronology from the Bighorn Basin, Wyoming, USA: implications for tectonostratigraphic evolution and paleogeography. Geological Society of America Bulletin, **125**: 1403–1422. doi:10.1130/B30824.1.

Mendoza, O.T., and Suastegui, M.G. 2000. Geochemistry and isotopic composition of the Guerrero terrane (western Mexico): implications for the tectono-magmatic evolution of southwestern North America during the late Mesozoic. Journal of South American Earth Sciences, **13**: 297–324. doi:10.1016/S0895-9811(00)00026-2.

Merewether, E.A., and Cobban, W.A. 1986. Evidence of mid-Cretaceous tectonism in the Frontier Formation, Natrona county, Wyoming. Earth Science Bulletin, **1**: 142–152.

Merewether, E.A., Blackmon, P.D., and Webb, J.C. 1984. The mid-Cretaceous Frontier Formation near the Moxa Arch, southwestern Wyoming. United States Geological Survey Professional Paper 1290. United States Geological Survey, Denver, CO. 29p.

Miall, A.D., and Catuneanu, O. 2019. The Western Interior Basin. *In* The sedimentary basins of the United States and Canada. *Edited by* A.D. Miall. Amsterdam, The Netherlands, Elsevier, pp. 401–443.

Miller, D.M., Miller, R.J., Nielson, J.E., Wilshire, H.G., Howard, K.A., and Stone, P. 2007. Geologic map of the East Mojave National Scenic Area, California. *In* Geology and mineral resources of the East Mojave National Scenic Area, San Bernardino County, California. *Edited by* T.G. Theodore. United States Geological Survey Bulletin 2160, Scale 1:125,000. United States Geological Survey, Denver, CO.

Mitrovica, J.X., Beaumont, C., and Jarvis, G.T. 1989. Tilting of continental interiors by the dynamical effects of subduction. Tectonics, **8**: 1079–1094. doi:10.1029/TC008i005p01079.

Molnar, P., England, P. C., and Jones, C.H. 2015. Mantle dynamics, isostasy, and the support of high terrain. Journal of Geophysical Research, Solid Earth, **120**: 1932–1957. doi:10.1002/2014JB011724.

Monger, J.W.H., Price, R.A., and Templeman-Kluitt, D. 1982. Tectonic accretion and the origin of two metamorphic and plutonic welts in the Canadian Cordillera. Geology, **10**: 70–75. doi:10.1130/0091-7613(1982)10⟨70:TAATOO⟩2.0.CO;2.

Monod, O., Busnardo, R., and Guerrero-Suastegui, M. 2000. Late Albian ammonites from the carbonate cover of the Teloloapan arc volcanic rocks (Guerrero State, Mexico). Journal of South American Earth Sciences, **13**: 377–388. doi:10.1016/S0895-9811(00)00030-4.

Mori, H. 2009. Dinosaurian faunas of the Cedar Mountain Formation with detrital zircon ages for three stratigraphic sections and the relationship between the degree of abrasion and U-Pb LA-ICP-MS ages of detrital zircons. M.S. thesis, Brigham Young University, Provo, UT. 102p.

Morris, R.A., DeBari, S.M., Busby, C., Medynski, S., and Jicha, B.R. 2019. Building arc crust: plutonic to volcanic connections in an extensional oceanic arc, the southern Alisitos arc, Baja California. Journal of Petrology, **60**: 1195–1228. doi:10.1093/petrology/egz029.

Mueller, P.A., Wooden, J.L., Mogk, D.W., and Foster, D.A. 2011. Paleoproterozoic evolution of the Farmington zone: implications for terrane accretion in southwestern Laurentia. Lithosphere, **3**: 401–408. doi:10.1130/L161.1.

Murphy, D.C. 1997. Geology of the McQuesten River region, northern McQuesten and Mayo map area, Yukon Territory, (115P/14, 15, 16; 105 M/13, 14). Exploration and Geological Services Division, Yukon, Indian and Northern Affairs Canada, Bulletin 6. Yukon, Indian and Northern Affairs Canada, Whitehorse, YT. 122p.

Nelson, S., Harris, R., Dorais, M., Heizler, M., Constenius, K., and Barnett, D. 2002. Basement complexes in the Wasatch fault, Utah, provide new limits on crustal accretion. Geology, **30**: 831–834. doi:10.1130/0091-7613(2002)030⟨0831:BCITWF⟩2.0.CO;2.

Norris, D.K., Stevens, R.D., and Wanless, R.K. 1965. K-Ar age of igneous pebbles in the McDougall-Segur conglomerate, southeastern Canadian Cordillera. Geological Survey of Canada, Paper 65-26. Geological Survey of Canada, Ottawa, ON. 11p.

Ogg, J.G., and Hinnov, L.A. 2012. Cretaceous. *In* The geologic time scale 2012. *Edited by* F.M. Gradstein, J.G. Ogg, M. Schmitz and G. Ogg. Elsevier, Amsterdam. pp. 793–853. doi:10.1016/B978-0-444-59425-9.00027-5.

Oriel, S.S., and Platt, L.B. 1980. Geologic map of the Preston 1° x 2° quadrangle, southeast Idaho and western Wyoming. United States Geological Survey, Geologic Investigations Map I-1127, scale 1:250,000. United States Geological Survey, Denver, CO.

Page, W.R., Lundstrom, S.C., Harris, A.G., Langenheim, V.E., Workman, J.B. Mahan, S.A., et al. 2005. Geologic and geophysical maps of the Las Vegas 30° x 60° Quadrangle, Clark and Nye Counties, Nevada,

and Inyo County, California. United States Geological Survey Scientific Investigations Map 2814, scale 1:100,000. United States Geological Survey, Denver, CO.

Painter, C.S., Carrapa, B., DeCelles, P.G., Gehrels, G.F., and Thomson, S.N. 2014. Exhumation of the North American Cordillera revealed by multi-dating of Upper Jurassic–Upper Cretaceous foreland basin deposits. Geological Society of America Bulletin, **126**: 1439–1464. doi:10.1130/B30999.1.

Pana, D.I., and van der Pluijm, B.A. 2015. Orogenic pulses in the Alberta Rocky Mountains: radiometric dating of major faults and comparison with the regional tectono-stratigraphic record. Geological Society of America Bulletin, **127**: 480–502. doi:10.1130/B31069.1.

Pana, D.I., Poulton, T.P., and DuFrane, S.A. 2019. U-Pb detrital zircon dating supports early Jurassic initiation of the Cordilleran foreland basin in southwestern Canada. Geological Society of America Bulletin, **131**: 318–334. doi:10.1130/B31862.1.

Pana, D.I., Poulton, T.P., and Heaman, L.M. 2018a. U-Pb zircon ages of volcanic ashes integrated with ammonite biostratigraphy, Fernie Formation (Jurassic), Western Canada, with implications for Cordilleran-foreland basin connections and comments on the Jurassic time scale. Bulletin of Canadian Petroleum Geology, **66:** 595–622.

Pana, D.I., Rukhlov, A.S., Heaman, L.M., and Hamilton, M. 2018b. Geochronology of selected igneous rocks in the Alberta Rocky Mountains, with an overview of the age constraints on the host formations. Alberta Energy Regulator/Alberta Geological Survey Open-File Report 2018-03. Alberta Geological Survey, Edmonton, AB. 67p.

Pape, D.E., Spell, T.L., Bonde, J.W., Fish, B., and Rowland, S.M. 2011. $^{40}Ar/^{39}Ar$ isotopic dates for the fossiliferous Willow Tank Formation (Cretaceous) in Valley of Fire State Park, Nevada. Geological Society of America Abstracts with Programs, **43**(5): 586.

Pavlis, T.L., Amato, J.M., Trop, J.M., Ridgway, K.D., Roeske, S.M., and Gehrels, G.E. 2020. Subduction polarity in ancient arcs: a call to integrate geology and geophysics to decipher the Mesozoic tectonic history of the northern Cordillera of North America. GSA Today, **29**: 4–10. doi:10.1130/GSATG465Y.1.

Pearce, J.A., Harris, N.B.W., and Tindle, A.G. 1984. Trace element discrimination diagrams for the tectonic interpretation of granitic rocks. Journal of Petrology, **25**: 956–983. doi:10.1093/petrology/25.4.956.

Peccerillo, A. 2005. Plio-Quaternary volcanism in Italy: Petrology, Geochemistry, Geodynamics. New York, Springer-Verlag, 365p with CD-ROM.

Peterson, T.D., Currie, K.L., Ghent, E.D., Bégin, N.J., and Beiersdorfer, R.E. 1997. Petrology and economic geology of the Crowsnest volcanics, Alberta. *In* Exploring for minerals in Alberta. *Edited by* R.W. MacQueen. Geological Survey of Canada Geoscience Contributions, Canada-Alberta agreement on mineral development (1992–1995). Geological Survey of Canada Bulletin 500. Geological Survey of Canada, Ottawa, ON. pp. 163–184.

Plint, A.G. 2000. Sequence stratigraphy and paleogeography of a Cenomanian deltaic complex: the Dunvegan and lower Kaskapau formations in subsurface and outcrop, Alberta and British Columbia, Canada. Bulletin of Canadian Petroleum Geology, **48**: 43–79. doi:10.2113/48.1.43.

Plint, A.G., Krawetz, J.R., Buckley, R.A., Vannelli, K.M., and Walaszczyk, I. 2018. Tectonic, eustatic and climatic controls on marginal-marine sedimentation across a flexural depocentre: Paddy Member of Peace River Formation (Late Albian), western Canada foreland basin. Depositional Record, **4**: 4–58. doi:10.1002/dep2.37.

Plint, A.G., Tyagi, A., Hay, M.J., Varban, B.L., Zhang, H., and Roca, X. 2009. Clinoforms, paleobathymetry, and mud dispersal across the Western Canada Cretaceous foreland basin: evidence from the Cenomanian Dunvegan Formation and contiguous strata. Journal of Sedimentary Research, **79**: 144–161. doi:10.2110/jsr.2009.020.

Plint, A.G., Tyagi, A., McCausland, P. J. A., Krawetz, J.R., Zhang, H., Roca, X., et al. 2012. Dynamic relationship between subsidence, sedimentation, and unconformities in mid-Cretaceous, shallow-marine strata of the Western Canada foreland basin: links to Cordilleran tectonics, chapter 24. *In* Tectonics of sedimentary basins: Recent advances. *Edited by* C. Busby and A. Azor. Blackwell Publishing, Oxford, UK. pp. 480–507.

Porter, K.W., Dyman, T.S., Cobban, W.A., and Reinson, G.E. 1998. Post-Manville/Kootenai Lower Cretaceous rocks and reservoirs, north-central Montana, southern Alberta and Saskatchewan. *In* Eighth International Williston Basin Symposium. *Edited by* J.E. Christopher et al. Saskatchewan Geological Society Special Publication 13. Saskatchewan Geological Society, Regina, SK. pp.123–127.

Price, R.A. 1973. Large scale gravitational flow of supracrustal rocks, southern Canadian Rockies. *In* Gravity and tectonics. *Edited by* K.A. De Jong and K. Scholten. John Wiley, New York, pp. 491–502.

Price, R.A. 1994. Chapter 2: Cordilleran tectonics and the evolution of the Western Canada sedimentary basin. *In* Geological atlas of the western Canada sedimentary basin. *Edited by* G. Mossop and I. Shetsen. Canadian Society of Petroleum Geologists and Alberta Research Council, Calgary, AB. pp. 13–24.

Price, R.A., and Sears, J.W. 2000. A preliminary palinspastic map of the Mesoproterozoic Belt-Purcell Supergroup, Canada and USA: implications for the tectonic setting and structural evolution of the Purcell anticlinorium and the Sullivan deposit. *In* The geological environment of the Sullivan deposit, British Columbia. *Edited by* J.W. Lydon, T. Höy, J.F. Slack and M.E. Knapp. Geological Association of Canada Special Publication 1. Geological Association of Canada, St. John's, NL. pp. 61–81.

Pubellier, M., Rangin, C., Rascon, B., Chorowicz, J., and Bellon, H. 1995. Cenomanian thrust tectonics in the Sahuaripa region, Sonora: implications about northwestern Mexico megashears. *In* Studies on the Mesozoic of Sonora and adjacent areas. *Edited by* C. Jacques-Ayala, C.M. González-León and J. Roldán-Quintana. Geological Society of America Special Paper 301. Geological Society of America, Boulder, CO. pp.111–120. doi:10.1130/0-8137-2301-9.111.

Pujols, E.J., Stockli, D.F., Constenius, K.N., and Horton, B.K. 2020. Thermo-chronological and geochronological constraints on late Cretaceous unroofing and proximal sedimentation in the Sevier orogenic belt, Tectonics, **39**: e2019TC005794. doi:10.1029/2019TC005794.

Quick, J.D., Hogan, J.P., Wizevich, M., Obrist-Farner, J., and Crowley, J.L. 2020. Timing of deformation along the Iron Springs thrust, southern Sevier fold-and-thrust belt, Utah: evidence for an extensive thrusting event in the mid-Cretaceous. Rocky Mountain Geology, **55**: 75–89. doi:10.24872/rmgjournal.55.2.75.

Quinn, G.M., Hubbard, S.M., van Drecht, R., Guest, B., Matthews, W.A., and Hadlari, T. 2016. Record of orogenic cyclicity in the Alberta foreland basin, Canadian Cordillera. Lithosphere, **8**: 317–332. doi:10.1130/L531.1.

Quintero-Legorreta, O. 1992. Geología de la región de Comanja, estados de Guanajuato y Jalisco. Universidad Nacional Autónoma de México, Instituto de Geología. **10**: 6–25.

Rasmussen, K.L. 2013. The timing, composition and petrogenesis of syn- to post-accretionary magmatism in the northern Cordilleran miogeocline, eastern Yukon and southwestern Northwest Territories. Ph.D. dissertation. University of British Columbia, Vancouver, BC. 788p.

Redden, J.A., and DeWitt, E. 2008. Maps showing geology, structure, and geophysics of the central Black Hills, South Dakota. United States Geological Survey, Scientific Investigations Map 2777, scale 1:100,000.

Reed, J.C., Jr., Wheeler, J.O., and Tucholke, B.E. 2005. Geologic map of North America. Decade of North American Geology Continental Scale Map 001, scale 1:5,000,000. Geological Society of America, Boulder, CO

Reese, J.A. 1989. Initial deposition in the Sevier foreland basin of southern Nevada; conglomerates of the Cretaceous Willow Tank Formation, Clark county, Nevada. M.S. Thesis, University of Nevada, Las Vegas, NV, 145p.

Reeside, J.B., Jr., and Cobban, W.A. 1960. Studies of the Mowry Shale (Cretaceous) and contemporary formations in the United States and Canada. United States Geological Survey Professional Paper 355. United States Geological Survey, Denver, CO. 126p.

Reinson, G.E., Warters, G.E., Cox, J., and Price, P.R. 1994. Chapter 21 – Cretaceous Viking Formation of the western Canada sedimentary basin. *In* Geological atlas of the western Canada sedimentary basin. G.D. Mossop and I. Shetsen. Canadian Society of Petroleum Geologists and Alberta Research Council, Calgary, AB. pp. 353–363.

Roberts, L.N.R., and Kirschbaum, M.A. 1995. Paleogeography of the Late Cretaceous of the Western Interior of middle North America: Coal distribution and sediment accumulation. U.S. Geological Survey Professional Paper 1561. U.S. Geological Survey, Denver, CO. 115p.

Roca, X., Rylaarsdam, J.R., Zhang, H., Varban, B.L., Sisulak, C.F., Bastedo, K., and Plint, A.G. 2008. Regional allostratigraphic correlation of Up-

per Albian to Lower Cenomanian foreland basin strata in the Rocky Mountain foothills and adjacent subsurface of Alberta and British Columbia: a genetic framework for a lower Colorado allogroup. Bulletin of Canadian Petroleum Geology, **56**: 259–299. doi:10.2113/gscpgbull.56.4.259.

Ross, G.M., Patchett, R.J., Hamilton, M., Heaman, L., DeCelles, P.G., Rosenberg, E., and Giovanni, M.K. 2005. Evolution of the Cordilleran orogen (southwestern Alberta, Canada) inferred from detrital mineral geochronology, geochemistry, and Nd isotopes in the foreland basin. Geological Society of America Bulletin, **117**: 747–763. doi:10.1130/B25564.1.

Royse, F., Jr. 1993. An overview of the geologic structure of the thrust belt in Wyoming, northern Utah, and eastern Idaho. *In* Geology of Wyoming. *Edited by* A.W. Snoke, J.R. Steidtmann and S.M. Roberts. Geological Survey of Wyoming Memoir 5. Geological Survey of Wyoming, Laramie, WY. pp. 272–311.

Royse, F., Jr., Warner, M.A., and Reese, D.L. 1975. Thrust-belt structural geometry and related stratigraphic problems, Wyoming-Idaho-northern Utah. *In* Deep drilling frontiers of the central Rocky Mountains. Rocky Mountain Association of Geologists Symposium 1975. Rocky Mountain Association of Geologists, Denver, CO. pp. 41–54.

Rubey, W.M. 1929. Origin of the siliceous Mowry shale of the Black Hills region. *In* Shorter contributions to general geology, 1928. United States Geological Survey Professional Paper 154-D. United States Geological Survey, Denver, CO. pp. 153–170.

Rubey, W.M. 1973. New Cretaceous formations in the western Wyoming thrust belt. United States Geological Survey Bulletin 1372-I, United States Geological Survey, Denver, CO. 35p.

Sabbatino, M., Tavani, S., Vitale, S., Orgacta, K., Corradetti, A., Consorti, L., et al. 2021. Forebulge migration in the foreland basin system of the central-southern Apennine fold-thrust belt (Italy): new high-resolution Sr-isotope dating constraints. Basin Research, **33**: 2817. doi:10.1111/bre.12587.

Sabbatino, M., Vitale, S., Tavani, S., Consorti, L., Corradetti, A., Cipriani, A., et al. 2020. Constraining the onset of flexural subsidence and peripheral bulge extension in the Miocene foreland of the southern Apennines (Italy) by Sr-isotope stratigraphy. Sedimentary Geology, **401**: 105634. doi:10.1016/j.sedgeo.2020.105634.

Samson, S.D. 2009. Dinosaur odyssey: Fossil threads in the web of life. University of California Press, Berkeley, CA. 332p.

Schröder-Adams, C.J., Cumbaa, S.L., Bloch, J., Leckie, D.A., Craig, J., Seif El-Dein, S.A., et al. 2001. Late Cretaceous (Cenomanian to Campanian) paleoenvironmental history of the eastern Canadian margin of the Western Interior seaway: bonebeds and anoxic events. Palaeogeography, Palaeoclimatology, Palaeoecology, **170**: 261–289. doi:10.1016/S0031-0182(01)00259-0.

Schröder-Adams, C.J., Leckie, D.A., Bloch, J., Craig, J., McIntyre, D.J., and Adams, P.J. 1996. Paleoenvironmental changes in the Cretaceous (Albian to Turonian) Colorado Group of Western Canada: microfossil, sedimentological and geochemical evidence. Cretaceous Research, **17**: 311–365. doi:10.1006/cres.1996.0022.

Schwans, P. 1995. Controls on sequence stacking and fluvial to shallow-marine architecture in a foreland basin. *In* Sequence stratigraphy of foreland basin deposits. *Edited by* J.A. Van Wagoner and G.T. Bertram. American Association of Petroleum Geologists Memoir 64. American Association of Petroleum Geologists, Tulsa, OK. pp. 55–102.

Sharman, G.R., Sharman, J.P., and Sylvester, Z. 2018. detritalPy: a Python-based toolset for visualizing and analyzing detrital geothermochronologic data. Depositional Records, **4:** 202–215. doi:10.1002/dep2.45.

Silver, L.T., and Chappell, B. 1988. The Peninsular Ranges batholith: an insight into the Cordilleran batholiths of southwestern North America. Earth and Environmental Science Transactions of the Royal Society of Edinburgh, **79**: 105–121. doi:10.1017/S0263593300014152.

Silver, L.T., Taylor, H.P., Jr., and Chappell, B. 1979. Some petrological, geochemical and geochronological observations of the Peninsular Ranges batholith near the international border of the U.S.A. and Mexico. *In* Mesozoic crystalline rocks. *Edited by* P.L. Abbott and V.R. Todd. Department of Geological Sciences, California State University, San Diego, CA. pp. 83–110.

Sinclair, H.D. 1997. Tectonostratigraphic model for underfilled peripheral foreland basins: an alpine perspective. Geological Society of America Bulletin, **109**: 324–346. doi:10.1130/0016- 7606(1997)109⟨0324:TMFUPF⟩2.3.CO;2.

Singer, B.S., Jicha, B.R., Sawyer, D., Walaszczyk, I., Buchwaldt, R., and Mutterlose, J. 2021. Geochronology of Late Albian-Cenomanian strata in the U.S. western interior. Geological Society of America Bulletin, **133**: 1665–1678. doi:10.1130/B35794.1.

Skipp, B. 1987. Basement thrust sheets in the Clearwater orogenic zone, central Idaho and western Montana. Geology, **15**: 220–224. doi:10.1130/0091-7613(1987)15⟨220:BTSITC⟩2.0.CO;2.

Skipp, B., and Hait, M.H., Jr. 1977. Allochthons along the northeast margin of the Snake River Plain, Idaho. *In* Rocky Mountain thrust belt geology and resources. *Edited by* E.L. Heisey and D.E. Lawson. Annual Field Conference 29. Wyoming Geological Association, Casper, WY. pp. 499–516.

Spieker, E.M. 1946. Late Mesozoic and early Cenozoic history of central Utah. U.S. Geological Society Professional Paper 205-D. U.S. Geological Society, Denver, CO. pp. 117–161.

Sprinkel, D.A. 1994. Stratigraphic and time-stratigraphic cross sections: a north-south transect from near the Uinta mountains axis across the Basin and Range transition zone to the western margin of the San Rafael Swell, Utah. U.S. Geological Survey Miscellaneous Investigations Series I-2184-D. U.S. Geological Survey, Denver, CO. 31p. Scale 1:500,000.

Sprinkel, D.A., Madsen, S.K., Kirkland, J.I., Waanders, G.L., and Hunt, G.J. 2012. Cedar Mountain and Dakota formations around Dinosaur National Monument—evidence of the first incursion of the Cretaceous Western Interior seaway into Utah. Utah Geological Survey Special Study 143. Utah Geological Survey, Salt Lake City, UT. 21p. compact disc.

Sprinkel, D.A., Weiss, M.P., Fleming, R.W., and Waanders, G.L. 1999. Redefining the Lower Cretaceous stratigraphy within the central Utah foreland basin. Utah Geological Survey Special Studies **97**: 21p.

Stapp, R.W. 1967. Relationship of Lower Cretaceous depositional environment to oil accumulation, northeastern Powder River basin, Wyoming. AAPG Bulletin, **51**: 2044–2055. doi:10.1306/5D25C1F5-16C1-11D7-8645000102C1865D.

Stelck, C.R. 1962. Upper Cretaceous, Peace River area, British Columbia. *In* Peace River. *Edited by* E.E. Pelzer. Edmonton Geological Society Guidebook, Fourth Annual Field Trip. Edmonton Geological Society, Edmonton, AB. 10–21. pp.

Stelck, C.R. 1975. The upper Albian *Miliammina manitobensis* zone in northeastern British Columbia. *In* The Cretaceous system in the western interior of North America. *Edited by* W.G.E. Caldwell. Geological Association of Canada, Special Paper 13. Geological Association of Canada, St. John's, NL. pp. 253–275.

Stelck, C.R., and Koke, K.R. 1987. Foraminiferal zonation of the Viking interval in the Hasler Shale (Albian), northeastern British Columbia. Canadian Journal of Earth Sciences, **24**: 2254–2278. doi:10.1139/e87-212.

Stelck, C.R., and Leckie, D.A. 1990. Biostratigraphy of the Albian Paddy Member (Lower Cretaceous Peace River Formation). Canadian Journal of Earth Sciences, **27**: 1159–1169. doi:10.1139/e90-123.

Stockmal, G.S., and Beaumont, C. 1987. Geodynamic models of convergent margin tectonics: the southern Canadian Cordillera and the Swiss Alps. *In* Sedimentary basins and basin-forming mechanisms. *Edited by* C. Beaumount and A.J. Tankard. Canadian Society of Petroleum Geologists, Memoir 12 and Atlantic Geoscience Society, Special Publication 5. Canadian Society of Petroleum Geologists. Calgary, AB. pp. 393–411.

Stockmal, G.S., Beaumont, C., and Boutilier, R. 1986. Geodynamic models of convergent margin tectonics: transition from rifted margin to overthrust belt and consequences for foreland-basin development. American Association of Petroleum Geologists Bulletin, **70**: 181–190.

Stokes, W.L. 1976. What is the Wasatch line? *In* Geology of the Cordilleran hingeline. *Edited by* J.G. Hill. Rocky Mountain Association of Geologists, Denver, CO. pp. 11–25.

Stott, D.F. 1982. Lower Cretaceous Fort St. John Group and Upper Cretaceous Dunvegan Formation of the foothills and plains of Alberta, British Columbia, District of Mackenzie and Yukon Territory. Geological Survey of Canada Bulletin 328. Geological Survey of Canada, Ottawa, ON. 124p.

Stroup, C.N., Link, P.K., Janecke, S.U., Fanning, C.M., Yaxley, G.M., and Beranek, L.P. 2008. Eocene to Oligocene provenance and drainage in extensional basins of southwest Montana and east-central Idaho: evidence from detrital zircon populations in the Renova Formation and equivalent strata. *In* Ores and orogenesis: circum-Pacific tectonics, geologic evolution and ore deposits. *Edited by* J.E. Spencer and S.R. Titley. Arizona Geological Society Digest 22. Arizona Geological Society, Tucson, AZ. pp. 529–546.

Suarez, C.A., González, L.A., Ludvigson, G.A., Kirkland, J.I., Cifelli, R.L., and Kohn, M.J. 2014. Multi-taxa isotopic investigation of paleohydrology in the Lower Cretaceous Cedar Mountain Formation, eastern Utah, U.S.A.: deciphering effects of the Nevada Plano plateau on regional climate. Journal of Sedimentary Research, **84**: 975–987. doi:10.2110/jsr.2014.76.

Talavera-Mendoza, O., Ruiz, J., Gehrels, G. E., Valencia, V. A., and Centeno-García, E. 2007. Detrital zircon U/Pb geochronology of southern Guerrero and western Mixteca arc successions (southern Mexico): new insights for the tectonic evolution of the southwestern North America during the late Mesozoic. Geological Society of America Bulletin, **119**: 1052–1065. doi:10.1130/B26016.1.

Tardy, M., Lapierre, H., Freydier, C., Coulon, C., Gill, J.B., and Mercier De Lepinay, B., 1994. The Guerrero suspect terrane (western Mexico) and coeval arc terranes (the Greater Antilles and the Western Cordillera of Colombia): a Late Mesozoic intra-oceanic arc accreted to cratonal America during the Cretaceous. Tectonophysics, **230**: 49–73. doi:10.1016/0040-1951(94)90146-5.

Tesauro, M., Kaban, M.K., and Mooney, W.D. 2015. Variations of the lithospheric strength and elastic thickness in North America. Geochemistry, Geophysics, Geosystems, **16**: 2197–2220. doi:10.1002/2015GC005937.

Thomson, D., Schroëder-Adams, C.J., Hadlari, T., Dix, G., and Davis, W.J. 2011. Albian to Turonian stratigraphy and paleoenvironmental history of the northern Western Interior sea in the Peel Plateau region, Northwest Territories, Canada. Palaeogeography, Palaeoclimatology, Palaeoecology, **302**: 270–300. doi:10.1016/j.palaeo.2011.01.017.

Tizzard, P.G., and Lerbekmo, J.F. 1975. Depositional history of the Viking Formation, Suffield area, Alberta, Canada. Bulletin of Canadian Petroleum Geology, **23**: 715–752.

Troyer, R., Barth, A.P., Wooden, J.L., and Jacobson, C. 2006. Provenance and timing of Sevier foreland basin sediments in the Valley of Fire, southern Nevada, from U-Pb geochronology. Geological Society of America Abstracts with Programs, **38**(7): 369.

Tucker, R.T., Zanno, L.E., Huang, H-Q., and Makovocky, P.J. 2020. A refined temporal framework for newly discovered fossil assemblages of the upper Cedar Mountain Formation (Mussentuchit Member), Mussentuchit Wash, central Utah. Cretaceous Research, **110**: 104384. doi:10.1016/j.cretres.2020.104384.

Tulloch, A.J., and Kimbrough, D.L. 2003. Paired plutonic belts in convergent margins and the development of high Sr/Y magmatism: Peninsular Ranges batholith of Baja-California and Median batholith of New Zealand. *In* Tectonic evolution of northwestern Mexico and the southwestern USA. *Edited by* S.E. Johnson, S.R. Patterson, J.M. Fletcher, G.H. Girty, D.L. Kimbrough and A. Martín-Barajas. Geological Society of America Special Paper 374. Geological Society of America, Boulder, CO. pp. 275–295. doi:10.1130/0-8137-2374-4.275.

Turcotte, D.L. 1979. Flexure. *In* Advances in geophysics. *Edited by* B. Saltzman, B. Academic Press, New York, **v. 21**, pp. 51–86.

Turcotte, D.L., and Schubert, G. 1982. Geodynamics: Applications of continuum physics to geological problems. John Wiley & Sons, New York. 450p.

Tyagi, A., Plint, A.G., and McNeil, D.H. 2007. Correlation of physical surfaces, bentonites, and biozones in the Cretaceous Colorado group from the Alberta Foothills to southeast Saskatchewan, and a revision of the Belle Fourche – Second White Specks formational boundary. Canadian Journal of Earth Sciences, **44**: 871–888. doi:10.1139/e07-004.

Tysdal, R.G., Dyman, T.S., and Nichols, D.J. 1989. Correlation chart of Lower Cretaceous rocks, Madison Range to Lima Peaks area, southwestern Montana. United States Geological Survey, Miscellaneous Field Studies Map MF-2067. United States Geological Survey, Denver, CO. pp. 1–16.

Ullmann, P.V., Varricchio, D., and Knell, M.J. 2012. Taphonomy and taxonomy of a vertebrate microsite in the mid-Cretaceous (Albian-Cenomanian) Blackleaf Formation, southwest Montana. Historical Biology, **24**: 311–328.

van der Meulen, M.J., Kouwenhoven, T.J., van der Zwaan, G.J., Meulenkamp, J.E., and Wortel, M.J.R. 1999. Late Miocene uplift in the Romagnan Apennines and the detachment of subducted lithosphere. Tectonophysics, **315**: 319–335. doi:10.1016/S0040-1951(99)00282-6.

van der Meulen, M.J., Meulenkamp, J.E., and Wortel, M.J.R. 1998. Lateral shifts of Apenninic foredeep depocentres reflecting detachment of subducted lithosphere. Earth and Planetary Science Letters, **154**: 203–219. doi:10.1016/S0012-821X(97)00166-0.

Varricchio, D.J., Martin, A.J., and Katsura, Y. 2007. First trace and body fossil evidence of a burrowing, denning dinosaur. Proceedings of the Royal Society B: Biological Sciences, **274**: 1361–1368. doi:10.1098/rspb.2006.0443.

Vorobieva, O. 2000. A multidisciplinary subsurface study of the Albian Bow Island and Westgate formations in southwestern Alberta, Canada. M.S. thesis, Carleton University, Ottawa, ON, 202p.

Vuke, S.M. 1984. Depositional environments of the early Cretaceous Western Interior seaway in southwestern Montana and the northern United States. *In* The Mesozoic of middle North America. *Edited by* D.F. Stott and D.J. Glass. Canadian Society of Petroleum Geologists Memoir 9. Canadian Society of Petroleum Geologists, Calgary, AB. pp. 127–144.

Walaszczyk, I., and Cobban, W.A. 2016. Inoceramid bivalves and biostratigraphy of the Upper Albian and Lower Cenomanian of the United States Western Interior Basin. Cretaceous Research, **59**: 30–68. doi:10.1016/j.cretres.2015.10.019.

Walker, J.D., Burchfiel, B.C., and Davis, G.A. 1995. New age controls on initiation and timing of foreland belt thrusting in the Clark Mountains, southern California. Geological Society of America Bulletin, **107**: 742–750. doi:10.1130/0016-7606(1995)107⟨0742:NACOIA⟩2.3.CO;2.

Wallace, C.A., Lidke, D.J., and Schmidt, R.G. 1990. Faults of the central part of the Lewis and Clark line and fragmentation of the Late Cretaceous foreland basin in west-central Montana. Geological Society of America Bulletin, **102**: 1021–1037. doi:10.1130/0016-7606(1990)102⟨1021:FOTCPO⟩2.3.CO;2.

Waring, J. 1976. Regional distribution of environments of the Muddy Sandstone, southeastern Montana. *In* Geology and energy resources of the Powder River; 28th Annual Field Conference Guidebook. Wyoming Geological Association, Casper, WY. pp. 83–96.

Warzeski, E.R. 1987. Revised stratigraphy of the Mural Limestone: a lower Cretaceous carbonate shelf in Arizona and Sonora. *In* Mesozoic rocks of southern Arizona and adjacent areas. *Edited by* W.R. Dickinson and M.F. Klute. Arizona Geological Society Digest 18, Arizona Geological Society, Tucson, Arizona. pp. 335–363.

Weimer, R.J. 1986. Relationship of unconformities, tectonics, and sea level changes in the Cretaceous of the Western Interior, United States. *In* Paleotectonics and sedimentation in the Rocky Mountain Region, United States. *Edited by* J.A. Peterson. American Association of Petroleum Geologists, Memoir 41. American Association of Petroleum Geologists, Tulsa, OK. pp.397–422. doi:10.1306/M41456.

Wells, M.L. 2016. A major mid-Cretaceous shortening event in the southern Sevier orogenic belt: continental record of global plate reorganization. Geological Society of America Abstracts with Programs, **48**(7). doi:10.1130/abs/2016AM-287809.

Wetmore, P.H., and Ducea, M.N. 2009. Geochemical evidence of a near-surface history for source rocks of the central Coast Mountains batholith, British Columbia. International Geology Review **1**: 1–31.

Whalen, J.B., and Hildebrand, R.S. 2019. Trace element discrimination of arc, slab failure, and A-type granitic rocks. Lithos, **348-349**: 105179. doi:10. 1016/j.lithos.2019.105179.

Whiteford, Stanley D., Jr. 1962. Regional aspects of the Muddy Formation in the Wind River Basin, Wyoming. Proceedings of the Iowa Academy of Science, **69**: 411–430.

Wilson, J.T. 1968. Static or mobile earth: the current scientific revolution. Proceedings of the American Philosophical Society, **112**: 309–320.

Wulf, G.R. 1962. Lower Cretaceous Albian rocks in the northern Great Plains. Bulletin of the American Association of Petroleum Geologists, **46**: 1371–1415.

Yanagi, T., Baadsgaard, H., Stelck, C.R., and McDougall, I. 1988. Radiometric dating of a tuff bed in the middle Albian Hulcross Formation at Hudson's Hope, British Columbia. Canadian Journal of Earth Sciences, **25**: 1123–1127. doi:10.1139/e88-109.

Yang, T., and Gurnis, M. 2016. Dynamic topography, gravity and the role of lateral viscosity variations from inversion of global mantle flow. Geophysical Journal International. **207**: 1186–1202. doi:10.1093/gji/ggw335.

Yingling, V.L., and Heller, P.L. 1992. Timing and record of foreland sedimentation during the initiation of the Sevier orogenic belt in central Utah. Basin Research, **4**: 279–290. doi:10.1111/j.1365-2117.1992.tb00049.x.

Yonkee, W.A., and Weil, A.B. 2015. Tectonic evolution of the Sevier and Laramide belts within the North American Cordillera orogenic system. Earth-Science Reviews, **150**: 531–593. doi:10.1016/j.earscirev.2015.08.001.

Yonkee, W.A., Eleogram, B., Wells, M.L., Stockli, D.F., Kelley, S., and Barber, D.E. 2019. Fault slip and exhumation history of the Willard thrust sheet, Sevier fold-thrust belt, Utah: relations to wedge propagation, hinterland uplift, and foreland basin sedimentation. Tectonics, **38**: 2850–2893. doi:2018TC005444.

Yonkee, W.A., Parry, W.T., and Bruhn, R.L. 2003. Relations between progressive deformation and fluid-rock interaction during shear zone growth in a basement-cored thrust sheet, Sevier orogenic belt, Utah. American Journal of Science, **303**: 1–59. doi:10.2475/ajs.303.1.1.

Zartman, R.E., Dyman, T.S., Tysdal, R.G., and Pearson, R.C. 1995. U-Pb ages of volcanogenic zircon from porcellanite beds in the Vaughn Member of the mid-Cretaceous Blackleaf Formation, southwestern Montana. United States Geological Survey Bulletin 2113-B. United States Geological Survey, Denver, CO. pp. 1–16.

Zuber, M.T., Bechtel, T.D., and Forsyth, D.W. 1989. Effective elastic thicknesses of the lithosphere and mechanisms of isostatic compensation in Australia. Journal of Geophysical Research, **94**: 9353–9367. doi:10.1029/JB094iB07p09353.

Zupanic, J. 2017. Lateral heterogeneity and architectural analysis of the Wall Creek Member of the Upper Cretaceous (Turonian) Frontier Formation., Unpublished MSc Thesis. University of Montana, Missoula, MT. 145p.